Volume 9 | Issue 1 | June 2019 ISSN 2182-0287

Journal of Integrated OMICS

a methodological journal

JIOMICS

Journal of Integrated OMICS

Focus and Scope

Journal of Integrated OMICS, JIOMICS, provides a forum for the publication of original research papers, preliminary communications, technical notes and critical reviews in all branches of pure and applied "-omics", such as genomics, proteomics, lipidomics, metabolomics or metallomics. The manuscripts must address methodological development. Contributions are evaluated based on established guidelines, including the fundamental nature of the study, scientific novelty, and substantial improvement or advantage over existing technology or method. Original research papers on fundamental studies, and novel sensor and instrumentation development, are especially encouraged. It is expected that improvements will also be demonstrated within the context of (or with regard to) a specific biological question; ability to promote the analysis of molecular mechanisms is of particular interest. Novel or improved applications in areas such as clinical, medicinal and biological chemistry, environmental analysis, pharmacology and materials science and engineering are welcome.

Editors-in-Chief

Regional editors

Associated editors

AUSTRALIA AND NEW ZEALAND

SOUTH AMERICA

Alessandro Farias
Neuroimmunomodulation Group, department of Genetics, Evolution and Bioagents, University of Campinas - SP – Brazil
Alexandra Sawaya
Department of Plant Biology, Institute of Biology, UNICAMP, Campinas, São Paulo, Brazil
Andréa P.B. Gollucke
Hexalab/Catholic University of Santos, Brazil
Arlindo Moura
Department of Animal Science - College of Agricultural Sciences - Federal University of Ceara, Fortaleza, Brasil
Bruno Lomonte
Instituto Clodomiro Picado, Universidad de Costa Rica
Deborah Schechtman
Department of Biochemistry, Chemistry Institute, University of São Paulo, Brazil
Edson Guimarães Lo Turco
São Paulo Federal University, Brasil
Elisabeth Schwartz
Department of Physiological Sciences, Institute of Biological Sciences, University of Brasilia, Brazil
Fabio Ribeiro Cerqueira
Department of Informatics and NuBio (Research Group for Bioinformatics), University of Vicosa, Brazil
Fernando Barbosa
Faculty of Pharmaceutical Sciences of Ribeirão Preto University of São Paulo, Brazil
Hugo Eduardo Cerecetto
Grupo de Química Medicinal, Facultad de Química, Universidad de la República, Montevideo, Uruguay
Luis Pacheco
Institute of Health Sciences, Federal University of Bahia, Salvador, Brazil
Mário Hiroyuki Hirata
Laboratório de Biologia Molecular Aplicado ao Diagnóstico, Departamento de Análises Clínicas e Toxicológicas, Faculdade de Ciências Farmacêuticas, Universidade de São Paulo, Brazil
Jan Schripsema
Grupo Metabolômica, Laboratório de Ciências Quimicas, Universidade Estadual do Norte Fluminense, Campos dos Goytacazes, Brazil
Jorg Kobarg
Centro Nacional de Pesquisa em Energia e Materiais, Laboratório Nacional de Biociências, Brazil
Marcelo Bento Soares
Cancer Biology and Epigenomics Program, Children's Memorial Research Center, Professor of Pediatrics, Northwestern University's Feinberg School of Medicine
Mario Palma
Center of Study of Social Insects (CEIS)/Dept. Biology, Institute of Biosciences, Univesity of São Paulo State (UNESP), Rio Claro - SP Brazil
Rinaldo Wellerson Pereira
Programa de Pós Graduação em Ciências Genômicas e Biotecnologia, Universidade Católica de Brasília, Brazil
Roberto Bobadilla
BioSigma S.A., Santiago de Chile, Chile
Rossana Arroyo
Department of Infectomic and Molecular Biology, Center of Research and Advanced Studies of the National, Polytechnical Institute (CINVESTAV-IPN), Mexico City, Mexico
Rubem Menna Barreto
Laboratorio de Biología Celular, Instituto Oswaldo Cruz, Fundaçao Oswaldo Cruz, Rio de Janeiro, Brazil
Vasco Azevedo
BiologicalSciencesInstitute, Federal University of Minas Gerais, Brazil

NORTH AMERICA

Adam Vigil
University of California, Irvine, USA
Akeel Baig
Hoffmann-La Roche Limited, Pharma Research Toronto, Toronto, Ontario, Canada
Alexander Statnikov
Center for Health Informatics and Bioinformatics, New York University School of Medicine, New York
Amosy M'Koma
Vanderbilt University School of Medicine, Department of General Surgery, Colon and Rectal Surgery, Nashville, USA
Amrita Cheema
Georgetown Lombardi Comprehensive Cancer Center, USA
Anthony Gramolini
Department of Physiology, Faculty of Medicine, University of Toronto, Canada
Anas Abdel Rahman
Department of Chemistry, Memorial University of Newfoundland and Labrador St. John's, Canada
Christina Ferreira
Purdue University - Aston Laboratories of Mass Spectrometry, Hall for Discovery and Learning Research, West Lafayette, US
Christoph Borcher
Biochemistry & Microbiology, University of Victoria, UVic Genome British Columbia Proteomics Centre, Canada
Dajana Vuckovic
University of Toronto, Donnelly Centre for Cellular + Biomolecular Research, Canada
David Gibson
University of Colorado Denver, Anschutz Medical Campus, Division of Endocrinology, Metabolism and Diabetes, Aurora, USA
Deyu Xie
Department of Plant Biology, Raleigh, USA
Edgar Jaimes
University of Alabama at Birmingham, USA
Eric McLamore
University of Florida, Agricultural & Biological Engineering, Gainesville, USA
Eustache Paramithiotis
Caprion Proteomics Inc., Montreal, Canada
FangXiang Wu
University of Saskatchewan, Saskatoon, Canada
Fouad Daayf
Department of Plant Science, University of Manitoba, Winnipeg, Manitoba, Canada
Haitao Lu
Washington University School of Medicine, Saint Louis, USA
Hexin Chen
University of South Carolina, Columbia, USA
Hsiao-Ching Liu
232D Polk Hall, Department of Animal Science, North Carolina State University Raleigh, USA
Hui Zhang
Johns Hopkins University, MD, USA
Ing-Feng Chang
Institute of Plant Biology, National Taiwan University, Taipei, Taiwan

JOURNAL OF INTEGRATED OMICS

A methodological Journal

SPECIAL ISSUE: COMMEMORATING THE 2ND CONGRESS OF THE BELARUSIAN SOCIETY OF BIOCHEMISTS AND MOLECULAR BIOLOGISTS

ORIGINAL ARTICLES

SPECIAL ISSUE

COMMEMORATING THE 2ND CONGRESS OF THE BELARUSIAN SOCIETY OF BIOCHEMISTS AND MOLECULAR BIOLOGISTS

2018

JOURNAL OF INTEGRATED OMICS
A METHODOLOGICAL JOURNAL
HTTP://WWW.JIOMICS.COM

ORIGINAL ARTICLE | DOI: 10.5584/jiomics.v9i1.258

Therapeutic potential of autologous bone marrow mononuclear cells preconditioned with Erythropoietin implantation in laser channels in patients with Cardiac arteria disease

Alexander Lykov [1,2*], Olga Poveshchenko [1,2], Maria Surovtseva [1,2], Alexander Cherniavsky [1], Alexei Fomichev [1].

[1]Meshalkin National Medical Research Center, Ministry of Health of Russian Federation, Rechkunovskaya Str., 15, Novosibirsk, 630055, Russian Federation; [2]Research Institute of Clinical and Experimental Lymphology – Branch of the Institute of Cytology and Genetics, Siberian Branch of Russian Academy of Science, Timakova Str., 2, Novosibirsk, 630090, Russian Federation

Received: 10 July 2018 **Accepted:** 31 December 2018 **Available Online**: 08 March 2019

Abstract

The problem of incomplete myocardial revascularization for diffuse and distal lesions of the myocardium is still relevant. We assessed the clinical and instrumental long-term results of autologous bone marrow mononuclear cell (BM-MNCs) implantation in laser channels in ischemic heart disease with diffuse and distal coronary disease. In 2015-2018, 50 ischemic heart disease patients with diffuse and distal coronary arterial disease during coronary artery bypass grafting (CABG) underwent BM-MNCs short-term pre-treated with Erythropoietin implantation in laser channels (BM-MNCs group) and in 50 patients only CABG was done in the clinic of National Medical Research Center n.a. E.N. Meshalkin (Novosibirsk, Russia). Therapeutic potential of pre-treated BM-MNCs with Erythropoietin implantation was carried out at two weeks, six and twelfth months after surgery. Changes on morphofunctional properties of BM-MNCs after pre-treatment with Erythropoietin was carried out on basis phenotype, cell cycle, cell death, proliferation, migration, tube formation and cytokine production. In this study, we observed the presence in cellular graft of the hematopoietic stem cells (HSCs), and endothelial progenitor cells (EPCs) at the different stage of maturation/differentiation, and mesenchymal stem cells (MSCs). Precondition BM-MNCs with Erythropoietin increased number of HSCs carrying erythropoietin receptor (EpoR), and EPCs carrying CD184. Also, Epo detained CB34+ cells in a rest phase of cell cycle (G0G1). Condition media from BM-MNCs treated with Erythropoietin augment tube formation and wound healing by EA.hy 929. After six months postoperatively, the severity of angina and heart failure based NYHA functional class (NYHA FC) was significantly less in the BM-MNCs group than in control group (p=0.04). according to perfusion scintigraphy, there was a slight decrease of stable perfusion defects (SPD) in the early postoperative period. Left ventricular ejection fraction in BM-MNCs group have tendency to increase six months after treatment.

Аннотация

Проблема неполной реваскуляризации миокарда при диффузных и дистальных поражениях миокарда остается актуальной. Проведена оценка клинико-инструментальных отдаленных результатов имплантации аутологичных мононуклеарных клеток костного мозга (КМ-МНК) в лазерные каналы при ишемической болезни сердца с диффузной и дистальной ишемической болезнью сердца. В 2015-2018 годах, у 50 больных с ишемией сердца, обусловленной диффузным и дистальным коронарным атеросклерозом во время аортокоронарного шунтирования (АКШ) была проведена имплантация КМ-МНК предварительно проинкубированных с эритропоэтином в лазерные каналы (КМ-МНК группа) и у 50 больных проведено только АКШ на базе клиники Национального медицинского научно-исследовательского центра им. акад. Е. Н. Мешалкина (Новосибирск, Россия). Терапевтический потенциал имплантации предварительно обработанных КМ-МНК с эритропоэтином оценивали через две недели, шесть и двенадцатый месяцев после операции. Изменения морфофункциональных свойств КМ-МНК после предварительной обработки эритропоэтином осуществляли на основе фенотипа, клеточного цикла, гибели клеток, пролиферации, миграции, образования сосудисто-подобных структур и продукции цитокинов. В данном исследовании мы наблюдали наличие в клеточном трансплантате гемопоэтических стволовых клеток (ГСК) и эндотелиальных прогениторных клеток (ЭПК) на разной стадии созревания/дифференцировки, а также мезенхимальных стволовых клеток. Предварительная культивация КМ-МНК с эритропоэтином способствовала увеличению количества ГСК, несущих рецептор эритропоэтина, и ЭПК, несущих CD184. Кроме того, обработка клеток эритропоэтином удерживало CD34+ клеток в фазе покоя клеточного цикла (G0G1). Кондиционная среда от КМ-МНК проинкубированных с эритропоэтином увеличивало формирование сосудисто-подобных структур и заживление раневого дефекта монослоя EA.hy 929. Через полгода после операции тяжесть стенокардии и сердечной недостаточности по функциональному классу NYHA была достоверно меньше в группе КМ-МНК, чем в контрольной группе (P=0,04). По данным перфузионной сцинтиграфии в раннем послеоперационном периоде отмечено незначительное снижение стабильных перфузионных дефектов. Фракция выброса левого желудочка в группе КМ-МНК имеет тенденцию к увеличению через полгода после лечения.

Keywords: Coronary artery disease, erythropoietin, bone marrow mononuclear cells, intramyocardial injection, NYHA class, Borg class

***Corresponding author:** Alexander Lykov, Ph.D., e-mail: aplykov2@mail.ru

1. Introduction

In Cardiovascular diseases are the leading cause of morbidity, and mortality, and development of heart failure (1-2). The lack of capillary network and perfusion after acute myocardium infarction (AMI) caused oxygen and nutrients deficiency and leads to endothelial apoptosis, and an increase in the area of heart attack and left ventricular dysfunction. Also, after AMI, several processes occurred, including the irreplaceable loss of a part of cardiomyocytes, structural remodeling of a myocardium associated with inflammation, scar formation, and development of interstitial fibrosis in peri-infarction zone, and remodeling of blood supply of a myocardium, that are also the starting factors of heart failure development (3-4). Although pharmacological and surgical treatments can significantly improve patient outcomes, no treatment currently available is able to generate new contractile myocardium or revers ischemic myocardium, therefore new methods of therapy are necessary to repair myocardium function. In many reports the successful use of the stem cells to regenerate damaged myocardium in both animal and human AMI has been shown (5-6). Stem cell-based therapy is emerging as a potential therapeutic approach for damaged tissue regeneration and an important strategy for the treatment of heart failure (7-10). Implantation of autologous bone marrow stem cells into injured myocardium may be considered as a promising therapy for myocardium regeneration and ventricular contractility restoration (11-19). Analysis of obtained data from randomized clinical trials of intramyocardial bone marrow cells to treat ischemic heart disease showed increased left ventricular ejection fraction (LVEF), reduced left ventricular end-systolic volume (LVESV), and trend toward the decrease of left ventricular end-diastolic volume (LVEDV). The best efficacy of intramyocardial bone marrow cells injection observed on the left ventricular ejection fraction in patients with suitable for revascularization with coronary artery bypass grafting compared with patients unsuitable for revascularization (20). Numerous clinical trials have previously investigated the clinical outcomes in patients after myocardium infarction and reported significant efficacy in improving contractility and reducing infarction scar (13, 15, 18-19, 21). However, there was a problem of the limited efficacy: improvement of left-ventricular ejection fraction and reduction of infarction size, viability of stem cells. Under this situation, precondition of the adult stem cells before implantation would be a very feasible and safe way to augment the therapeutic efficacy. Erythropoietin (Epo), cytokine that controls erythropoiesis, also appears to have pleiotropic effects, such as anti-ischemic and anti-apoptotic properties, promotion of neovascularization, mobilization of EPCs, and enhancement of angiogenesis (22). The aim of this study was to investigate the therapeutic efficiency of intramyocardial administration of short-term preconditioning autologous bone marrow mononuclear cells in patients with cardiac arteria disease.

2. Material and Methods

2.1. Ethics Statement and Patients Characteristics

The Research involving humans was performed with the prior approval of the Ethics Committee of Institute of Clinical and Experimental Lymphology-Branch of National Research Centre Institute of Cytology and Genetics Siberian Division of Russian Academy of Sciences, and of the Ethics Committee of Meshalkin National Medical Research Center, Ministry of Health of Russian Federation, and all procedure was conducted in accordance with the principles and guidelines of the Declaration of Helsinki. All participants signed written informed consent prior to the study. One hundred ischemic heart disease patients with diffuse and distal coronary arteria disease (CAD) were enrolled from Meshalkin National Medical Research Center, Ministry of Health of Russian Federation (Novosibirsk, Russian Federation) in January 2016 – May 2018. Patients had to be at least 50 years old, suffering from chronic ischemic heart disease, and receiving constant state-of-the-art pharmacotherapy for at least 3 months prior to enrolment. 95% were men. All were in angina NYHA functional class II-III. Arterial hypertension was presented in 90%, peripheral atherosclerosis in 60%. The inclusion criteria were as follows: age ≥50 and <75 years; presence of coronary artery lesions; chronic ischemia heart failure; myocardial infarction within previous 12 months; New York Heart Association (NYHA) functional class II-III within last 6 months; systolic dysfunction with LVEF ≤35%; fixed perfusion defect on Tc-99m technetril single-photon emission computed tomography (SPECT). The exclusion criteria comprised the following factors: eligibility for percutaneous coronary intervention; eligibility for coronary artery bypass grafting; previous valve surgery; surgical remodeling of the left ventricle or cardiac resynchronization therapy; hemorrhagic symptoms; severe renal and liver dysfunction; malignancy. Patients who meet eligibility criteria will be scheduled for bone marrow harvest. Indications for surgery were: severe angina refractory to clinical antianginal therapy; diffuse coronary artery lesion of the distal bed or small coronary vessel diameter (less than 1 mm) or a viable (hibernating) myocardium. 50 patients received only coronary artery bypass grafting (CABG) – control group, 50 patients during CABG underwent autologous bone marrow mononuclear cells pre-treated with Epo implantation in laser channels – BM-MNCs group. Clinical and instrumental assessment of the therapeutic efficiency was carried out at two weeks, six and twelfth months after surgery. One of the main conditions of the operation was the presence of a viable myocardium in the revascularization area. In this regard, we analyzed two-staged myocardial scintigraphy with Tc-99

data for myocardial viability, as well as to assess the effectiveness of indirect revascularization. The status of the infarction was assessed on a 5-point scale: 4 – rule; 3 – ischemia (hibernating myocardium); 2 – small focal scarring; 1 – tripe; 0 –aneurysm. The main parameters were stable perfusion defect (SPD, %) and transient perfusion defect (TPD, %).

2.2 Human Bone Marrow Mononuclear Cells Morphofunctional Properties

Bone marrow samples of fifty patients with CAD were harvested for autologous transmyocardial implantation. Bone marrow aspirates were diluted with PBS and bone marrow mononuclear cells (BM-MNCs) were isolated by density gradient centrifugation with Ficoll-Paque. The BM-MNCs were washed three times with 50 mL of PBS, counted, and viability testing was performed with trypan blue exclusion (≥ 95%), and used for the experiments. The 106 BM-MNCs/cm2 from patients with CAD were plated in PBS supplemented completed with 10% autologous serum and Epo (33.4 IU/mL of Recormon) for 1 hour. BM-MNCs phenotype was performed for CD18 (Integrin β2), CD29 (Integrin β1), CD31 (Platelet endothelial cell adhesion molecule-1, PECAM-1), CD34 (Glycoprotein), CD44 (Cell-surface glycoprotein), CD45 (Transmembrane glycoprotein), CD49a (Integrin alpha-1), CD54 (Inter-cellular adhesion molecule 1), CD62E (E-selectin), CD73 (68kDa GPI-anchored cell-surface protein with enzymatic and signal transduction activities), CD90 (GPI-anchored membrane glycoprotein of the Ig superfamily, Thy-1), CD105 (Endoglin, a major glycoprotein of human vascular endothelium), CD131(βIL-3 (AIC2A) and βc (AIC2B) cytokine receptor subunits), CD133(Promenin-1), CD146 (Cell surface glycoprotein MUC18), CD184 (CXC chemokine receptor, CXCR4), CD202b (Angiopoetin-1 receptor), KDR (Vascular endothelial growth factor receptor -2), and Erythropoietin-receptor (EpoR) expression. Cell cycle distribution were performed by using Propidium Iodide. The apoptosis assay was performed using an Annexin V-FITC/PI Apoptosis Detection kit. Proliferative potential of 2 x 105 BM-MNCs/well were done with Concanavalin A (10 μg/mL), Phytohemagglutinin A (10 μg/mL), Lipopolysaccharide (1 μg/mL), Epo (33.4 IU/mL of Recormon), and H2O2 (1, 3, and 5 mM) in DMEM plus 10% FCS, 0.3 mg/mL L-glutamine, 5 mM HEPES buffer), and 80 μg/mL of gentamycin during 72 hours in CO2-incubator, then cells were supplemented with fresh medium containing 5 mg/mL 3-[4, 5-dimethylthiazol-2-yl]-2, 5-diphenyl-tetrazolium bromide (MTT) and incubated for 4 hours at 37 0C. The formazan in viable cells was dissolved with 100 μL of dimethyl sulfoxide and determined by reading optical densities (OD) in microplate reader (Stat Fax 2100) at an absorption wave length of 570 nm. For enzyme-linked immunosorbent assay (ELISA), and wound healing test, and tubule-formation, media were collected from plates of BM-MNCs (CM-MNCs) after 72 hours of culture in DMEM plus 10% FCS, 0.3 mg/mL L-glutamine, and 80 μg/mL of gentamycin, and Epo (0 and 33.4 IU/mL of Recormon), aliquoted and storage at -70 0C before using in testing in vitro. IL-1β, TNF-α, TGF-β1, IL-6, IL-8, IL-10, PDGF-AB, VEGF, basal GFG, IGF-1, Epo, CXCL-12/SDF-1a, MMP-9, TIMP-1, and NO in CM-MNCs were determined by ELISA. NO inhibition assay was conducted using Griess reagent kit for nitrite determination. Wound healing was tested on EA.hy 926 cells (kindly gifted by Dr. C.J. Edgel, Caroline University, USA) scratched monolayer cultured or tubule-formation on In vitro angiogenesis assay kit in 100 μL of DMEM plus 0% or 10% FCS (negative and positive control), in mixture of 70% DMEM and 30% of CM-MNCs growth in the presence or absence of Epo (experimental wells) in CO2-incubator for 24 hours.

2.3 Indirect Method of Coronary Revascularization and Short -term Preconditioning Autologous Bone Marrow Mononuclear Cells with Erythropoietin Intramyocardial Implantation

In fifty patients with CAD after performed the distal anastomoses, 5-7 radially arranged blind laser channels in fifth points were formed by using laser surgical unit of LSP-IRE-Polus (Russia) with wavelength of 1.56 microns with a power of 15 watts. Laser was applied in pulsed mode, with a pulse duration of 20 ms and an interval between pulses of 20 ms. Channel length was determined by the size of scar area. Further, in order to create a closed cavity in the channel mouth, an n-stitch was superimposed, the 20 x 106 BM-MNCs pre-treated with Epo infusion was performed, and the n-stitch arose. The efficacy of treatment was assed in 2 weeks, 6 and 12 months by changes in the LVEF, LVESV, LVEDV by echocardiography and myocardial perfusion by ECG-synchronized SPECT using technetium (Tc-99m technetril) at rest and during pharmacological stress caused by intravenous administration of adenosine (0.14 mg/kg/min over 6 min). The results were assessed in 10 segments; score range in each segment from 0 to 4 (0 – normal activity, 4 – no activity). Also, efficiency of treatment was estimated using NYHA FC, and Borg dyspnea scale.

2.4 Statistical Analysis

All data analyses were performed by Statistica 10 statistical program. In this study, the normality of the distribution was determined by the w-Shapiro-Wilkes criterion, in tables the obtained data were presented as median with lower and upper quartiles (Me; LQ-UQ) with no less than three replicates for each experimental condition, the data were analyzed by Mann-Whitney U test for pairwise comparisons data, and correlation coefficient using the Spearman rank correlation (Rs). If p-value was less than 0.05, it was considered statistically significant.

3. Results and discussion

3.1. Morphofunctional properties of Bone Marrow Mononuclear Cells from Patients with CAD

Among mononuclear cells derived from bone marrow samples from patients with CAD we observed a higher number of hematopoietic stem cells (HSCs), endothelial progenitor cells (EPCs) and mesenchymal stem cells (MSCs). So, among HSCs the number of CD45+/CD34- cells were more than 30%, CD45+/CD184+ cells more than 16%, and CD45+/EpoR+ more than 3%. Among EPCs the number of CD45-/CD34+ cells were more than 0.6%, CD34+/CD31+ cells more than 0.9%, CD34+/VEGFR2+ cells more than 1.25%, CD34+/CD133+ cells more than 0.95%, CD34+/CD131+ cells more than 1.15%, CD34+/CD184+ cells more than 2.6%, CD34+/EpoR+ cells more than 0.85%, and CD31+/CD184+ cells more than 5.5%. Among MSCs the number of CD73+/CD90+ cells were more than 1.3%, CD73+/CD105+ cells more than 3.7, and CD90+/CD105+ cells more than 0.9%. These findings indicated that BM-MNCs from patients with CAD contained heterogeneous stem cells populations. Information on BM-MNCs phenotypes changes after short-term conditioning with Erythropoietin was summarized in Table 1. Conditioning BM-MNCs with Epo significantly increased the number of HSCs expressed EpoR (CD45+/EpoR+ cells), and the number of EPCs expressed CD184 (CD31+/CD184+ cells), wherease the number of EPCs expressed CD133 (CD34+/CD133+ cells) significantly decreased. Also, we find a trend towards the decrese of the number of CD34+/CD133+ cells, CD34+/EpoR+ cells, CD34+/CD184+ and CD34+/CD131+ cells, and the trend towards the increase of the number of CD34+/VEGFR2+ cells and MSCs with CD73+/CD90+, CD73+/CD105+ and CD90+/CD105+ phenotype. We showed strong correlation between the number of CD34+/CD133+, and the number of CD34+/EpoR+ cells with the age of patients (R=0.52 and R=0.49, p ≤0.05). We found that pre-treatment of BM-MNCs with Epo significantly increased the number of CD34+ cells in subG0G1, G0G2 cell cycle phase, and significantly decreased the number of CD34+ cells in G2/M and S cell cycle phase (Table 2). Whereas, we did not observe any significant difference in the number of CD34+ cells in apoptosis and necrosis when we used an Annexin V-FITC/PI Apoptosis Detection kit, but we observed the trend towards the decrease of the number of CD34+ cells after pre-treatment with Epo on apoptosis/necrosis. Data of the effect of pre-treatment of BM-MNCs with Epo on expression of CD18, CD54, CD29, CD44, CD49a, CD62E, CD146, CD202b was summarized in Table 3. We found the trend towards the increase in the number of CD34+/CD54+, CD34+/CD18+, CD49a and CD202b cells among BM-MNCs after pre-treatment with Epo. Whereas, the number of CD18+/CD54+, CD29+, CD44+, CD62E+ and CD146+ cells tend to reduce among BM-MNCs after pre-treatment with Epo. BM-MNCs proliferation spontaneous or in the presence of stimulating factors or inductors of oxidative stress after pre-treatment with Epo was significantly reduced compared with basal and stimulated proliferation capacity of BM-MNCs without pre-treatment with Epo (Table 4). We

Table 1 | The effect of short-term preconditioning of the bone marrow mononuclear cells on the number of stem cells (%, Me; LQ-UQ). Эффект кратковременной экспозиции КМ-МНК с эритропоэтином на количество стволовых клеток.

Phenotype	*Basal*	*Epo -preconditioning*	*p-value*
Hematopoietic stem cells			
CD45+/EpoR+	4.76 (0.5-6.25)	10.91 (1.75-16.24)	0.01159
Endothelial progenitor cells			
CD34+/CD31+	0.94 (0.4-1.0)	0.92 (0.5-1.0)	0.41699
CD34+/CD133+	0.87 (0.5-1.06)	0.33 (0.1-0.7)	0.01052
CD34+/VEGFR2+	1.09 (0.5-1.3)	1.51 (0.1-2.5)	0.29870
CD34+/EpoR+	0.8 (0.4-0.9)	0.55 (0.3-0.55)	0.14634
CD34+/CD184+	2.46 (1.0-3.0)	1.69 (0.4-2.0)	0.19361
CD34+/CD131+	0.78 (0.2-1.45)	0.55 (0.2-0.5)	0.97278
CD31+/CD184+	6.13 (2.0-8.5)	11.48 (5.0-11.0)	0.02778
Mesenchymal stem cells			
CD73+/CD90+	0.85 (0.25-2.2)	1.15 (0.1-2.7)	0.96
CD73+/CD105+	1.75 (0.35-7.2)	2.0 (0.1-5.4)	0.91
CD90+/CD105+	0.5 (0.21-1.3)	0.95 (0.6-2.0)	0.34

Table 2 | The effect of short-term preconditioning of the bone marrow mononuclear cells on the cell cycle distribution and apoptosis/necrosis. Эффект краткосрочной экспозиции КМ-МНК с эритропоэтином на распределение клеток в фазах клеточного цикла и апоптоз/некроз

Parameters	*Basal*	*Epo - preconditioning*	*p-value*
Cell cycle			
subG0G1	5.58 (5.0-5.0)	6.12 (6.0-6.0)	0.011975
G0G1	78.25 (78.0-78.0)	85.29 (85.0-85.0)	0.001914
G2/M	15.85 (13.0-13.0)	7.1 (7.0-7.0)	0.000052
S	3.25 (3.0-3.0)	1.08 (1.0-1.0)	0.000052
Apoptosis/Necrosis			
Annexin V+/PI- (early apoptosis)	6.98 (1.7-10.0)	5.47 (0.85-5.0)	0.076424
Annexin V+/PI+ (apoptosis)	3.07 (0.1-3.6)	4.2 (0.6-2.95)	0.310768
Annexin V-/PI+ (necrosis)	2.72 (0.25-1.05)	1.58 (0.2-1.0)	0.966427

Table 3 | Effect of short-term preconditioning of the bone marrow mononuclear cells on the expression of adhesion molecules. Эффект краткосрочной экспозиции КМ-МНК на экспрессию молекул адгезии

Phenotype	*Basal*	*Epo -preconditioning*	*p-value*
CD34+/CD54+	1.77 (0.55-3.0)	2.0 (0.7-3.9)	0.67
CD34+/CD18+	1.4 (0.55-2.25)	1.7 (0.2-4.2)	0.52
CD18+/CD54+	59.47 (43.9-75.0)	54.27 (34.8-70.7)	0.94
CD29a+	97.27 (95.8-98.75)	89.2 (75.8-96.7)	0.83
CD44+	91.25 (84.6-97.9)	86.97 (64.5-99.8)	0.28
CD49a+	37.92 (22.65-53.2)	56.0 (51.1-63.4)	0.62
CD62E+	44.6 (21.95-67.25)	42.4 (8.4-73.7)	0.57
CD146+	6.85 (1.0-12.65)	5.9 (0.1-12.1)	0.94
CD202b+	13.65 (3.75-23.55)	17.63 (9.3-24.1)	1.0

established the trend to increase TNF-α, Epo, PDGF-AB and IGF-1production by BM-MNCs after pre-treatment with Epo (Table 5). Whereas, levels of IL-1β, IL-8, IL-10 and TGF -β1 production by BM-MNCs pre-treated with Epo did not change. Also, we did not establish significant differences between the basal levels of cytokines production by BM-MNCs and by BM-MNCs cultured in the presence of Epo ($p>0.05$). Conditioned media from BM-MNCs cultured with or without Epo stimulated vessel-like structures formation (Table 6). In the presence of CM from pre-treated with Epo BM-MNCs we observed increased wound healing (Figure 1) and tend to increase vessel-like structures formation (Figure 2).

Table 4 | Effect of short-term preconditioning of the bone marrow mononuclear cells on proliferative activities. Эффект краткосрочной экспозиции КМ-МНК с эритропоэтином на пролиферацию

Parameters	*Basal*	*Epo -conditioning*	*p-value*
Spontaneous	0.66 (0.58-0.68)	0.45 (0.4-0.45)	0.00072
Concanavalin A (10 μg/mL)	0.57 (0.56-0.6)	0.42 (0.36-0.46)	0.011384
Phytogemagglutinin A (10 μg/mL)	0.61 (0.6-0.67)	0.44 (0.37-0.46)	0.000083
Lipopolysaccharide (10 μg/mL)	0.69 (0.66-0.7)	0.49 (0.44-0.51)	0.00057
Hydrogen peroxide 1 μM	0.65 (0.57-0,76)	0.34 (0.32-0.36)	0.0000001
Hydrogen peroxide 3 μM	0.55 (0.51-0.57)	0.35 (0.3-0.42)	0.000541
Hydrogen peroxide 5 μM	0.48 (0.48-0.57)	0.37 (0.34-0.38)	0.048652
Erythropoietin (33.4 IU/mL)	0.69 (0.57-0.82)	0.5 (0.49-0.54)	0.006027

3.2. Efficacy of intramyocardial administration of autologous bone marrow mononuclear cells pre-treated with Erythropoietin

Six months after treatment, the severity of angina and heart failure based on NYHA FC significantly reduced in BM-MNCs group than in control group (0 ± 0 vs 1.6 ± 0.1, $p=0.01$). 12 months after surgery angina and heart insufficiency were at the same levels. Additionally, in BM-MNCs group we observed the increase in exercise tolerance from 321 m (285 – 385 m) to 356.5 m (325 – 420 m) during the 6 minutes walking test, and reduced Borg dyspnea scale

Table 5 | Effect of Erythropoietin on the cytokines production by bone marrow mononuclear cells. Эффект эритропоэтина на уровни продукции цитокинов КМ-МНК

Cytokine	*Basal (1)*	*Epo in culture media (2)*	*Epo -conditioning (3)*	*p-value (1-2/1-3)*
IL-1β	22.3 (12.3-51.2)	34.25 (2.67-67.95)	26.8 (0.15-40.2)	0.93/0.54
TNF-α	7.04 (1.31-21.85)	7.9 (2.54-22.85)	10.3 (0.42-369.7)	0.97/0.69
IL-6	1615 (1208-1743)	1651 (1208.5-1776)	1560 (824-1666)	0.85/0.25
IL-8	1260 (1225-1320)	1270 (1164-1353)	1268 (1218-1280)	1.0/0.9
IL-10	164.15 (13.95-269)	62 (12.7-193.7)	13.9 (4.84-57)	0.65/0.39
Epo	240.9 (46.8-650.25)	843.7 (557.7-848.65)	561 (180.9-822.4)	0.07/0.06
PDGF-AB	97.5 (76,8-153.1)	95.4 (65.5-736.8)	66.8 (46.8-1240)	0.95/0.32
IGF-1	0.18 (0.15-0.21)	0.23 (0.18-0.28)	0.22 (0.16-0.25)	0.13/0.43
TGF-β1	7.7 (2.73-31.4)	2.36 (1.52-4.94)	5.7 (2.04021.2)	0.09/0.17
NO	1.1 (1-1.2)	1.05 (0.95-1.2)	1 (0.5-1.20	0.92/0.41

Table 6 | Effect of conditioned media from bone marrow mononuclear cells on vessel formation in vitro. Эффект кондиционных сред от КМ-МНК на формирование сосудисто-подобных структур

Hours	*Basal*	*Epo -conditioning*	*p-value*
Vessel length			
On 3 hours	20.58 (17.77-25.35)	19.78 (18.24-22.9)	0.849995
On 24 hours	43.3 (34.97-45.91)	41.43 (35.21-49.46)	0.969827
Vessel width			
On 3 hours	12,81 (10.05-16.98)	13.18 (12.02-14.08)	0.849995
On 24 hours	32.09 (27.24-33.53)	30.22 (23.94-38.31)	0.909654

the 6 minutes walking test, and reduced Borg dyspnea scale from 2 (2 -3) to 1 (0 -1). In BM-MNCs group we detected a slight decreased stable perfusion defects, reflecting irreversible scarring of the myocardium and partially hibernating myocardium, (7.9 ± 5.1% vs 7.4 ± 3.9% in control group and BM-MNCs group respectively). Intramyocardial implantation of BM-MNCs pre-treated with Epo additional to CABG increased left ventricule contractility (LVEDV 91 ± 45 mL and LVEF 63 ± 28% in control group vs LVEDV 83 ± 34 mL and LVEF 65 ± 25% in BM-MNCs group). There was an inversed correlation between the number of CD45+/EpoR+, the number of CD34+/EpoR+ cells, and NYHA (R=-0.49 and R=-0.43, p ≤0.05).

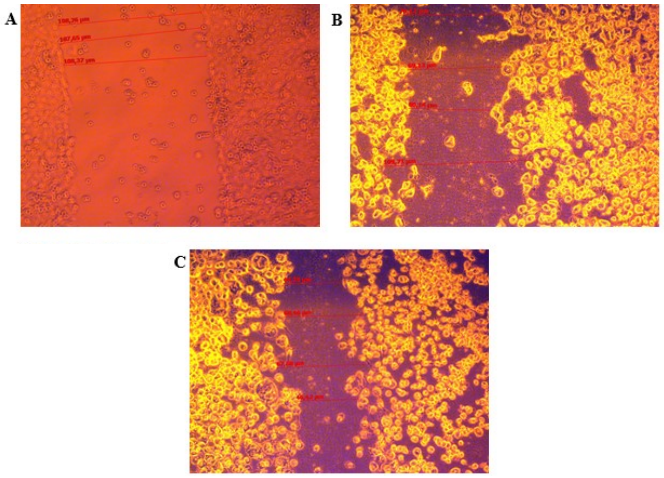

Figure 1 | Effect of condition media from BM-MNCs treated with Erythropoietin on EA.hy 929 wound healing. a, micrograph of a wound closure in media without growth factors at 24 hours (negative control). b, micrograph of a wound closure in media with 10% FSC at 24 hours (positive control). c, micrograph of a wound closure in media with 30% (v/v) conditioned media from Erythropoietin treated BM-MNCs at 24 hours. Эффект кондиционной среды от КМ-МНК проинкубированных с эритропоэтином на заживление раневого дефекта монослоя клеток EA.hy 929. a – закрытие раневого дефекта через 24 часа в культуральной среде без ростовых факторов (отрицательный контроль). b – закрытие раневого дефекта в присутствие 10% ЭТС через 24 часа (положительный контроль). c – закрытие раневого дефекта в присутствие 30% от объема кондиционной среды от КМ-МНК проинкубированных с эритропоэтином через 24 часа

4. Discussion

Ischemic heart failure (IHF) is an important cause of morbidity and mortality (13). The main reason of IHF development is myocardium infarction, because of the structural remodeling of a myocardium associated with inflammation, formation of scar, and development of interstitial fibrosis in peri-infarct zone, with the remodeling of blood supply of a myocardium (4). Bone marrow mononuclear cells contain EPCs and MSCs valuable in stem cell therapy for enhanced postischemic neovascularization (15, 18). Numerous clinical trials have previously investigated the clinical outcomes in patients after myocardium infarction and reported significant efficacy in improving contractility and reducing infarction scar (4, 13, 15, 18-19, 21). But the problem was in the limited efficacy: the improvement of left-ventricular ejection fraction and the reduction of infarction size, the viability of stem cells. Under this situation, precondition of the adult stem cells before implantation would be a very feasible and safe way to augment the therapeutic efficacy. Epo, cytokine that controls erythropoiesis, appears to have pleiotropic effects, such as

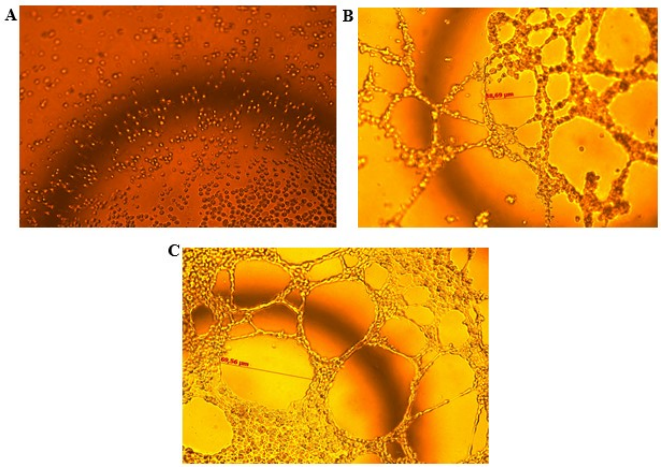

Figure 2 | Effect of condition media from BM-MNCs treated with Erythropoietin on EA.hy 929 vessel-like formation. A, - micrograph of a vessel-like formation by EA.hy 929 at 0 hour. B, - micrograph of a vessel-like formation by EA.hy 929 in presence of 30% (v/v) conditioned media from BM-MNCs with Erythropoietin 0 IU/mL at 24 hours (negative control). c, - micrograph of a vessel-like formation by EA.hy 929 in presence of 30% (v/v) conditioned media from BM-MNCs with Erythropoietin 33.4 IU/mL at 24 hours. Эффект кондиционной среды от КМ-МНК проинкубированных с эритропоэтином на формирование сосудисто-подобных структур клетками EA.hy 929. a – исходная картина (0 часов). b – формирование сосудистых образований клетками EA.hy 929 в присутствии 30% от объема кондиционной среды от КМ-МНК проинкубированных с 0 МЕ/мл эритропоэтина через 24 часа (отрицательный контроль). c – сосудо-образование клетками EA.hy 929 в присутствии 30% от объема кондиционной среды от КМ-МНК проинкубированных с 33,4 МЕ/мл эритропоэтина через 24 часа

anti-ischemic and anti-apoptotic properties, promotion of neovascularization, mobilization of EPCs, and enhancement of angiogenesis (22). This article presents the results of 6-12 months follow-up of patients who underwent coronary bypass surgery and transmyocardial laser revascularization, combined with implantation of autologous bone marrow mononuclear cells short-term pre-treated with Epo. We analyzed effect of short-term pre-treatment BM-MNCs with Epo on morphofunctional properties in vitro, and the clinical status of the patients, the dynamics of myocardium contractility, and local contractility of the left ventricule on echocardiography, as well as myocardium perfusion changes. Through this study we have showed the beneficial effect of in vitro Epo treatment to increase the vasculogenic potential of human bone marrow stem cells. First of all, we established that in bone marrow of patients with CAD there are three main stem cells populations (HSC, EPCs and MSCs). Moreover, BM-MNCs presented a higher number of 'early', and a lower number of 'late' EPCs (CD34-/CD133+, and CD34+/CD133- cells, respectively). Also, in BM-MNCs from patients with CAD there are 'mature' EPCs (CD34+/KDR+, and CD34+/CD31+ cells). Moreover, BM-MNCs from patients with CAD is characterized as a high proliferating cells, because 12% of CD34+ cells are in G2/M phase of cell cycle and spontaneous proliferation measured by MTT test was OD=0.66. Moreover, we observed that among CD34+ BM-MNCs there is very low number of apoptotic cells.

Ahmed and coworkers (2015), also Hur and coworkers (2004) demonstrated that EPCs expressed CD34 or VEGFR-2(KDR), and EPCs, which carried both surface markers (CD34+/KDR+ EPCs) is an independent predictor of clinical performance at cardiovascular pathology (23-24). About 1% of BM-MNCs were positive for EpoR and these cells were used to evaluate the specific effects of Epo treatment through its receptor. Epo treated BM-MNCs show the increase in HSCs bearing EpoR (increased in a 6.87-fold). Epo treatment also induced CD34+/CD133+ - EPCs decrease (on 30%) and increase CD31+/CD184+ ("homing-receptor") - EPCs (in a 5-fold). Epo treatment also leads to accumulation of CD34+ cells in G0G1 phase of cell cycle (on 8.97%). Epo treated BM-MNCs produced angiogenic factors, because addition of 30% (v/v) of the conditioned media from Epo treated BM-MNCs augment capillary-like structure formation by EA.hy 929, hybridoma cell line with a "mature" EPCs phenotype properties. Bone marrow cells can migrate from niches into blood stream through "homing" involve CXCR-4 (CD184), a specific receptor for the SDF-1/CXCL12, and CD144 to engraftment onto target organs, including ischemic tissues (25). The results of presented study show that a large number of HSCs and EPCs expressed CD184.

Moreover, Epo treatment of BM-MNCs increased a count of EPCs co-expressed CD31 and CD184 surface markers. It is well known, that EpoR is expressed on surface not only of erythroid progenitor cells, but also on other type of cells [16-19]. Epo maintains survival of different types of cells through interaction with EpoR (26). Epo binding with EpoR alone or in cooperation with CD131 leads to cytoprotective effect (27). Bennis and coworkers (2012) demonstrated that Epo in dosage of 5 IU/mL stimulates proliferative potential, migration, tubule-formation capacity, closure of wound made in monolayer of EPCs, and increased resistance of EPCs to oxidation stress (27). The unfavorable microenvironment present in the ischemic tissue might impair the effectiveness of stem cell transplantation. Additionally, the results of presented study shown that Epo treatment of BM-MNCs prevent cells from oxidative stress (proliferative activity of Epo treated BM-MNCs in the presence of H_2O_2). Kang and coworkers (2014) demonstrated that treatment of bone marrow stem cells with Epo increased the expression of pro-angiogenic factors, including IL-8, and IL-10, and b-FGF, and PDGF, and MMP -9, and levels of adhesion molecule such as integrin (28). Taken together, the presented study demonstrated that Epo has the potential to augment regenerative effect of BM-MNCs. CABG is preferred method for treatment of patients with ischemic heart disease, but sometimes coronary vessel diameter is insufficient for direct myocardium revascularization. Laser channels accompanied with stem cells implantation can improve the quality of life in patients with ischemic heart disease. Our data indicates that laser indirect revascularization with BM-MNCs pre-treated with Epo improves NYHA FC, exercise tolerance, dyspnea, and left ventricule contractility. Intramyocardial implantation of stem cells is used for restoring of ischemic myocardium microvasculature. There are no publications on pre-treated BM-MNCs with Epo and laser revascularization. It's known that pre-treatment with Epo of the organ injured and dysfunctionalized by hemorrhagic shock exerts tissue-protective effect as a result of mobilization of bone marrow endothelial progenitor cells (29). In animal model of myocardium infarction therapy with Epo and Granulocyte colony stimulating factor stabilized LVEF and improved LVEDV, and histopathology revealed increased areas of viable myocardium and vascular density (30). Authors evaluated therapeutic efficiency on animal model after systemic administration of Epo. But there is no information on the effect of the pre-treatment of bone marrow mononuclear cells with Epo and its implantation on laser channels into ischemic myocardium in human yet. Currently, in this article we have not studied enough patients, and so the results are contradictory. The small sample size, the number of BM-MNCs necessary for implantation, survival rate of implanted BM-MNCs do not allow to conclude that the pre-treatment with Epo BM-MNCs is really effective. Also, the effect of laser exposure on myocardium is not studied yet. We believe that our results suggest a cumulative effect of laser revascularization and short-term pre-treatment of bone marrow mononuclear cells, and they will improve the surgical treatment results of coronary arteria disease in the near period.

5. Concluding Remarks

Summarizing all the above, we can conclude that the short -term pre-treatment of bone marrow mononuclear cells with Epo increased count of EPCs with CD31+/CD184+ phenotype, increased a count of CD34+ cells in G0G1 phase of cell cycle, increased vasculogenic effect of conditioned media from Epo treated BM-MNCs on tube formation by EA.hy 929. Also, direct revascularization and combination of direct and indirect (laser channels) revascularization with Epo pre-treated bone marrow mononuclear cells implantation of the ischemic myocardium leads to myocardium perfusion improvement, and left ventricular contractility. Myocardial perfusion improvements at the early period after surgery is a result of direct revascularization, whereas at the long-term period it is a result of angiogenesis and vasculogenesis in the hibernate area, and the reduction of perfusion defects due to BM-MNCs implantation in laser channels. These findings strongly suggest that in vitro Epo treatment of BM-MNCs can be a feasible and effective method to augment the efficacy of BM-MNCs stem cells therapy for patients with CAD

Заключение

Показано, что кратковременная экспозиция костномозговых мононуклеаров с эритропоэтином способствует увеличению количества пула эндотелиальных прогениторных клеток с фенотипом CD31+/CD184+, количества CD34+ клеток в фазе G0G1 клеточного цикла и возрастанию васкулогенного потенциала кондиционных сред костномозговых мононуклеаров, предобработанных с эритропоэтином в модели in vitro образования сосудисто-подобных структур эндотелиальными клетками EA.hy 929. Кроме этого, прямая реваскуляризация и сочетание с прямой и непрямой (лазерные каналы) реваскуляризации, обусловленной имплантацией эритропоэтин предобработанных костномозговых мононуклеаров в ишемизированный миокард ведет к улучшению перфузии миокарда и сократимость левого желудочка. Параметры перфузии миокарда на ранние сроки после хирургического вмешательства являются следствием прямой реваскуляризации миокарда, тогда как на более поздних сроках наблюдения это следствие ангио- и васкулогенеза в гибернированной области миокарда, а также ответом на имплантацию костномозговых мононуклеаров в лазерные каналы. Полученные данные, указывают, что in vitro предобработка костномозговых мононуклеаров безопасный и эффективный способ увеличения терапевтического потенциала клеточной терапии стволовыми клетками больных с ишемической болезнью сердца

Acknowledgements

The study was funded by a Russian Scientific Foundation grant (project no. 16-15-00057).

Author Contribution

This work was carried out in equivalent collaboration of all authors.

References

[1] Cook MM, Kollar K, Brooke GP, Atkonson K. Cellular therapy for repair of cardiac damage after acute myocardial infarction. International Journal Cell Biology. 2009; 2009: 906507. DOI doi:10.1155/2009/906507.

[2] Roth GA, Forouzanfar MH, Moran AE, Barber R, Nguyen G, Feigin VL, et al. Demographic and epidemiologic drivers of global cardiovascular mortality. The New England Journal of Medicine. 2015; 372(14): 1333-1341.

[3] Liang J, Huang W, Yu X, Ashraf A, Wary KK, Xu M, et al. Suicide gene reveals the myocardial neovascularization role of mesenchymal stem cells over expressing CXCR4 (MSCCXCR4). PLoS ONE. 2012; 7(9): e46158. DOI: 10.1371/journal.pone.0046158.

[4] Park JH, Yoon JY, Ko SM, Jin SA, Kim JH, Cho CH, et al. Endothelial progenitor cell transplantation decreases lymphangiogenesis and adverse myocardial remodeling in a mouse model of acute myocardial infarction. Experimental Molecular Medicine. 2011; 43(8): 479-485.

[5] Pavo IJ, Michel-Behnke I. Clinical cardiac regenerative studies in children. World Journal of Cardiology. 2017; 9(2): 147-153.

[6] Rupp S, Jux C, Bonig H, Bauer J, Tonn T, Seifried E, et al. Intracoronary bone marrow cell application for terminal heart failure in children. Cardiology of Young. 2012; 22(5): 558-563.

[7] Ambastha C, Bittle GJ, Morales D, Parchment N, Saha P, Mishra R, et al. Regenerative medicine therapy for single ventricule congenital heart disease. Translational Pediatrics. 2018; 7(2): 176-187.

[8] Ayala-Cuellar AP, Kang JH, Jeung EB, Choi KC. Roles of Mesenchymal Stem Cells in Tissue Regeneration and Immunomodulation. Biomolecular Therapy. 2018; DOI: 10.4062/biomolther.2017.260.

[9] Charwat S, Lang I, Dettke M, Graf S, Nyolczas N, Hemetsberger R, et al. Effect of intramyocardial delivery of autologous bone marrow mononuclear stem cells on the regional myocardial perfusion. NOGA-guided subanalysis of the MYSTAR prospective randomised study. Thrombosis and Haemostasis. 2010; 103(3): 564-571.

[10] Tabatabaei Qomi R, Sheykhhasan M. Adipose-derived stromal cell in regenerative medicine: A review. World Journal of Stem Cells. 2017; 9(8): 107-117.

[11] Bartunek J, Davison B, Sherman W, Povsic T, Henry TD, Gersh B, et al. Congestive Heart Failure Cardiopoietic Regenerative Therapy (CHART-1) trial design. European Journal of Heart Failure. 2016; 18: 160–168.

[12] Collantes M, Pelacho B, Gracia-Velloso MJ, Gavira JJ, Abizanda G, Palacios I, et al. Non‐invasive in vivo imaging of cardiac stem/progenitor cell biodistribution and retention after intracoronary and intramyocardial delivery in a swine model of chronic ischemia reperfusion injury. Journal of

Translational Medicine. 2017; 15: 56. DOI: 10.1186/s12967-017-1157-0.

[13] Fisher SA, Doree C, Brunskill SJ, Mathur A, Martin-Rendon E. Bone Marrow Stem Cell Treatment for Ischemic Heart Disease in Patients with No Option of Revascularization: A Systematic Review and Meta-Analysis. PLoS ONE. 2013; 8(6): e64669. https://doi.org/10.1371/journal.pone.006.

[14] Henry TD, Schaer GL, Traverse JH, Povsic TJ, Davidson C, Lee JS, et al. Autologous CD34+ Cell Therapy for Refractory Angina: 2-Year Outcomes from the ACT34-CMI Study. Cell Transplantation. 2016; 25: 1701–1711.

[15] Kandala J, Upadhyay GA, Pokushalov E, Wu S, Drachman DE, Singh JP. Meta-analysis of stem cell therapy in chronic ischemic cardiomyopathy. American Journal of Cardiology. 2013; 112(2): 217-225.

[16] Kastrup J, Schou M, Gustafsson I, Nielsen OW, Mogelvang R, Kofoed K., et al. Rationale and Design of the First Double-Blind, Placebo-Controlled Trial with Allogeneic Adipose Tissue-Derived Stromal Cell Therapy in Patients with Ischemic Heart Failure: A Phase II Danish Multicentre Study. Stem Cells International. 2017; https://doi.org/10.1155/2017/8506370.

[17] Mozid A, Yeo C, Arnous S, Ako E, Saunders N, Locca D, et al. Safety and feasibility of intramyocardial versus intracoronary delivery of autologous cell therapy in advanced heart failure: the REGENERATE-IHD pilot study. Regenerative Medicine. 2014; 9(3): 269–278.

[18] Seurder D, Radrizzani M, Turchetto L, Lo Cicero V, Soncin S, Muzzarelli S, et al. Combined Delivery of Bone Marrow-Derived Mononuclear Cells in Chronic Ischemic Heart Disease: Rationale and Study Design. Clinical Cardiology. 2013; 36(8): 435-441.

[19] Vrtovec B, Poglajen G, Haddad F. Stem cell therapy in patients with heart failure. Methodist Debakey Cardiovascular Journal. 2013; 9(1): 6-10.

[20] Tian T, Chen B, Xiao Y, Yang K, Zhou X. Intramyocardial autologous bone marrow cell transplantation for ischemic heart disease: A systematic review and meta-analysis of randomized controlled trials. Atherosclerosis. 2014; 233: 485-492.

[21] Cogle CR, Wise E, Meacham AM, Zierold C, Traverse JH, Henry TD, et al. Detailed analysis of bone marrow from patients with ischemic heart disease and left ventricular dysfunction: BM CD34, CD11b, and clonogenic capacity as biomarkers for clinical outcomes. Circulation Research. 2014; 115(10): 867-874.

[22] Tsai TH, Lu CH, Wallace CG, Chang WN, Chen SF, Huang CR, et al. Erythropoietin improves long-term neurological outcome in acute ischemic stroke patients: a randomized, prospective, placebo-controlled clinical trial. Critical Care. 2015; 19: 49. https://doi.org/10.1186/s13054-015-0761-8.

[23] Ahmed SH, Sabry D, Noh O, Samir M. Potential proliferative effect of lipopolysaccharide preconditioning on human umbilical blood-derived endothelial cells. African Journal of Biotechnology. 2015; 14(13): 1167-1173.

[24] Hur J, Yoon CH, Kim HS, Choi JH, Kang HJ, Hwang KK, et al. Characterization of Two Types of Endothelial Progenitor Cells and Their Different Contributions to Neovasculogenesis. Arteriosclerosis Thrombosis, and Vascular Biology. 2004; 24: 288-293.

[25] Hristov M, Zernecke A, Bidzhekov K, Liehn EA, Shagdarsuren E, Ludwig A, et al. Importance of CXC chemokine receptor 2 in the homing of human peripheral blood endothelial progenitor cells to sites of arterial injury. Circulation Research. 2007; 100(4): 590-597.

[26] Beleslin-Cokic BB, Cokic VP, Yu X, Weksler BB, Schechter AN, Noguchi CT. Erythropoietin and hypoxia stimulate erythropoietin receptor and nitric oxide production by endothelial cells. Blood. 2004; 104: 2073-2080.

[27] Bennis Y, Sarlon-Bartoli G, Guillet B, Lucas L, Pellegrini L, Velly L, et al. Priming of late endothelial progenitor cells with erythropoietin before transplantation requires the CD131 receptor subunit and enhances their angiogenic potential. Journal of Thrombosis and Haemostasis. 2012; 10(9): 1914-1928.

[28] Kang J, Yun JY, Hur J, Kang JA, Choi JI, Ko SB, et al. Erythropoietin priming improves the vasculogenic potential of G-CSF mobilized human peripheral blood mononuclear cells. Cardiovascular Research. 2014; 104(1): 171-182.

[29] Nandra KK, Collin M, Rogazzo M, Fantozzi R, Patel NS, Thiemermann C. Pharmacological preconditioning with erythropoietin attenuates the organ injury and dysfunction induced in a rat model of hemorrhagic shock. Disease Model and Mechanisms. 2013; 6(3): 701-709.

[30] Angeli FS, Amabile N, Shapiro M, Mirsky R, Bartlett L, Zhang Y, et al. Cytokine combination therapy with erythropoietin and granulocyte colony stimulating factor in a porcine model of acute myocardial infarction. Cardiovascular drug and therapy. 2010; 24(5-6): 409-420

JOURNAL OF INTEGRATED OMICS
A METHODOLOGICAL JOURNAL
HTTP://WWW.JIOMICS.COM

ORIGINAL ARTICLE | DOI: 10.5584/jiomics.v9i1.260

The role of metallothioneins in the maintance of zinc homeostasis and redox state in erythrocytes of cardiologic patients with the metabolic disorders

Y.M. Harmaza *, A.V. Tamashevski, E.I. Slobozhanina

Institute of Biophysics and Cell Engineering of National Academy of Sciences, 220072 Minsk, Akademicheskaya st.27, Belarus

Received: 18 October 2018 **Accepted:** 31 Decemeber 2018 **Available Online**: 08 March 2019

ABSTRACT

The comparative analysis of the intracellular labile zinc pool, level of the reduced glutathione and cystein-rich proteins metallothioneins considering the viability of erythrocytes was conducted in patients suffered from coronary heart disease with diagnosed arterial hypertension and type 2 diabetes mellitus. Fluorescent probes (FluoZin-3-AM and Calcein-AM), Ellman's reagent and monoclonal antibody (anti-metallothionein UC1MT) have been used. The obtained results demonstrated an important role of zinc homeostasis (decrease in cytosolic Zn^{2+} level) in the etiopathogenesis of type 2 diabetes mellitus and in the development of metabolic syndrome in general. Increasing metallothioneins expression in erythrocytes of evaluated patients implied its functioning as an additional antioxidant in human erythrocytes defense system in this pathology. The present data show that these proteins could be selected as a target for some antioxidant treatment strategies for CHD patients with metabolic disorders.

Аннотация

Проведен сравнительный анализ внутриклеточного пула ионов цинка, содержания восстановленного глутатиона и цистеин-обогащенных белков металлотионеинов с учетом жизнеспособности эритроцитов у пациентов с диагностированной артериальной гипертензией и сахарным диабетом 2 типа на фоне ишемической болезни сердца. В работе использованы флуоресцентные зонды (FluoZin-3-AM и Calcein-AM), реактив Эллмана и моноклональные антитела (анти-металлотионеин UC1MT). Полученные результаты демонстрируют важную роль цинкового гомеостаза (снижение цитозольного уровня Zn^{2+}) в этиопатогенезе сахарного диабета 2 типа и развитии метаболических нарушений в целом. Увеличение уровня металлотионеинов в эритроцитах исследуемых пациентов свидетельствует о функционировании данных белков в качестве дополнительной антиоксидантной защитной системы эритроцитов человека при данной патологии. Полученные результаты демонстрируют, что эти белки могут быть выбраны в качестве мишени при назначении терапии кардиологическим пациентам с метаболическими нарушениями

Keywords: Metallothioneins, Labile zinc pool, Reduced glutathione, Erythrocytes, Type 2 diabetes mellitus, Coronary heart disease.

1. Introduction

Zinc (Zn^{2+}) is an essential trace element that controls the processes of proliferation, differentiation and cell death. It can mimic the action of hormones, growth factors, cytokines, thereby acting as a "signal molecule" [1]. At the end of 2010, the Protein Data Bank (PDB) contained 6170 structures of zinc-binding proteins but only 4882 are to be considered as true zinc proteins (they bind at least one Zn^{2+} with a physiological role). Over half of the true zinc proteins in the PDB (i.e., 2759 proteins) are enzymes, with most of the others being zinc finger proteins [2]. Currently there are already 14410 entries in PDB that contain Zn2+ cations. In metalloenzymes, zinc has three main functions: the involvement in catalysis, the maintenance of structural stability and the regulation of the cellular processes [3]. Knowledge about the proteins that control cellular zinc provides a basis for understanding how Zn^{2+} can regulate cellular processes.

Physiological concentration of zinc in human serum is

***Corresponding author:** Harmaza Yuliya, PhD.(Biol.), Senior Researcher in the Laboratory of Medical Biophysics, Institute of Biophysics and Cell Engineering of National Academy of Sciences of Belarus, 220072, Minsk, Akademicheskaya st. 27, Belarus. E-mail: garmaza@yandex.ru; tel. +375172842633 .

about 2-15 μM, while its intracellular content is extremely low (~ 1 nM) [4]. The intracellular Zn^{2+} pool is controlled via the expression and the functioning of 14 zinc importers (ZIPs / SLC39s), 10 zinc exporters (ZnTs / SLC30s) and Zn-binding proteins such as metallothioneins (MTs) [1, 4, 5]. Zrt- and Irt-like (zinc and iron regulated transporter) proteins (ZIPs) are also named solute carrier family 39 (SLC39) A1–A14, while members of the zinc transporter (ZnT) family are denoted to SLC30A1–A10. A few of these transporters have an additional role in Mn^{2+} and Fe^{2+} transport, while MTs also have a function in Cu^{2+} metabolism [4]. Most of the ZIP and ZnT transporters are located in the plasma membrane, but others – in mitochondrial, Golgi network, lysosomal and vesicular or endoplasmic reticulum membranes [1, 4].

MTs are the family of intracellular cysteine-rich, low molecular weight (6–7 kDa) metal-binding proteins. They have a single peptide chain containing 61–68 amino acids, 20 of them are cysteines distributed in two domains α and β-clusters, and they bind in total 7 ions of divalent metals [6]. The single polypeptide chain of MT has the structure Cys-X-Cys, Cys-XY-Cys, and Cys-Cys where X and Y represent noncysteine amino acids; the stoichiometric form of the protein shows 7 ions for each 20 cysteines forming metal-thiolate complexes [6, 7, 8]. MT binds to metals through a thiol group (SH) found in cysteine residues; the metal-free protein named as apo-metallothionein (Apo-MT) or thionein. Four isoforms of MTs – I, II, III and IV were discovered. MT-I and MT-II which are the major isoforms found in the most tissues, whereas MT-III and MT-IV have cell type-specific expression [7]. Traditionally, MTs have been considered as an intracellular proteins which are localized in the cytoplasm and can also be found in the nucleus upon translocation; however, more recent reports suggest that MT can be localized in a variety of extracellular spaces [9]. MTs are involved in many physiological and pathophysiological processes such as intracellular storage, transport and metabolism of metal ions, whereas in vivo they regulate essential trace metal homeostasis such as zinc and copper and play a protective role in heavy metal detoxification reactions such as cadmium and mercury [6]. However, under physiological conditions MTs have high binding affinity exactly to Zn^{2+} and play a significant role in maintaining its stable intracellular availability through sequestration or release of zinc ions. Intracellular Zn^{2+} is strictly regulated by binding to MTs via compartmentalization through the activities of ZnT [1]. When intracellular Zn^{2+} level is insufficient to stabilize the protein, the MTs are rapidly proteolyzed, so the Zn^{2+} is released by the degradation of MTs causing the intracellular Zn^{2+} to remain at a balanced concentration [10].

In addition, MTs are vital proteins in the cellular defense antioxidant system, and their protective role against reactive oxygen species (ROS) damage in biological systems has been widely reported. Different studies have shown that the thiolate ligands in cysteine residues confer the redox activity of MTs; these residues can be oxidized by cellular oxidants, and during this process zinc is released causing a decrease in lipid peroxidation levels [11]. It is known that, when oxidative stress level increases, MTs are able to scavenge a variety of ROS including hydroxyl radicals and superoxide anion, hydrogen peroxide, radicals of reactive nitrogen species, and nitric oxide radicals [12]. Compared to other antioxidants such as super oxide dismutase, catalase, glutathione peroxidase, MT could be considered as a more effective antioxidant [13]. It is known that the low-molecular weight thiol glutathione (L-g-glutamyl-L-cysteinylglycine) (GSH) is the major attribute of a redox buffer in cells because of its high cellular abundance (2–10 mM) and low redox potential of -240 mV [14]. However, it was shown that all 20 cysteine sulfur atoms of MTs are involved in the radical quenching process, and the rate constant for the reaction of hydroxyl radical with MT is about 340-fold higher than that with GSH [15].

So, MTs and two zinc transporter families – zinc importers (ZIPs / SLC39s) and zinc exporters (ZnTs / SLC30s) – control the intracellular Zn^{2+} pool and dysfunction of such complex regulatory system may lead to Zn dyshomeostasis that is associated with many pathological processes in the human organism [1, 4, 5].

Metabolic syndrome (MS) is a group of conditions that put people at risk for heart disease and diabetes. These conditions or so-called metabolic risk factors include high blood pressure, high blood glucose levels, high levels of triglycerides, low levels of high-density lipoprotein in the blood, excessive fat deposits around the waist. Diabetes mellitus (DM) is the major cause of morbidity and mortality world-wide, and also the major risk factor for early onset of coronary heart disease (CHD). Type 1 diabetes is characterized by the lack of insulin production and type 2 diabetes is characterized primarily by the resistance to insulin effects. It is known that pancreatic β cells contain large amounts of zinc which participates in the binding of insulin in hexamers [16]. Decade ago, it has been established that SLC30A8 gene, encoding zinc transporter ZnT8, is expressed exclusively in the secretory granules of the pancreatic β-cells [17], thereby playing an important role in the pathogenesis of type 2 DM, where single nucleotide polymorphism in SLC30A8, rs13266634 (Arg325Trp) has been reported [18]. Later, Rutter and Sladek et al. [19, 20] demonstrated that normal cellular zinc homeostasis is a crucial factor of the insulin release maintaining physiological glucose levels, and decreasing the behavioral risk for type 2 DM. The reduced Zn^{2+} level in atherosclerotic plaques of patients with type 2 diabetes mellitus, as well as in the blood plasma of patients with pathology under evaluation was shown [21, 22]. Zinc deficiency has also been observed in patients with metabolic syndrome [23] and arterial hypertension [24]. These results indicate that zinc is strongly associated with lipid and glucose status. It can be assumed that cellular zinc concentration could be a predictive for metabolic disorders. Singh et al. [25] concluded that lower

consumption of dietary zinc and low serum zinc levels were associated with an increased prevalence of CHD and several associated risk factors including hypertension and hypertriglyceridemia.

There are many studies [19, 26, 27] which have confirmed that type 2 DM caused by oxidative stress plays an important role in the development of cardiological disorders. At the same time, Zn dyshomeostasis (due to a change in the expression of zinc transporter ZnT8) also induces the development of oxidative stress in type 2 DM cells [1, 4, 5, 17], but MTs expression in this cell type was not investigated. Recently, it was revealed that the high urinary excretion of zinc caused the reduction in its blood plasma levels being indicative of disturbance in Zn-based antioxidant mechanism [28]. Thus, a simultaneous investigation of the parameters that characterize both cellular zinc metabolism and redox state of cardiologic patients with metabolic disorders may be useful for selecting a treatment strategy (e.g.: zinc or antioxidant supplementation) that could regulate the cellular metabolic processes.

The aim of this study is to investigate the level of expression of cystein-rich proteins metallothioneins in erythrocytes of patients suffered from coronary heart disease with the metabolic syndrome (representing arterial hypertension and type 2 diabetes mellitus) and to find out their role in the maintenance of zinc homeostasis (estimating the intracellular labile Zn^{2+} pool) and redox state (estimating the reduced glutathione concentration) under these pathological states.

It is known that when zinc compounds enter the human blood, more than 90% of Zn^{2+} accumulates in red blood cells [1]. So, human erythrocytes were used as a model system and as a potential indicator of zinc status in humans. Moreover, the absence of nuclei in mature mammalian red blood cells provides an opportunity to exclude a genotoxic effect of Zn^{2+}.

2. Material and Methods

All the chemicals in the experiment were used without further purification. FluoZin-3-AM was obtained from Molecular Probes (USA); anti-metallothionein UC1MT, anti -mouse IgG1-FITC, mouse IgG1 were obtained from Abcam (Great Britain); Calcein-AM, twin 20, paraformaldehyde, pluronic F-127, 5,5'-dithio-bis-[2-nitrobenzoic acid], bovine serum albumin (BSA) were obtained from Sigma-Aldrich (Germany); trichloroacetic acid (TCA) and all salts were obtained from “Belleschimcomplect” (Belarus).

Peripheral blood from patients with coronary heart disease (n = 18, age 59.7±2.7 years) was supplied by Republic scientific and practical Centrum "Cardiology" (Minsk, Belarus) and from healthy donors (n = 10) was supplied by Republic scientific and practical Centrum “Transfusiology and medical biotechnologies” of Ministry of Health of Belarus (Minsk, Belarus). All blood samples were in the conservative agent "citrate-Na". Erythrocytes were separated from serum by centrifugation of blood at 1500g, 15 min.

Diagnostic evaluation of CHD patients for formation of three tested groups were conducted by cardiologists of Republic scientific and practical Centrum "Cardiology" (Minsk, Belarus). The first group is CHD patients who had arterial hypertension and diabetes mellitus type 2 (Ah+DM+), the second group is CHD patients who had only arterial hypertension (Ah+DM–) and the third group is CHD patients without any diagnosed component of metabolic disorder (Ah–DM–).

Intracellular labile zinc pool ($[Zn^{2+}]i$) was assessed using fluorescent dye FluoZin-3-AM. Cells were loaded with 2 μM FluoZin-3-AM (λex/em=494/516 nm) in the presence of 0.02% Pluronic F-127 for 30 min at 37°C. Cells were washed (2000g, 10 min) and incubated for an additional 30 min at room temperature in PBS buffer (KH2PO4 – 2 mM, Na2HPO4*12H2O – 10 mM, NaCl – 137 mM, KCl – 2.7 mM, pH 7.4) with 0.3% BSA. After loading, erythrocytes were washed twice with the same solution. Then cells were analyzed by the flow cytometry at the FL-1H channel.

The concentration of reduced glutathione (GSH) in erythrocytes was estimated by Ellman’s method. For this purpose 10% TCA was added to cell suspension for 15 min at room temperature. After that cells were centrifugated (2000g, 10 min) and then 0.1 M Na-phosphate buffer pH 8.0 supplemented with 1 mM Ellman’s reagent (5.5'-dithio-bis-[2-nitrobenzoic acid]) were added to supernatant for 15 min at room temperature. Then optical density of solution was measured and GSH concentration (mM) was calculated (ε=13.6 $mM^{-1}cm^{-1}$, L=1 cm).

Metallothioneins expression level (MT-I/MT-II) was evaluated using monoclonal antibody – anti-metallothionein UC1MT. Erythrocytes suspension was fixed by 2% paraformaldehyde (60 min, t=4°C), washed (2000g, 10 min), permeabilized using 0.5% twin 20 in PBS pH 7.4 (10 min, t=4°C) and incubated with UC1MT overnight at 4°C. Then cells were rinsed in PBS (2000g, 10 min) and further incubated with secondary antibodies labeled with fluorophore – anti-mouse IgG1-FITC (dilution 1:500) for 120 min at 4°C. Mouse IgG1 was used as an isotype control that was incubated in parallel with cells as describe above. After washing in PBS a cytofluorimetric analysis was performed. Fluorescence intensity of complex: metallothioneins-UC1MT-FITC was used as a marker of these proteins expression in erythrocytes.

The viability of erythrocytes was controlled by cell esterase activity using high lipophilic dye calcein-AM – a highly lipophilic dye that rapidly enters to viable cells, where it is converted by intracellular esterases to its deesterified form Calcein with an intense green emission (CAL, λex/ em=496/516 nm). It should be noted that Calcein is retained by cells with intact plasma membrane [29]. Erythrocytes were loaded with 5 μM Calcein-AM in PBS for 40 min at 37° C. After cells were washed (2000g, 10 min) and analyzed by flow cytometry at the FL-1H channel.

Cytofluorimetric analysis was performed on flow cytometer FACSCanto II (Beckton Dickenson) and spectrophotometric analysis – on the Specord M-40 spectrophotometer.

Statistical analysis of experimental results was carried out using non-parametric Mann–Whitney U test and Spearman test. Data were expressed as mean ± SEM. The results were considered statistically significant at $p<0.05$. Statistical analysis program (STATISTICA, version 8.0) was used for evaluations.

3. Results and discussion

At the first stage, the cytofluorimetric study of the intracellular level of labile zinc pool in erythrocytes of patient's blood samples was carried out. We have used a recently developed fluorimetric probe (FluoZin-3) with high affinity to Zn^{2+} (Kd=15 nM) and low affinity to Ca^{2+} or Mg^{2+} [30]. FluoZin-3 is particularly sensitive to changes in zinc concentration because of the high ratio between the fluorescence of the probe saturated with Zn^{2+} and that in its absences [31]. A significant decrease (on 15–20%) of the intracellular zinc level in red blood cells of CHD patients with presenting arterial hypertension and type 2 diabetes mellitus ($Ah^{+}DM^{+}$) in comparison to the last one in healthy donors was established (Figure 1A). But it was revealed that there is only a tendency to reduction of the cytoplasmic zinc pool in groups of CHD patients without diagnosed type 2 diabetes mellitus ($Ah^{+}DM^{-}$) and without both signs of metabolic disorders ($Ah^{-}DM^{-}$) (Figure 1A).

As mentioned above, type 2 diabetes mellitus mediated the changes in redox state behavior in blood cells [19, 26, 27]. Therefore, in our previous study, the alterations in intracellular zinc ions pool of erythrocytes and activation of the programmed cell death process under H_2O_2-induced oxidative stress in vitro were found [32]. So, in order to avoid the experimental artifacts associated with cell death, it is necessary to take into account their viability when evaluating the intracellular Zn^{2+} pool.

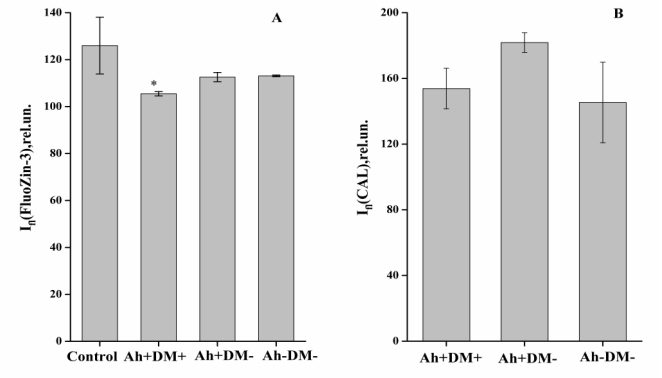

Figure 1 | Fluorescence intensity of FluoZin-3 (A) and Calcein (B) incorporated into erythrocytes of donors (Control) and patients with coronary heart disease ($Ah^{+}DM^{+}$, $Ah^{+}DM^{-}$, $Ah^{-}DM^{-}$); * – $p<0.05$ compared to control. Интенсивность флуоресценции FluoZin-3 (А) и Кальцеина (Б), встроенного в эритроциты доноров (контроль) и пациентов с ишемической болезнью сердца ($АГ^{+}СД^{+}$, $АГ^{+}СД^{-}$, $АГ^{-}СД^{-}$). * – $p<0.05$ по сравнению с контролем

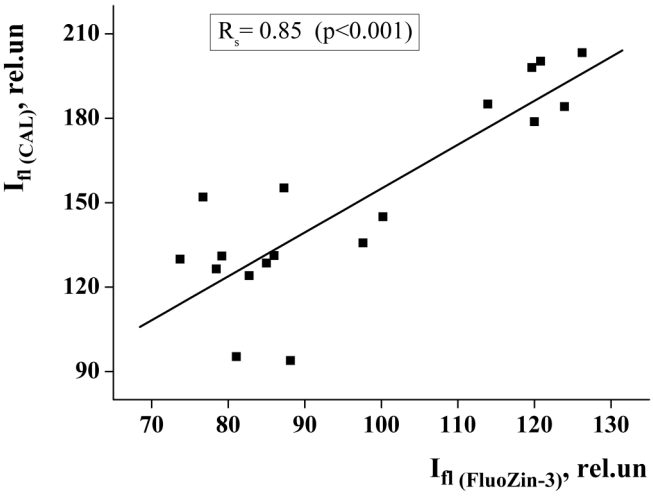

Figure 2 | Correlation between values of FluoZin-3 fluorescence intensity and Calcein fluorescence intensity in erythrocytes of patients with coronary heart disease where Ifl – fluorescence intensity; CAL – desterified form of calcein. Корреляционная связь между значениями интенсивности флуоресценции FluoZin-3 и кальцеина в эритроцитах пациентов с ишемической болезнью сердца, где, Iфл – интенсивность флуоресценции; CAL – деэстерифицированная форма кальцеина

Additionally a comparative evaluation of the erythrocytes esterase activity (a marker of their viability) using Calcein-AM in the tested groups of patients with coronary heart disease was conducted. This methodology is based on the ability of living cells to hydrolyze calcein-acetoxymethyl ester by intracellular esterases and on the association of Calcein-AM hydrolysis rates with a specific cell status (e.g. pre-apoptotic stage), both in physiological and pathological conditions [29]. However, we did not reveal the significant difference in the fluorescence of Calcein for tested cells (Figure 1B). But, the viability of erythrocytes in CHD patients was slightly reduced in comparison to donors' cells. Based on the correlation analysis (positive correlation parameters were approximately Rs=0.85, p=0.001), we found that values of fluorescence intensity for FluoZin-3 (characterizing the cytosolic labile zinc ions level) and Calcein (characterizing cell viability) correspond to CHD patients of the third tested groups (Figure 2). These results may help to predict the risk of involvement of Zn dyshomeostasis in activation of apoptotic process in cells of CHD patients.

It worth to notice that decrease of erythrocytes viability under modification of zinc homeostasis enables us to assume the crucial role of these processes in the etiology and pathogenesis of metabolic disorders in general and of type 2 diabetes mellitus in particular.

Previously, it was established that among the pathogenetic mechanisms underlying some metabolic and endocrine diseases, the relationship between the alteration of Zn^{2+} level

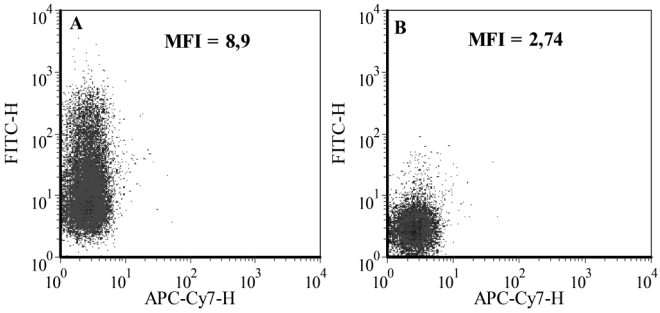

Figure 3 | Representative diagrams of distribution of UC1MT-IgG1-FITC fluorescence intensity (A) and IgG1-FITC fluorescence intensity (B) in the total population of donor's erythrocytes where MFI – mean fluorescence intensity. Репрезентативные диаграммы распределения интенсивности флуоресценции комплексов UC1MT–IgG1–FITC (А) и IgG1–FITC (Б) в суммарной популяции эритроцитов донора где, MFI – значение интенсивности флуоресценции комплексов.

and activation of free radical processes is of particular importance due to disturbance of glutathione homeostasis and cellular cascade of reactions dependent on NFκβ [26]. Moreover, Zn^{2+} is an important regulator of GSH synthesis. The importance of zinc in the metabolism of glutathione underscores the finding that in many studies a decrease of reduced glutathione under zinc deficiency conditions was revealed [33, 34]. Therefore, in the next step, the content of GSH, as the main cellular antioxidant, in erythrocytes was evaluated. Its significant reduction (2–2.8-fold) was found in all tested groups of CHD patients: 0.36±0.02 mM – in Ah^+DM^+ group; 0.40±0.02 mM – in Ah^+DM^- group; 0.47±0.03 mM – in Ah^-DM^- group. At the same time, GSH concentration in erythrocytes of healthy donors was approximately 0.91±0.07 mM.

It is known that cysteine-rich low-molecular proteins metallothioneins are markers of oxidative stress of both mRNA and protein levels [11, 12]. Nordberg and Arnér in their study [35] have demonstrated that MTs "co-operate" with also low-molecular weight thiol – GSH, in maintaining the cellular redox state and act as an additional antioxidant in the cellular defense system [35]. These results testify about antioxidant features of MTs in the extreme conditions under oxidative stress. Moreover, the enhanced MTs expression in the cell line with blocked glutathione synthesis was detected [36]. In our previous studies, it was found an increased MTs level in human erythrocytes, both under H_2O_2-induced oxidative stress when zinc releases from its intracellular depots [32], and Zn-deficient state [37]. Kumar et al. [38] showed that the introduction of Zn^{2+} into the diet of diabetic mice led to a significant inhibition of lipid peroxidation and to a decrease in the level of superoxide anions and oxidized glutathione. Besides, they also found that the introduction of Zn^{2+} causes the decrease in GSH level and MTs mRNA expression, and also superoxide dismutase activation.

In this regard, an assessment of the content of MTs, functioning as an auxiliary protective antioxidant system [12, 13, 15], in erythrocytes of tested groups of CHD patients was conducted. Figure 3 demonstrates the dot diagrams of the fluorescence of UC1MT-IgG1-FITC and IgG1-FITC complexes showing the order of fluorescence intensities values of these complexes (MFI parameter – mean fluorescence intensity) in donor's erythrocytes. It is known that UC1MT are the specific mouse monoclonal antibodies for two classes of MTs – MTI and MTII. We estimated the relative content of MTs in human erythrocytes by using the ratio of the fluorescence intensity of the UC1MT-IgG1-FITC complex (I1) to the fluorescence intensity of the isotype control IgG1-FITC (I2) which characterized the non-specific binding of antibodies in cells. It is clearly seen that the ratio of the fluorescence intensity of donor's erythrocytes antibodies to the isotype control was about 3.04±0.60, while in the cells of CHD patients with arterial hypertension (Ah^+DM^-) – 4.16±0.38 (Figure 4). At the same time, this value was in the range of 5.6±0.6 for the group of patients having arterial hypertension and type 2 diabetes mellitus (Ah^+DM^+).

A comparative analysis of the content of metallothioneins in the erythrocytes of tested groups of patients revealed a principal trend – an increase in the content of low-molecular weight polypeptides with antioxidant properties in red blood cells of CHD patients. Moreover, in the Ah^+DM^+ group these changes were more pronounced as 1.8-fold increase in the MTs content was observed compared to the healthy donors' erythrocytes.

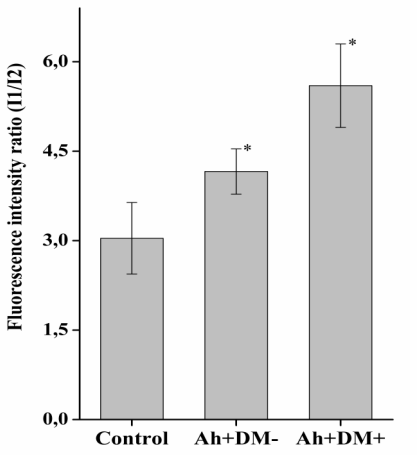

Figure 4 | Relative level of metallothioneins in the donor's erythrocytes and two examined groups of patients with coronary heart disease: Ah^+DM^- and Ah^+DM^+, where, control – healthy donors; I1 – the fluorescence intensity of the UC1MT-IgG1-FITC complex (relative units); I2 – intensity of fluorescence of isotype control IgG1-FITC (relative units). * – $p<0.05$ compare with control. Относительный уровень содержания металлотионеинов в эритроцитах доноров и двух обследованных подгрупп пациентов с ИБС: $АГ^+СД^-$ и $АГ^+СД^+$, где, контроль – здоровые доноры; I1 – интенсивность флуоресценции комплекса UC1MT–IgG1-FITC (отн. ед); I2 – интенсивность флуоресценции изотипического контроля IgG1 -FITC (отн. ед). * – $p<0.05$ по сравнению с контролем

5. Concluding Remarks

Thus, it was revealed that the observed decrease in the intracellular level of labile zinc in CHD cells appears to be an inductor of modification of cellular redox state (2–2.8-fold decrease in GSH concentration). The increase in metallothioneins expression and significant decrease in the reduced glutathione level in erythrocytes of CHD patients with the metabolic disorders imply functioning cysteine-rich proteins as an additional antioxidant in human erythrocytes defense system under these pathologies. It is clear that the potential of MTs as the scavengers of reactive species is not fully understood, but the present data show that these proteins could be selected as a target for some antioxidant treatment strategies for CHD patients with metabolic disorders in general and with type 2 diabetes mellitus in particular.

Заключение

Обнаруженное снижение внутриклеточного уровня лабильного цинка в эритроцитах ИБС-пациентов, по-видимому, является индуктором в нарушении редокс-статуса клеток, что проявляется в 2–2.8-кратном снижении концентрации восстановленного глутатиона. Увеличение уровня экспрессии металлотионеинов на фоне значительного снижения уровня восстановленного глутатиона в эритроцитах ИБС-пациентов с метаболическими нарушениями свидетельствует о функционировании данных цистеин-содержащих белков в качестве дополнительной антиоксидантной защитной системы эритроцитов человека при данной патологии. Разумеется, роль MTs, как захватчиков свободных радикалов до конца не выявлена, но представленные данные демонстрируют, что эти белки могут быть выбраны в качестве мишени при назначении терапии кардиологическим пациентам с метаболическими нарушениями в целом и при наличии сахарного диабета 2 типа в частности.

Acknowledgements

The authors thank Prof. L.G. Gelis (Minsk, Belarus) and MD A.A. Miadzvedzeva (Minsk, Belarus) for giving peripheral blood of CHD patients for current investigation and their characterization. Also, we thank Dr. I. Iatsunskyi (Poznan, Poland) for providing language help.

References

[1] Y.M. Harmaza, E.I. Slobozhanina, Biophysics 59 (2014) 234–275. DOI: 10.1134/s0006350914020092
[2] C. Andreini, I. Bertini, J. Inorg. Biochem. 111 (2012) 150–156. DOI: 10.1016/j.jinorgbio.2011.11.020
[3] W. Maret, Adv. Nutr. 4 (2013) 82–91. DOI: 10.3945/an.112.003038.
[4] D.J. Eide, Biochim. Biophys. Acta. 1763 (2006) 711–722. DOI: 10.1016/j.bbamcr.2006.03.005
[5] G.K. Andrews, Biometals 14 (2001) 223–237. DOI: 10.1023/a:1012932712483
[6] M. Vasak, D. W. Hasler, Curr. Opin. Chem. Biol. 4 (2000) 177–183. DOI: 10.1016/S1367-5931(00)00082-X
[7] M. Vasak, G. Meloni, J. Biol. Inorg. Chem. 16 (2011) 1067–1078. DOI: 10.1007/s00775-011-0799-2
[8] A.T. Miles, G.M. Hawksworth, J.H. Beattie, V. Rodilla, Crit. Rev. Biochem. Mol. Biol. 35 (2000) 35–70. DOI: 10.1080/10409230091169168
[9] M. Penkowa, FEBS J. 273 (2006) 1857–1870. DOI: 10.1111/j.1742-4658.2006.05207.x
[10] T. Kimura and T. Kambe, Int. J. Mol. Sci. 17 (2016) 336. DOI: 10.3390/ijms17030336.
[11] Y.J. Kang, Exp. Biol. Med. 231 (2006) 1459–1467. DOI: 10.1177/153537020623100903
[12] N. Thirumoorthy, A. Shyam Sunder, K. Manisenthil Kumar,M. Senthil Kumar, G. Ganesh, M. Chatterjee, World J. Surg. Oncol. 9 (2011) 54. DOI: 10.1186/1477-7819-9-54.
[13] M. Sato, M. Kondoh, Tohoku J. Exp. Med. 196 (2002) 9–22. DOI: 10.1620/tjem.196.9 ·
[14] M. Deponte , Antioxid. Redox. Signal. 27 (2017) 1130–1161. DOI: 10.1089/ars.2017.7123
[15] P.J. Thornalley, M. Vasak, Biochim Biophys Acta. 827 (1985) 36–44. DOI: 10.1016/0167-4838(85)90098-6
[16] J. Goldman, F.H. Carpenter, Biochemistry. 13 (1974) 4566–4574. DOI: 10.1021/bi00719a015
[17] F. Chimienti, S. Devergnas, A. Favier, M. Seve, Diabetes 53 (2004) 2330–2337. DOI: 10.2337/diabetes.53.9.2330
[18] J. Xu, J. Wang, B. Chen, Genet Mol Res. 11 (2012) 1592–1598. DOI: 10.4238/2012.
[19] G.A. Rutter, P. Chabosseau, E.A. Bellomo, W. Maret, R.K. Mitchell, D.J. Hodson, A. Solomou, M. Hu, Proc. Nutr. Soc. 1 (2015) 1–12. DOI: 10.1017/S0029665115003237
[20] R. Sladek, G. Rocheleau, J. Rung, C. Dina, L. Shen, D. Serre, P. Boutin, D. Vincent, A. Belisle, S. Hadjadj, B. Balkau, B. Heude, G. Charpentier, T.J. Hudson, A. Montpetit, A.V. Pshezhetsky, M. Prentki, B.I. Posner, D.J. Balding, D. Meyre, C. Polychronakos, P. Froguel, Nature 445 (2007) 881–885. DOI: 10.1038/nature05616
[21] A. Błazewicz, G. Orlicz-Szczesna, A. Prystupa, P.J. Szczesny, Trace Elem. Med. Biol. 242 (2010) 14–19. DOI: 10.1016/j.jtemb.2009.08.001
[22] N. Stadler, S. Heeneman, S. Vöö, N. Stanley, G.I. Giles, B.P. Gang, K.D. Croft, T.A. Mori, V. Vacata, M.J. Daemen, J. Waltenberger, M.J. Davies, Atherosclerosis 222 (2012) 512–518. DOI: 10.1016/j.atherosclerosis.2012.03.015
[23] J.A. Seo, S.W. Song, K. Han, K.J. Lee, H.N. Kim, PLoS One 9 (2014) e105990. DOI: 10.1371/journal.pone.0105990
[24] K. Marcinek, J. Sulibursкa, Z. Krejpcio, P. Bogdanski, Rocz. Panstw. Zakl. Hig. 66 (2015) 61–67. https://pdfs.semanticscholar.org/5284/79ed31cc4e10aff3ee102a0c751a5b8670 d1.pdf
[25] R.B. Singh, M.A. Niaz, S.S. Rastogi, S. Bajaj, Z. Gaoli, Z. Shoumin, J. Am. Coll. Nutr. 17 (1998) 564–570. DOI: 10.1080/07315724.1998.10718804
[26] M. Foster, S. Samman, Antioxid. Redox. Signal 13 (2010) 1549–1573. DOI: 10.1089/ars.2010.3111
[27] D. Popovici, D. Pereţianu, Med. Interne. 27 (1989) 57–64.
[28] S. Praveeena, S. Pasula, K. Sameera, J. Clin. Diagn. Res. 7 (2013) 1863–1865. DOI: 10.7860/JCDR/2013/5464.3335
[29] D. Bratosin, L. Mitrofan, C. Palli, J. Estaquier, Cytometry A. 66A (2005) 78–84. DOI: doi.org/10.1002/cyto.a.20152

[30] K.R. Gee, Z.L. Zhou, D. Ton-That, S.L. Sensi, J.H. Weiss, Cell Calcium 31 (2002) 245–251. DOI: 10.1016/S0143-4160(02) 00053-2

[31] A.R. Kay, BMC Physiol 4 (2004) 4. DOI: 10.1186/1472-6793-4-4

[32] Y.M. Harmaza, A.V. Tamashevski, J.S. Kanash, G.P. Zubritskaya, A.G. Kutko, E.I. Slobozhanina, Biophysics 61 (2016) 950–958. DOI: 10.1134/s0006350916060087

[33] A. Kojima-Yuasa, K. Umeda, T. Olikita, D.O. Kennedy, S. Nishiguchi, I. Matsui-Yuasa, Free Radic. Biol. Med. 39 (2005) 631–640. DOI: 10.1016/j.freeradbiomed.2005.04.015

[34] A. Kraus, H.P. Roth, M. Kirchgessner, J. Nutr. 127 (1997) 1290–1296. DOI:10.1093/jn/127.7.1290

[35] J. Nordberg, E.S. Arnér, Free Radic. Biol. Med. 31 (2001) 1287 –1312. DOI: doi.org/10.1016/s0891-5849(01)00724-9

[36] I. Nakagawa, M. Suzuki, N. Imura, A. Naganuma, Free Radic. Biol. Med. 24 (1998) 1390–1395. DOI: 10.1016/s0891-5849(98)00008-2

[37] Y.M. Harmaza, A.V. Tamashevski, J. Belarus. State Univ. Ecol. 3 (2017) 54–63. (in Russ.)

[38] S.D. Kumar, M. Vijaya, R.P. Samy, S.T. Dheen, M. Ren, F. Watt, Y.J. Kang, B.H. Bay, S.S. Tay, Free Radic. Biol. Med. 53 (2012) 1595–1606. DOI: 10.1016/j.freeradbiomed.2012.07.008

JOURNAL OF INTEGRATED OMICS
A METHODOLOGICAL JOURNAL
HTTP://WWW.JIOMICS.COM

ORIGINAL ARTICLE | DOI: 10.5584/jiomics.v9i1.252

Vitabolomics. New direction in the vitaminilogy

S. A. Petrov, N. L. Fedorko, A. K, Budnyak, V. E. Yakimenko, S. S. Chernadchuk, A. V. Sorokin, A. M.. Andrievskyi , A. V. Zakharov, K. V. Nikolaienko, A. V. Baydan, I. I. Zarovnaya, I. S. Gorbenko, S. O. Cherepneva-Khlyustova.

Department of Biochemistry, Odessa I.I. Mechnikov National University, Odessa, Ukraine

Received: 4 July 2018 **Accepted:** 31 December 2019 **Available Online**: 13 March 2019

Abstract

Modern studies of enzymovitamins are devoted to the study of the biochemical functions of their metabolically active forms. At the same time, it is not taken into account that in cells and in some cases in one compartment of the cell both the vitamin itself and its anabolites and catabolites co-exist together. It seems to us necessary to study the biochemical effect of the combined action of all the metabolites of a particular vitamin that present in the cells. We propose to name such a complex of all formed metabolites of individual vitamins as the vitabolome. Our studies, conducted with thiamine, riboflavin, and pantothenic vitabolomes, have demonstrated that in some cases the complexes of metabolites of these vitamins have regulatory properties that are fundamentally different from those of the corresponding vitamins and coenzymes. Thus, thiamine vitabolome significantly mitigates the activating action of thiamine and TPP on the activity of the pyruvate dehydrogenase complex in tissues and prevents the inhibitory effect of thiochrome on this multienzyme complex. Even more significant is the fact that thiamine vitabolome has a regulatory effect on certain enzymes, unlike thiamin or its metabolites alone. Studying the effect of individual metabolites of pantothenic acid and their complex on acetylation activity in tissues, we found that individual metabolites in physiological concentrations do not affect the recorded index, while pantothenic vitabolome exerted a pronounced effect, the direction of which depends on the terms after its introduction. Riboflavin vitabolome significantly activated succinate dehydrogenase, while riboflavin, FMN and FAD did not have such effect .

Аннотация

Современные исследования энзимовитаминов посвящены изучению биохимических функций их метаболически активных форм. В то же время не учитывается то обстоятельство, что в клетках, а в ряде случаев в одном компартменте клетки, сосуществуют как сам витамин, так и его анаболиты и катаболиты. Нам представляется необходимым изучение биохимического эффекта совместного действия всех присутствующих в клетках метаболитов того или иного витамина. Такой комплекс всех образующихся метаболитов отдельных витаминов мы предлагаем назвать витаболомом. Нашими исследованиями, проведенными с тиаминовым, рибофлавиновым, и пантотеновым витаболомами, продемонстрировали, что в некоторых случаях комплексы метаболитов выше указанных витаминов обладают регуляторными свойствами, принципиально отличающимися от таковых соответствующих витаминов и коферментов. Так, тиаминовый витаболом существенно смягчает активирующее действие тиамина и ТПФ на активность пируватдегидрогеназного комплекса в тканях и предотвращает ингибирующее действие тиохрома на этот мультиэнзимный комплекс. Еще более существенным является то, что тиаминовый витаболом оказывает регулирующее действие на некоторые ферменты, на которые ни тиамин, ни его метаболиты в отдельности не влияют. При изучении воздействия отдельных метаболитов пантотеновой кислоты и их комплекса на ацетилирующую активность в тканях нами установлено, что отдельные метаболиты в физиологических концентрациях не влияют на регистрируемый показатель, в то время как пантотеновый витаболом оказывал выраженное действие, направленность которого зависит от сроков после его введения. Рибофлавиновый витаболом существенно активировал сукцинатдегидрогеназу, в то время как рибофлавин, ФМН и ФАД таким эффектом не обладали

Keywords: Laser Vitabolomics, Vitamins, Coenzymes, Catabolites.

***Corresponding author:** Sergiy Anatoliyovich Petrov, doctor of biological sciences, professor of Odesa National Mechnykov I. I. University, Department of Biochemistry, 2, Dvoryanska Str., Odesa, 65082, Ukraine, email: serpet2015@ukr.net; budnyak2005@ukr.net

1. Introduction

In contemporary vitaminology, the predominant notion claims that the single biochemical function of an enzyme-vitamin appears to be the function of coenzyme for a corresponding enzyme.

However, during last three decades, a significant number of researches, disproving this notion, have been published. Their results indicate that the enzyme-vitamins and their metabolites have their own biochemical functions, which have nothing to do with the coenzyme activity [2-7]. In our laboratory, biochemical functions of catabolites of thiamine, riboflavin, pantothenic acid, nicotinic acid, pyridoxine and ascorbic acid have been studied [8-10].

In the process of investigation the functions of enzyme-vitamins and their catabolites in the body, one should keep in mind that the vitamin itself, its coenzymes and other metabolites are present simultaneously in the tissues. Therefore, the objective of this study was to study the possibility of the cooperative participation of metabolites of vitamins, found in tissues, in the regulation of various multistage biochemical processes.

Actually every vitamin, this applies in particular to coenzyme vitamins, is contained in cells in the form of certain metabolites through which it can realize its functions. For example, vitabolome of vitamin B1, thiamine, includes thiamine monophosphate, thiamine diphosphate, thiamine triphosphate, and also simple and mixed disulfides, recently found and studied adenylated thiamine triphosphate. In addition to these compounds, the cells contain a certain amount of other thiamine metabolites. The biochemical activity of thiochrome is intensively studied in our laboratory. Vitamin B_2 realizes its functions through the co-enzymes of FAD and FMN, however, the cells also contain the original form of the vitamin - riboflavin itself, in addition, other riboflavin catabolites are present in the cells, for example, lumichrome and lumiflavine. Earlier it was thought that these are inert compounds, which are unnecessary ballast in cells. Their functions are also investigated in our laboratory. Vitamin B_5, in a large number of publications, known as vitamin B_3, deciphering as pantothenic acid, has a basic coenzyme form called coenzyme A, which function of the transporting acyl groups to energy-significant enzyme cycles, for example, to the Krebs cycle, has long been known. But in the cells, apart from pantothenic acid, there are also other derivatives of pantothenic acid, and compounds which are structural units or metabolic products of coenzyme A. These are phosphopantothenate, β-alanine, sodium panthoate, pantethine A and other compounds. Other systems of metabolites of vitamins also exist in cells. For example, there is ascorbic acid metabolites system comprising, in fact, ascorbic acid, mono- and dehydroascorbic acids, diketogulonic, threonic, oxalic acids. There are publications devoted to other metabolites of vitamin C, for example, L-xylonic acid and its lactone, L-lyxonic and L-erythroaskorbic acids. Publications on the combined effect of vitamin C metabolites on cellular metabolism are limited, and this concept is not well developed and supported by all.

Professor S.A.Petrov proposed the term "vitabolome" by analogy with metabolone. In our therminology, vitabolome is a combination of a given vitamin and its metabolic-catabolite forms, which form a specific system in cells and are in certain ratios corresponding to a certain level of cellular metabolism. Their concentration and ratios in cells determine, regulate and limit the functional activity of cellular processes. In this article, we made an attempt to investigate the vitabolomes of vitamins B_1, B_2 and B_5.

2. Material and Methods

The experiments were conducted at the Department of Biochemistry of Odessa I. I. Mechnikov National University. Albino mongrel rats of different ages were used. As a biomaterial, extracts of organs lacking cell membranes were used. The use of such an object as tissue extracts devoid of cell membranes is caused by the necessity of having all components of the cell in the environment, since the realization of the functions of vitamin metabolites can be carried out in different cell compartments. Before determining the biochemical parameters, the membrane-free extracts of the organs were introduced into the incubation medium and all the metabolites were added in the ratios present in the tissues. In particular: metabolites of vitamin B_1: thiamine, thiamine pyrophosphate (TPP), thiochrome, 4-methyl-5-β-hydroxyethylthiazole, a mixture of these metabolites, called vitabolome of vitamin B_1; metabolites of vitamin B_2: riboflavin, FMN, FAD, lumichrome (LC), a mixture of these metabolites called vitamin's B_2 vitabolome; metabolites of vitamin B_5: phosphopantothenate, β-alanine, calcium α-pantothenate, sodium pantoate, pantetin A, CoA, a mixture of these metabolites, which was called vitamin's B_5 vitabolome. Activity of the pyruvate dehydrogenase complex and succinate dehydrogenase was defined by Potassium ferricyanide method; the activity of CoA transacetylases was defined by the speed of acetylation [12], the activity of acetylcholinesterase has been measured according to the standard protocol by colorimetric method of acetylcholine hydrochloride hydrolysis with the formation of choline and acetic acid, which caused a change in pH [13], and the activity of transketolase was defined by the photometric method for the intensity of the formation of a colored complex of pentose with orcine [14]. Earlier, we determined the average concentrations of vitamin metabolites in some organs. Therefore, in the study of vitabolomes, we used precisely these concentrations and ratios of the metabolites present in tissues in situ. As we established earlier, some catabolites of vitamins, even in insignificant concentrations compared to the vitamin itself, have a marked effect on the

Table 1 | The content of thiamine (μg/g), riboflavin (μg/g), pantothenic acid (nmol/g) and their main metabolites in the liver of white rats (n=8). * - significant in relation to the content of the corresponding vitamin, $p \leq 0.05$. Содержание тиамина (мкг / г), рибофлавина (мкг / г), пантотеновой кислоты (нмоль / г) и их основных метаболитов в печени белых крыс (n = 8). * - достоверно по отношению к содержанию соответствующего витамина, $p \leq 0,05$.

Thiamine and its metabolites (μg/g)		Riboflavin and its metabolites (μg/g)		Pantothenic acid and its metabolites (nmol//g)	
TPP+TMP	1,5±0,2*	FAD	124,0±2,0*	KoA	165,0±17,0*
Thiamine	0,4±0,1	FMN	6,2±0,7*	Panthetine	2,0±0,3*
Thiochrome	0,4±0,1	Riboflavin	0,8±0,1	Pantothenate	12,1±1,3
4-methyl-5-β-hydroxyethyl-thiazole	0,1±0,1*	Lumichrome	0,3±0,1*	Pantoate	0,8±0,1*

activity of certain enzymes. Everything related to laboratory animals (keeping, conducting experiments) were with strict compliance to international rules: «Guide for the Care and Use of Laboratory Animals». All obtained data was processed statistically. Values are reported as means ± SE. All data were analyzed using one-way ANOVA (Biostat). Statistical significance was considered to be $p \leq 0.05$ [16].

3. Results and discussion

In At the beginning of our research, we determined the average content of thiamine, riboflavin, pantothenic acid and their main metabolites in the liver of Albino mongrel rats. These data are presented in Table 1.

As it can be seen from the results presented in table 1, the prevailing metabolic form of all the studied vitamins is the coenzyme form. However, small amounts of free vitamins and even smaller amounts of their catabolites are present in the liver.

Therefore, in further studies of the effects of vitabolome, we used a mixture of catabolites in the concentrations and ratios indicated in Table 1, which are present in vivo in the liver.

During investigation of the regulatory properties of thiamine's vitabolome, the following patterns have been detected. In the liver of white rats, the sum of thiamine metabolites significantly mitigate the activating action of thiamine and thiamine pyrophosphate (TPP) on the activity of the pyruvate dehydrogenase complex (PDC) and prevents the inhibitory effect of thiochrome on it (Figure 1).

During the study of the activity of transketolase in the presence of thiamine, its metabolites and vitabolome, it was detected that the activity of transketolase is different in different organs and tissues (blood, liver, brain, adrenals). This activity is maximal in the brain and minimal in the liver. However, the nature of the effect of thiamine metabolites (thiamine and TPP) on the activity of transketolase is practically the same. Thiamine vitabolome also stimulated the activity of this enzyme, and this effect was a bit greater than in the case of TPP (Figure 2).

In the course of the study of the regulatory role of pantothenic acid, its metabolites and pantothenic acid's vitabolome on the transacetylating activity in the tissues of white rats (Figure 3), we found out that none of the metabolites of pantothenate had a significant effect on transacetylase activity in the kidneys and heart. Pantothenic acid's vitabolome also proved to be ineffective in these organs. In the liver, activating action was demonstrated by β -alanine, and in the brain by panthetine. The CoA effect was unexpected for us. The addition of CoA into the incubation medium reduced the investigated index in the liver by 10%. Pantothenic acid's vitabolome in the liver led to the decrease in transacetylase activity. In other organs studied, pantothenic acid's vitabolome did not affect the investigated

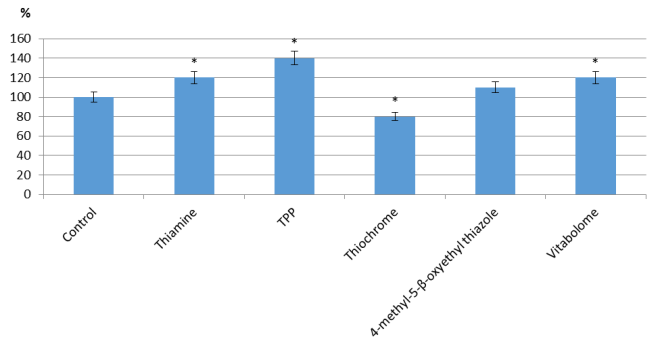

Figure 1 | Influence of individual thiamine metabolites and thiamine's vitabolome on the activity of the pyruvate dehydrogenase complex in the liver of white rats (n=8). Notes: * - $p \leq 0.05$ in comparison with the control. Влияние отдельных метаболитов тиамина и витаболома тиамина на активность пируватдегидрогеназного комплекса в печени белых крыс (n = 8). Примечания: * - $p \leq 0,05$ по сравнению с контролем

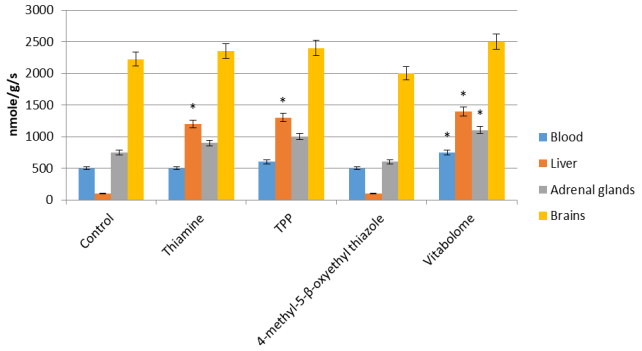

Figure 2 | Influence of pantothenate and its metabolites and pantothenic acid's vitabolome on transacetylase activity in tissues of white rats (% of control) (n=8). Notes: * - $p \leq 0.05$ in comparison with the control. Влияние пантотената и его метаболитов и витаболома пантотеновой кислоты на трансацетилазную активность в тканях белых крыс (% от контроля) (n = 8). Примечания: * - $p \leq 0,05$ по сравнению с контролем.

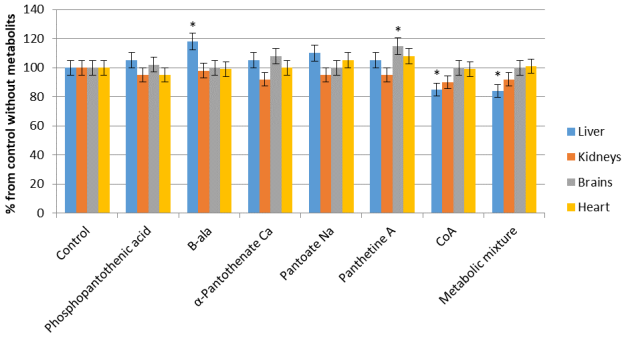

Figure 3 | Influence of pantothenate and its metabolites and pantothenic acid's vitabolome on transacetylase activity in tissues of white rats (% of control) (n=8). Notes: * - $p \leq 0.05$ in comparison with the control. Влияние пантотената и его метаболитов и витаболома пантотеновой кислоты на трансацетилазную активность в тканях белых крыс (% от контроля) (n = 8). Примечания: * - $p \leq 0,05$ по сравнению с контролем.

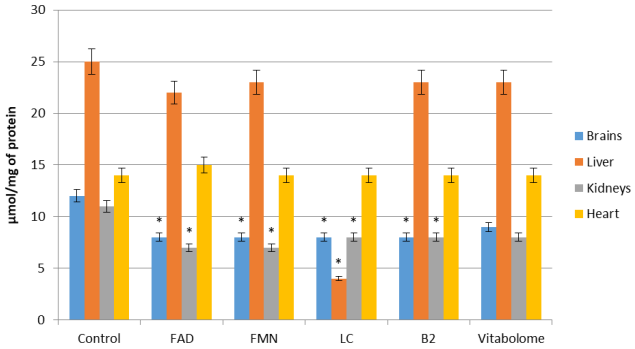

Figure 5 | Influence of riboflavin, its metabolites and riboflavin'svitabolome on the activity of PDC in the organs of mature (10-12 months) rats (μM / mg protein) (n=8). Notes: * - $p \leq 0.05$ in comparison with the control. Влияние рибофлавина, его метаболитов и витаболома рибофлавина на активность пируватдегидрогеназного комплекса в органах зрелых (10-12 месяцев) крыс (мкМ / мг белка) (n = 8). Примечания: * - $p \leq 0,05$ по сравнению с контролем.

index. To explain the effects, series of additional studies are required.

The most prominent features of riboflavin's vitabolome appeared in studies of the regulation of the activity of the multi-enzyme pyruvate dehydrogenase complex. The effect of riboflavin and its metabolites on the activity of the multienzyme pyruvate dehydrogenase complex depends on the age of animals used for the experiments. In particular, in the organs of old rats (22-24 months), neither riboflavin nor its metabolites and vitabolome had an effect on the activity of the pyruvate dehydrogenase complex (PDC) (Figure 4).

In the group of mature rats, it was detected that neither riboflavin, nor its metabolites (except lumichrome) and riboflavin vitabolome had any effect on the PDC activity in liver and heart. All studied metabolites of riboflavin reduce the activity of the PDC in brain and kidneys, while the vitabolome to some extent mitigated this inhibitory effect (Figure 5).

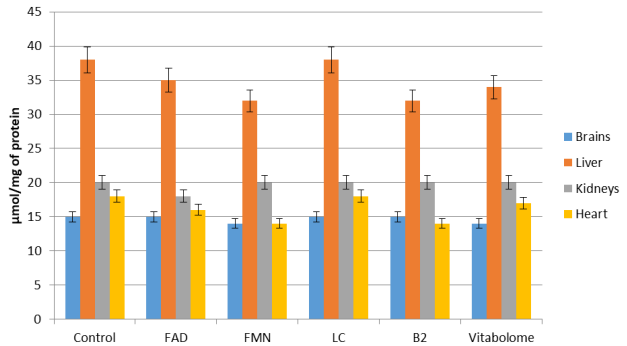

Figure 4 | Influence of riboflavin, its metabolites and riboflavin's vitabolome on the activity of PDC in the organs of old (22-24 months) rats (μM / mg protein) (n=8). Notes: * - $p \leq 0.05$ in comparison with the control. Влияние рибофлавина, его метаболитов и витаболома рибофлавина на активность пируватдегидрогеназного комплекса в органах старых (22-24 месяца) крыс (мкМ / мг белка) (n = 8). Примечания: * - $p \leq 0,05$ по сравнению с контролем.

In general, similar pattern was observed in the organs of young (5-6 months) rats (Figure 6). All metabolites of riboflavin reduce the activity of PDC in brain, while riboflavinic vitabolome returned the investigated index to the control values. Only FAD and lumichrome reduced the activity of PDC in liver, and the vitabolome had no protective effect as it was shown in previous organs. FMN significantly decreased the activity of PDC in kidneys. The riboflavinic vitabolome approximated the investigated index to the control values.

Besides, we conducted there the search on effects of riboflavin, its metabolites and vitabolome on the activity of succinate dehydrogenase (SDH) in organs of white rats. In old animals (22-24 months), the content of the riboflavin's metabolites and its vitabolome varied in different organs (Figure 7). FMN and LC showed the inhibitory action on SDH in heart. Vitabolome also reduced this effect. In brain, the addition of FMN into the medium led to the activation

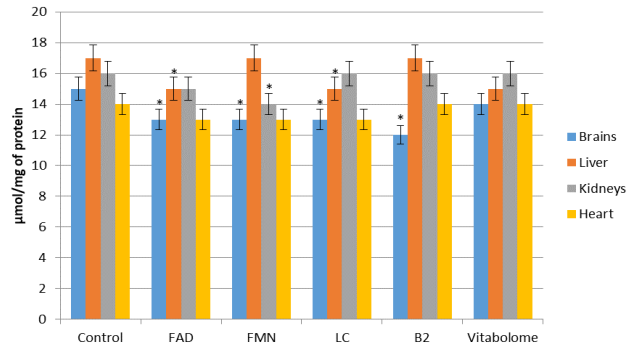

Figure 6 | Influence of riboflavin, its metabolites and riboflavin's vitabolome on the activity of PDC in the organs of young (5-6 months) rats (μM / mg protein)(n=8). Notes: * - $p \leq 0.05$ in comparison with the control. Влияние рибофлавина, его метаболитов и витаболома рибофлавина на активность пируватдегидрогеназного комплекса в органах молодых (5-6 месяцев) крыс (мкМ / мг белка) (n = 8).Примечания: * - $p \leq 0,05$ по сравнению с конт .

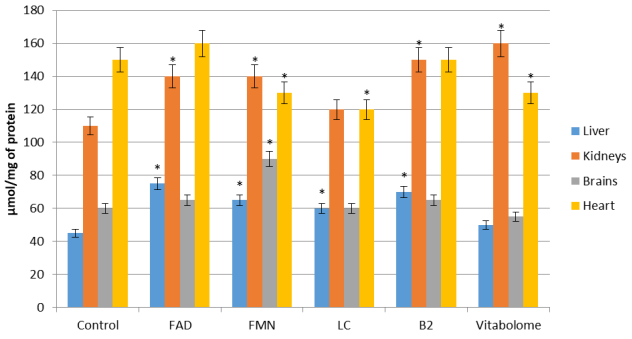

Figure 7 | Influence of riboflavin, its metabolites and its vitabolome on the activity of SDH in the organs of old (22-24 months) rats (nmol / mg protein) (n=8). Notes: * - $p \leq 0.05$ in comparison with the control. Влияние рибофлавина, его метаболитов и его витаболома на активность СДГ в органах старых (22-24 месяца) крыс (нмоль / мг белка) (n = 8). Примечания: * - $p \leq 0,05$ по сравнению с контролем.

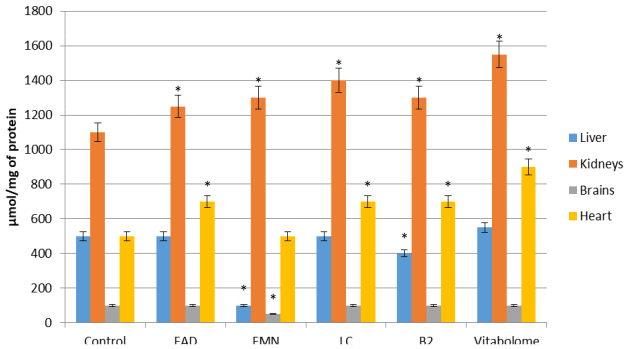

Figure 9 | The effect of riboflavin, its metabolites and vitabolome on the activity of SDH in the organs of young (5-6 months) rats (nmol/mg protein) (n=8). Notes: * - $p \leq 0.05$ in comparison with the control. Влияние рибофлавина, его метаболитов и витаболома на активность СДГ в органах молодых (5-6 месяцев) крыс (нмоль / мг белка) (n = 8). Примечания: * - $p \leq 0,05$ по сравнению с контролем.

of SDH. Vitabolome returned this pattern to the control values. The activating action of riboflavin, FMN, LC and FAD was significantly reduced in the presence of the vitabolome in the liver.

Riboflavin had an activating action on activity of SDG but FMN and LC decrease the activity of SDG in the liver of mature rats (10-12 months) (Figure 8). FAD increase the activity of SDG, but riboflavin and LC decrease the activity of SDG in the heart. All of the metabolites of riboflavin decrease the activity of SDG in the brain. In all these organs, riboflavin's vitabolome significantly changed these effects.

In the heart and kidneys of young animals (5-6 months) riboflavinic vitabolome activated SDH greater than individual metabolites. Riboflavin and FMN decreased the activity of SDG in liver,and the effect of the vitabolome does not differ from the effect of FAD on activity of SDG (Figure 9).

Discussion of the results obtained, while studying the effect of vitabolome on enzymes that do not contain vitamins' metabolites as coenzymes, deserve special attention. Acetylcholinesterase (AChE) was chosen as such an enzyme. The most noticeable fact is that riboflavin and its metabolites and vitabolome had an activating effect on the activity of acetylcholine esterase in the study of activity in the liver of old (22-24 months) rats. In the liver of young animals only riboflavinic vitabolome significantly increased the activity of AChE (Figure 10).

Thus, our studies have shown the need to take into account the simultaneous presence of various metabolites of vitamins in tissues when examining their effects on various biochemical processes. Our research has demonstrated that in a significant number of cases the action of the vitabolomes of various vitamins differs from the action of both coenzyme forms and catabolites.

The mechanisms of such action can be realized both at the level of individual enzymes, and in competition for the corresponding proteins

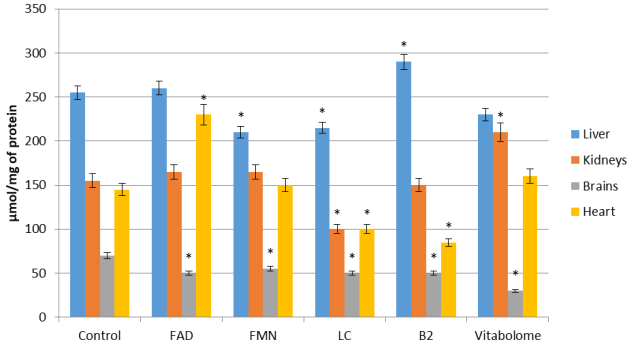

Figure 8 | Influence of riboflavin, its metabolites and vitabolome on the activity of SDH in the organs of mature (10-12 months) rats (nmol / mg protein) (n=8). Notes: * - $p \leq 0.05$ in comparison with the control. Влияние рибофлавина, его метаболитов и витаболома на активность СДГ в органах зрелых (10-12 месяцев) крыс (нмоль / мг белка) (n = 8). Примечания: * - $p \leq 0,05$ по сравнению с контролем .

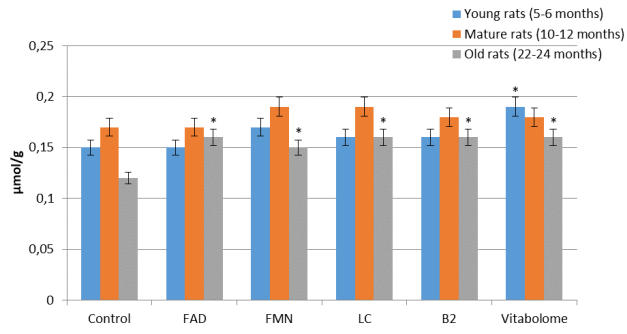

Figure 10 | Influence of riboflavin, its metabolites and vitabolome on AChE activity in liver of young (5-6 months), mature (10-12 months) and old (22-24 months) rats (µmol/g) (n=8). Notes: * - $p \leq 0.05$ in comparison with the control. Влияние рибофлавина, его метаболитов и витаболома на активность ацетилхолинэстеразы в печени молодых (5-6 месяцев), зрелых (10-12 месяцев) и старых (22-24 месяцев) крыс (мкмоль / г) (n = 8). Примечания: * - $p \leq 0,05$ по сравнению с контролем:

5. Concluding Remarks

1. The presence of the vitabolomes of the corresponding vitamins in tissues leads to modulating effects on the corresponding vitamin-dependent enzymes, which is manifested in a decrease in the activating effect and a weakening of the inhibitory action of catabolites.
2. The effectiveness of the action of the vitabolomes significantly depends on the age of the experimental animals.

Заключение

1. Наличие в тканях витаболомов соответствующих витаминов приводит к модулирующим эффектам в отношении соответствующих витаминзависимых ферментов, что выражается в снижении активирующих эффектов витаминов и ослаблении ингибиторного действия катаболитов.
2. Эффективность действия витаболомов существенно зависит от возраста экспериментальных животных

Acknowledgements

This research is co-financed by Greece and the European Union (European Social Fund- ESF) through the Operational Programme «Human Resources Development, Education and Lifelong Learning» in the context of the project “Strengthening Human Resources Research Potential via Doctorate Research” (MIS-5000432), implemented by the State Scholarships Foundation (ΙΚΥ). It was also supported from an ARISTEIA II grant (number 4045) to D. Vlahakos from the General Secretariat of Research and Technology of the Greek Ministry of Education.

References

[1] S.A. Petrov, O.V. Zaporozhchenko, O.K. Budnyak, S.S. Chernadchuk, N.L. Fedorko, in: Vitaminology: Textbook of Odessa: BMB, 2013. - 228 p.
[2] S.A. Petrov, V.E. Yakimenko, K.V. Nikolaenko, Journal of Education, health and sport,7(6) (2017) 591-596. DOI: http://dx.doi.org/10.5281/zenodo.828511
[3] O. Ustyanska, I. Vovchuk, S. Petrov, O. Budnjak, S. Gozhenko, Bulletin of the Taras Shevchenko National University of Kyiv, 71, №1 (2016) 77-81.
[4] S. A. A. Petrov, V. V. Zamorov, O. V. Ustyanskaya, O. K. Budnyak, S. S. Chernadchuk, O. M. Andrievskiy, O. O. Semyonova, Y. V. Karavanskiy, V. E. Yakimenko, I. O. Kravchuk Journal of Nutritional Science and Vitaminology 62 (2016) 6-11. DOI:https://doi.org/10.3177/jnsv.62.6.
[5] S.A. Petrov, V.E. Yakimenko, O Bytlan, Visnyk of Lviv National University. Biological series, 73 (2016) 352-355.
[6] S.A. Petrov, V.E. Yakimenko Bulletin of the Odessa National University, 20 1 (36) (2015) 7-13.
[7] S.A. Petrov, V.E.Yakimenko, Scientific Journal «ScienceRise», 8(1)(2016) 26-31.DOI: https://doi.org/10.15587/2313-8416.2016.76710.
[8] S.A. Petrov, V.E. Yakimenko, S.S. Chernadchuk, N.L. Fedorko, O.K. Budnyak, A.V. Sorokin, A.M. Andriyevsky, V.V. Zakharov, K.V. Nikolenko, A.V. Baidan, I.V. Zarovnaya, S.O. Cherepneva-Khlyustova., I.S. Gorbenko / NAS of Belarus; RNIIP "Institute of Biochemistry of Biologically Active Compounds of the National Academy of Sciences of Belarus"; under commonly Ed. I.N. Semeneni, AG Mosenok. Minsk: ICC Ministry of Finance, (2018) 463 - 468.
[9] S.A. Petrov, N.L. Fedorko, K.V. Nikolaenko, Journal of Education, Health and Sport, 7(7) (2017) 800-812. DOI: http://dx.doi.org/10.5281/zenodo.844093.
[10] S. Petrov, O. Budnyak, K., Ozherelyeva, O., Bytlan, K. Nikolaienko, K.Journal of Education, Health and Sport. - №7 (6) (2017) 583-590.DOI: http://dx.doi.org/10.5281/zenodo.827512.
[11] K.H. Kiessling, C.G., LunquistExperim. Cell. Kes, 26(1) (1962) 189-197.
[12] A.G. Moiseenok, Pantothenic acid (biochemistry and vitamin application) - Minsk: Science and Technology, (1980) 260.
[13] A.M. Goryachkovsky, Clinical biochemistry in laboratory diagnostics: A reference manual. - Ed. 3rd, and additional. - Odessa: "Ecology" (2005) 616.
[14] A.I. Karpishchenko (ed) Medical laboratory technologies: a guide to clinical laboratory diagnostics: in 2 toms / V2. - M.: GEOTAR-Media (2013) 792.
[15] Official Journal of the European Union L276/33. – Directive 2010/63/EU of the European parliament and of the council of 22 September 2010 on the protection of animals used for scientific purposes. 86/609/EC.20.10.2010.
[16] S. Glantz Medico-biological statistics. Trans. with English. - Moscow, Practice (1999) 459 .

JOURNAL OF INTEGRATED OMICS
A METHODOLOGICAL JOURNAL
HTTP://WWW.JIOMICS.COM

ORIGINAL ARTICLE | DOI: 10.5584/jiomics.v9i1.255

Detection and immunobiological characterization of bovine leukemia vírus in Russian Federation territory in dependence on geographical variations

M. V. Petropavlovskiy*, I. M. Donnik, N. A. Bezborodova, A. S. Krivonogova

Federal State Budgetary Scientific Institution "Ural Federal Agrarian Scientific Research Centre, Ural Branch of the Russian Academy of Sciences". 620142, Ekaterinburg, Belinskogo str. 112a.

Received: 13 September 2018 **Accepted:** 31 December 2018 **Available Online**: 30 April 2019

Abstract

BLV is a cancerous lymphoproliferative disease of cattle widely spread all over the world, including the Russian Federation. The genetic characterization of BLV is an important task in scientific research in many countries of the world. According to the phylogenetic analysis of routinely sequenced env gene region, BLV isolates are allocated in different geographical locations of the world, up to 10 different genetic groups of the virus were identified and classified. However, at the moment there are no detailed data on the immunobiological characteristics of BLV genotypes from Russia.

We selected groups of infected animals (n = 54) in Tyumen region by ELISA method. Immunological evaluation of animals in all test groups is given. A nested-PCR study was performed, which resulted in was received a fragment of the env 444 bp gene in the studied samples. RFLP analysis of this fragment allowed to establish that in 94% of the samples there was a «Belgian genotype» of the leukemia virus, in 4% of samples – «Australian» and in 2% - a «mixed type». In this region of Russia, the «Belgian genotype» eventually prevailed. Samples were sent for sequencing.

Аннотация

Вирус лейкоза – злокачественное лимфопролиферативное заболевание крупного рогатого скота, которое широко распространено во всем мире, включая Российскую Федерацию. Генетическая характеристика ВЛ КРС является важной задачей научно-исследовательских работ во многих странах мира. Согласно филогенетическому анализу секвенированных участков гена – env изолятов ВЛ КРС, выделенных в разных географических точках мира установлено и классифицировано до 10 различных генетических групп вируса. Однако на данный момент нет подробных данных об иммунобиологических характеристиках генотипов ВЛ КРС из Российской Федерации.

Нами были подобраны группы инфицированных животных (n=54) в Тюменской области методом ИФА. Дана иммунологическая оценка животных во всех опытных группах. Было выполнено nested-ПЦР исследование, в результате которого в исследуемых образцах был получен участок гена env 444 п.н. RFLP анализ этого фрагмента позволил установить в 94% образцов «Бельгийский генотип» вируса лейкоза, в 4% образцов - «Австралийский» и в 2% - «смешанный генотип». В исследуемом регионе Российской Федерации превалировал «Бельгийский генотип». Образцы были отправлены на секвенирование. Таким образом, исследованием фрагментов env области генома ВЛ КРС, выделенных на территории Тюменской области Российской Федерации, методом рестрикционного полиморфизма (RFLP) показано изменение генетического ландшафта и доминантного генотипа ВЛ КРС.

Keywords: Bovine leukemia virus in Russian Federation, nested PCR, RFLP analysis, several genetic groups

***Corresponding author:** Maxim Petropavlovskiy, petropavlovsky_m@mail.ru, tel: +7 (343) 257-20-44; fax: +7 (343) 257-82-63.

1. Introduction

Bovine leucosis is a cancerous lymphoproliferative disease, the etiologic factor of which is the bovine leukemia virus belonging to the family Retroviridae, the genus Deltaretrovirus.

The bovine leukemia virus is a huge problem for animal husbandry in many countries of the world, including the Russian Federation. In addition to the fact that the disease is widespread and causes billions of dollars in annual economic damage to the industry, there are also risks to public health [7]. The only effective method to eradicate the disease in cattle is the introduction of comprehensive recovery programs, including diagnostic studies of the entire population for the presence of antibodies to the capsid proteins of the pathogen, followed by the replacement of infected cattle. However, despite the relatively high efficiency of modern methods of diagnosing the disease, there is a possibility of incomplete identification of animals infected with leukemia virus in the healthy herds, which significantly affects the timing of the implementation of recovery programs. Earlier it was noted that this could be due, among other things, to the effect of genetic variability of individual virus isolates. The study of genetic diversity and regional phylogenetics of the virus is an important task in many countries around the world.

Molecular characterization of bovine leukemia virus

Like other retroviruses, the BLV gene contains the structural and regulatory genes: gag, pol and env. The env gene encodes the transmembrane glycoproteins gp51 and gp30 of the virus capsid, which cause the infectivity of the virus. In connection with this, the phylogenetic analysis of BLV genotypes was mainly based on the env gene [8, 10].

Characterization of the genetic diversity of BLV is an important task in scientific research in many countries of the world. According to the sequenced gene site – env BLV isolates are allocated in different geographical locations of the world, up to 10 different genetic groups of the virus were identified and classified [8].

The isolates allocated in Russia and published in NCBI Gene Bank are classified in 4, 7 and 8 genetic groups. Analysis of the amino acid sequences of isolated strains revealed that the main changes were localized in the C-part of the CD4+ epitope, the zinc binding peptide region, CD8+ T cell epitope and overlapping linear epitope E, and the greatest number of changes were noted in G4 («Belgian genotype») [3, 11].

However, there are no detailed data on the immunobiological characteristics of individual genetic groups, no difference in their effect on the animal's organism and no data on the detectability of the approved system tests (serological, molecular-genetic tests), and the recombinant interaction of several genetic groups.

Purpose of exploration: To study the antigenic landscape of bovine leukemia virus pathogens on the territory of the Tyumen region of the Russian Federation using PCR, nested PCR and polymorphism methods for following immunobiological and molecular genetic characteristics.

2. Material and Methods

As part of the research, we monitored the epizootic situation of the bovine leukemia virus in Russia. Groups of animals Holstein-Frisian (imported breed) and Russian Black Pied (local breed) breed (n = 54) were selected, belonging to agricultural organizations of the Tyumen region. Serological (ELISA, AGID) methods of screening the cattle population were used to identify infected animals. Studies by ELISA were performed using an IDEXX Leukosis Serum Screening test (IDEXX Montpellier SAS, France). For the AGID (agar gel immunodiffusion) - diagnostics used kit by the Kursk Biofactory - the "BIOK" company according to kit instructions.

Primary PCR study was performed using a standard commercial test system. Proviral DNA extraction was performed using the “Diatom DNA Prep 200” (IsoGen, Moscow) according to the manufacturer’s protocol.

For carrying out nested PCR, a BioMaster HS-Tag PCR kit (2x) by «Biolabmix» (Novosibirsk) was used. The concentrations of the solutions and the temperature regimes of the amplification reaction were established experimentally, a research protocol was formed. As a control, DNA isolated from cell culture FLK-BLV was used.

The env gene fragment was amplified using Nested PCR using the following primers: env 5032 TCT-GTG-CCA-AGT -CTC-CCA-GAT-A, env 5608 AAC-AAC-AAC-CTC-TGG-GAA-GGG-T, env 5099 CCC-ACA-AGG-GCG-GCG-CCG-GTT-T, env 5521 GCG-AGG-CCG-GGT-CCA-GAG-CTG-G [1], synthesized by «Syntol» (Moscow).

The DNA concentrations were determined on the MaxLife H100 Mod.2 kit of MVM Diagnostics (Barnaul). Amplification was performed using an Applied Biosystems 2720 thermal cycler (Singapore) with the following cycle parameters: 2 minutes at 94 ° C (1 cycle), 30 seconds at 95 ° C, 30 seconds at 62 ° C (external primers) or 30 seconds 70 ° C (internal primers), 60 seconds 72 ° C (40 cycles), 4 minutes 72ºC. PCR was performed in a 50 μl volume of the reaction mixture per sample (25 μl BioMaster set HS-Tag PCR (2x), 1 μl of each primer (1 pkm/μl), 1 μl MgCl2 (50 μM), 500 ng of genomic DNA, diluted bidistilled water.

The product was visualized on a 1.5% agarose gel in the presence of ethidium bromide.

At the first stage of the Nested PCR electrophoretic mobility amplicons corresponded to a fragment length of 600 bp. At the second stage of Nested PCR, positive amplicons correspond to a length of 444 bp.

To conduct genotyping of the env region (444bp-gp51 region), a polymorphism reaction (RFLP) was used, BamHI, BclI, PvuII were used as restriction enzymes. Amplification was performed with the following cycle parameters: BamHI, PvuII - 37ºC 2 hours; BclI - 55ºC 2 hours. PCR was performed in a volume of the reaction mixture of 20 μl per

sample (5 µl of PCR product, 1 µl of the enzyme, 2 µl of buffer, 12 µl of bidistilled water) [1].

3. Results

In As a result of the study, we obtained amplification products of the BLV env 444 bp gene region in 48 samples from the Tyumen region. In the process of research, there were animals that react negatively when examined with a standard commercial kit, however, during the Nested PCR reaction, the desired fragment of the virus gene site was found (Table 1).

RFLP analysis of this fragment allowed to establish that in 94% of the samples there was a «Belgian genotype» of the leukemia virus, in 4% of samples – «Australian genotype» and in 2% - a «mixed type» (Figure 1).

It is established that in Tyumen area of Russia the «Belgian genotype» of BLV dominates the «Australian». Mainly, this type was found in Holstein animals, the disease was characterized by a high rate of development of the acute form and rapid spread. The presence of negative samples in the study of the standard commercial test system could be associated with a low proviral load in the studied animals, as well as with the variability of the gene region in the primer sites. A complete picture characterizing the phylogenetic analysis and the nature of amino acid substitutions in the targeted part of the gene will be obtained from the results of DNA sequencing. The results of immunological studies of animals may allow to establish reliable correlations and to give immunobiological characteristics of individual isolates of the pathogen.

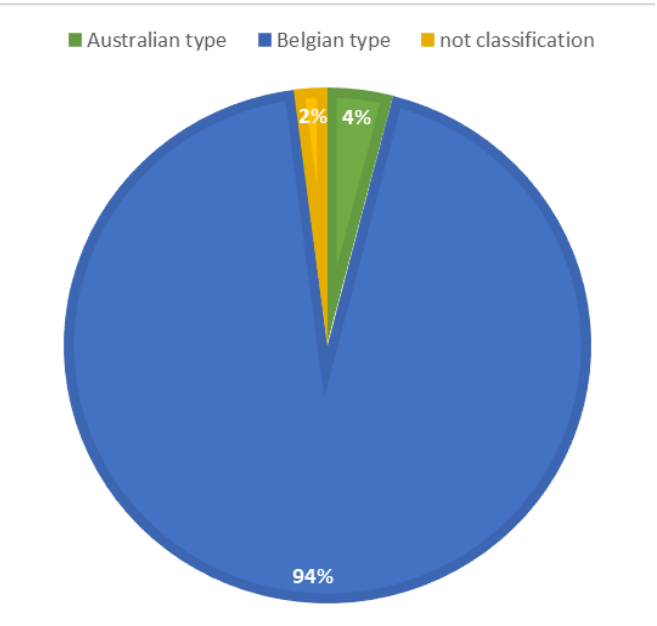

Figure 1 | Characterization of the genetic groups of the BLV in cattle of Tyumen area by RFLP method (n=48). Характеристика генетических групп вируса лейкоза крупного рогатого скота районов Тюменской области методом RFLP (ПДРФ), n=48.

4. Concluding Remarks

Summarizing the preliminary results, we can conclude that the application of the methodological approaches described in the article can serve to determine the geographical origin of leukemia virus isolates. So, we found that in the studied samples obtained from the Tyumen region mainly "Belgian genotype" of bovine leukemia virus is determined. The alleged source of infection could be local and imported cattle (previously imported in 2011) from America. It is also possible that there were false-negative serological tests in a batch of cattle from the Eastern Europe.

Earlier studies have determined that the territories of the Tyumen, Kurgan, and Sverdlovsk regions were dominated by the “Australian genotype”. We recorded the “Belgian genotype” in a smaller percentage in these areas [3, 11]. This genotype mainly dominated on the territory of the Chelyabinsk region, where the spread of the disease is the highest, and the course is characterized by severity and a rapid transition to the terminal stage (hematological). The high detection and dominance of the “Belgian genotype” on the territory of the Tyumen Region may be due to its more aggressive effect on the immune system of susceptible animals. In such animals, an increased proviral load is possible, which leads to a more rapid spread of the pathogen among susceptible herds. This is to be determined by the results of DNA sequencing and the results of immunological expertise of the studied cattle population.

Заключение

Установлено, что применение описанных в статье методологических подходов может служить для определения и установления географического происхождения изолятов вируса лейкоза. Так, нами было установлено, что в исследованных нами образцах, полученных из Тюменской области преимущественно, определялся «Бельгийский генотип» вируса лейкоза крупного рогатого скота.

Предполагаемым источником заражения мог являться местный и импортированный крупный рогатый скот (ранее импортированный в 2011 году) из Америки. Также возможно, что серологические тесты были ложноотрицательными в партии крупного рогатого скота из Восточной Европы.

Проведенными ранее исследованиями было определено, что на территориях Тюменской, Курганской, Свердловской областей циркулировал в доминирующем количестве (Австралийский генотип. Бельгийский генотип) нами регистрировался в меньшем процентном соотношении в этих областях [3,11]. Данный генотип в основном доминировал на территории Челябинской области, где распространение заболевания наиболее высоко, а течение характеризовано тяжестью и быстрым переходом в терминальную стадию (гематологическую). Высокое

Table 1 | List of samples and research results. Результаты исследований, выделенных образцов.
*Studies were conducted in the veterinary laboratory of the Tyumen region. Исследования проводились в районной ветеринарной лаборатории Тюменской области.

#	Origin	AGID*	ELISA	PCR	Nested PCR (second stage)	RFLP
1	Tyumen region, farm 1	+	no data	-	+	belgian type
2	Tyumen region, farm 1	+	no data	+	+	belgian type
3	Tyumen region, farm 1	+	no data	+	+	belgian type
4	Tyumen region, farm 1	+	no data	+	+	belgian type
5	Tyumen region, farm 1	+	no data	-	+	belgian type
6	Tyumen region, farm 1	+	no data	+	+	belgian type
7	Tyumen region, farm 1	+	no data	+	+	belgian type
8	Tyumen region, farm 1	+	no data	+	+	australian type
9	Tyumen region, farm 1	+	no data	-	+	belgian type
10	Tyumen region, farm 1	+	no data	+	+	belgian type
11	Tyumen region, farm 1	+	no data	-	-	-
12	Tyumen region, farm 1	+	no data	+	+	belgian type
13	Tyumen region, farm 1	+	no data	+	+	belgian type
14	Tyumen region, farm 1	+	no data	-	-	-
15	Tyumen region, farm 1	+	no data	+	+	belgian type
16	Tyumen region, farm 1	+	no data	-	-	-
17	Tyumen region, farm 1	+	no data	+	+	belgian type
18	Tyumen region, farm 1	+	no data	+	+	belgian type
19	Tyumen region, farm 1	+	no data	+	+	belgian type
20	Tyumen region, farm 1	+	no data	-	-	-
21	Tyumen region, farm 1	+	no data	+	+	belgian type
22	Tyumen region, farm 1	+	no data	-	-	-
23	Tyumen region, farm 1	+	no data	+	+	mixed type
24	Tyumen region, farm 1	+	no data	+	+	belgian type
25	Tyumen region, farm 1	+	no data	+	+	belgian type
26	Tyumen region, farm 1	+	no data	+	+	belgian type
27	Tyumen region, farm 1	+	no data	+	+	belgian type
28	Tyumen region, farm 1	+	no data	+	+	belgian type
29	Tyumen region, farm 1	+	no data	-	-	-
30	Tyumen region, farm 1	+	no data	+	+	belgian type
31	Tyumen region, farm 2	+	+	+	+	belgian type
32	Tyumen region, farm 2	+	+	+	+	belgian type
33	Tyumen region, farm 2	+	+	+	+	belgian type
34	Tyumen region, farm 2	+	+	+	+	belgian type
35	Tyumen region, farm 2	+	+	+	+	belgian type
36	Tyumen region, farm 2	+	+	+	+	belgian type
37	Tyumen region, farm 2	+	+	+	+	belgian type
38	Tyumen region, farm 2	+	+	+	+	belgian type
39	Tyumen region, farm 2	+	+	+	+	belgian type
40	Tyumen region, farm 2	+	+	+	+	belgian type
41	Tyumen region, farm 2	+	+	+	+	belgian type
42	Tyumen region, farm 2	+	+	+	+	belgian type
43	Tyumen region, farm 2	+	+	+	+	belgian type
44	Tyumen region, farm 2	+	+	+	+	belgian type
45	Tyumen region, farm 2	+	+	+	+	belgian type
46	Tyumen region, farm 2	+	+	+	+	belgian type
47	Tyumen region, farm 2	+	+	+	+	belgian type
48	Tyumen region, farm 2	+	+	+	+	belgian type
49	Tyumen region, farm 2	+	+	+	+	australian type
50	Tyumen region, farm 2	+	+	+	+	belgian type
51	Tyumen region, farm 2	+	+	+	+	belgian type
52	Tyumen region, farm 2	+	+	+	+	belgian type
53	Tyumen region, farm 2	+	+	+	+	belgian type
54	Tyumen region, farm 2	+	+	+	+	belgian type

обнаружение «Бельгийского генотипа» на территории Тюменской области может быть связано с его более агрессивным воздействием на иммунную систему восприимчивых животных. У таких животных возможна повышенная провирусная нагрузка, что приводит к более быстрому распространению возбудителя среди восприимчивого поголовья. Этот тезис предстоит установить по результатам секвенирования ДНК и результатам иммунологической экспертизы исследуемой популяции крупного рогатого скота.

Acknowledgements

The research was carried out at the expense of the Russian Science Foundation grant (project No. 17-76-10051).

References

[1] Beier D., Blankenstein P., Marquardt O., Kuzmak J, Identification of different BLV provirus isolates by PCR, RFLPA and DNA sequencing, // Berl. Munch.Tierarztl. Wschr., 2001, 114, no. 7–8: 252–256.

[2] Camargos MF, Pereda A, Stancek D, Rocha MA, dos Reis JK, Greiser-Wilke I, Leite RC (2007) Molecular characterization of the env gene from Brazilian field isolates of Bovine leukemia virus. Virus Genes 34(3):343–350.

[3] Donnik I., Petropavlovsky M. et al. (2016). Revisiting the issue of the molecular-genetic structure of the causative agent of the bovine leukemia virus in the Russian Federation. Indian Journal of Science and Technology, Vol 9(42): 1-11. doi: 10.17485/ijst/2016/v9i42/104253.

[4] Felmer R, Mun˜oz G, Zu´n˜iga J, Recabal M (2005) Molecular analysis of a 444 bp fragment of the bovine leukaemia virus gp51 env gene reveals a high frequency of non-silent point mutations and suggests the presence of two subgroups of BLV in Chile. Vet Microbiol 108(1–2):39–47.

[5] Lee E, Kim EJ, Ratthanophart J, Vitoonpong R, Kim BH, Cho IS, Song JY, Lee KK, Shin YK (2016) Molecular epidemiological and serological studies of bovine leukemia virus (BLV) infection in Thailand cattle. Infect Genet Evol 41:245–254.

[6] Lee E, Kim EJ, Joung HK, Kim BH, Song JY, Cho IS, Lee KK, Shin YK (2015) Sequencing and phylogenetic analysis of the gp51 gene from Korean bovine leukemia virus isolates. Virol J 12:64. doi:10.1186/s12985-015-0286-4.

[7] Mesa G., Ulloa J. C., Uribe A.M., Gutierrez M.F. Bovine Leukemia Virus Gene Segment Detected in Human Breast Tissue. Open Journal of Medical Microbiology, 2013, 3, 84-90 doi:10.4236/ojmm.2013.31013 Published Online March 2013 (http://www.scirp.org/journal/ojmm).

[8] Pluta A, Rola-Łuszczak M, Kubis´ P, Balov S, Moskalik R, Choudhury B, Kuzmak J (2018) Molecular characterization of bovine leukemia virus from Moldovan dairy cattle. Arch Virol 162(6):162:1563–1576.

[9] Polat M, Ohno A, Takeshima SN, Kim J, Kikuya M, Matsumoto Y,Mingala CN, Onuma M, Aida Y (2015) Detection and molecular characterization of bovine leukemia virus in Philippine cattle. Arch Virol 160(1):285–296. doi:10.1007/s00705-014-2280-3.

[10] Polat M, S Takeshima, Y Aida (2017) Epidemiology and genetic diversity of bovine leukemia virus. Virology Journal (2017) 14:209 DOI 10.1186/s12985-017-0876-4.

[11] Rola-Łuszczak M, Pluta A, Olech M, Donnik I, Petropavlovskiy M, Gerilovych A, Vinogradova I, Choudhury B, Kuz´mak J (2013) The molecular characterization of bovine leukemia virus isolates from Eastern Europe and Siberia and its impact on phylogeny. PLoS One 8(3):e58705. doi: 10.1371/journal.pone.0058705.

[12] Rice N. R., Stephens R.M., Couez D., Deschamps J., Keltmann R.. Burny A., Gilden R.V. The nucleotide sequence of the env gene and the post-env region of bovine leukemia virus // Virology. – 1984. – 138, 82-93.

[13] Wang M et all. (2018) Molecular epidemiology and characterization of bovine leukemia virus in domestic yaks (Bos grunniens) on the Qinghai-Tibet Plateau, China. Arch Virol 163(3):659-670.

[14] Yang Y, Kelly PJ, Bai J, Zhang R, Wang C. First molecular characterization of bovine leukemia virus infections in the Caribbean. PLoS One. 2016;11:e0168379.

JOURNAL OF INTEGRATED OMICS
A METHODOLOGICAL JOURNAL
HTTP://WWW.JIOMICS.COM

ORIGINAL ARTICLE | DOI: 10.5584/jiomics.v9i1.269

The potential benefits of shRNA-mediated MMP1 silencing for psoriasis

Julia A. Mogulevtseva [1], Sergey A. Bruskin [2], Alexandre Mezentsev [2]*

[1]K.A. Timiryazev Russian Agrarian University, Russian Ministry of Science and Higher Education, 49 Timiryazevskaya Street., Moscow 127550, Russia; [2]National N.I. Vavilov Institute of General Genetics, Russian Academy of Sciences, 3 Gubkina Street, Moscow 119333, Russia.

Received: 23 December 2018 **Accepted:** 03 February 2019 **Available Online**: 14 June 2019

Abstract

Matrix metalloproteinases (MMPs) orchestrate structural remodeling of psoriatic skin and accelerate the development of the inflammatory response.

In this paper, we explore whether knocking MMP1 down in epidermal keratinocytes can be beneficial for psoriasis.

We discovered that MMP1 silencing with specific shRNA reduced the migration of epidermal keratinocytes and made the cells susceptible to apoptosis in the presence of interferon-γ. Furthermore, MMP1-deficiency partially normalized the expression of genes involved in the pathogenesis of psoriasis (MMP9, -12, CCNA2, CCND1 and KRT17) and the terminal differentiation (KRT1, -10, IVL and LOR).

In conclusion, MMP1 silencing could be beneficial for psoriasis. MMP1-deficient cells exhibit lower proliferation rate. Moreover, MMP1-silencing makes the cells susceptable to the proinflammatory cytokine IFN-γ, which is abundant in lesional skin. In addition, knocking MMP1 down shifts the balance between proliferation and differentiation toward differentiation. The latter is important for psoriasis, which is a hyperproliferative skin disorder.

Аннотация

Матричные металлопротеиназы (MMP) принимают активное участие в структурной реорганизации эпидермиса, а также в стабилизации воспалительного процесса, которые происходят в пораженной псориазом коже.

Целью данной работы было оценить каким образом РНК-интерференция MMP1 в эпидермальных кератиноцитах человека может повлиять на патогенез псориаза.

Согласно полученным результатам, РНК-интерференция MMP1 в эпидермальных кератиноцитах человека приводит к снижению скоростей миграции и пролиферации данного типа клеток, а добавление в культуральную среду интерферона-γ инициирует их апоптоз. Кроме того, РНК-интерференция MMP1 частично нормализует экспрессию важных для патогенеза болезни генов (MMP9, -12, CCNA2, CCND1 и KRT17), а также генов-маркеров терминальной дифференцировки эпидермальных кератиноцитов (KRT1, -10, IVL и LOR).

Таким образом, РНК-интерференция MMP1 может иметь клиническое значение при псориазе, прежде всего, благодаря выраженному антипролиферативному эффекту. Более того, «нокдаун» MMP1 делает клетки восприимчивыми к провоспалительному цитокину IFN-γ, уровень которого повышен в пораженной болезнью коже. Наконец, РНК-интерференция MMP1 приводит к смещению баланса между пролиферацией и дифференцировкой клеток в сторону их дифференцировки. Последнее особенно важно для псориаза, который является гиперпролиферативным заболеванием кожи.

Keywords: Matrix metalloproteinase 1; Gene silencing; Th1-cytokine; Inflammatory response; Psoriasis.

***Corresponding author:** Alexandre Mezentsev, mesentsev@yahoo.com, tel: +7 (499) 132-0874; fax: +7 (499) 132-89-62 .

1. Introduction

Psoriasis is a chronic inflammatory disease driven by activated T-cells [1]. According to World Health Organization, more than 2% of the entire human population is suffering from psoriasis [2]. In Russia, where about 2.8 million people are diagnosed with psoriasis, the prevalence of the disease is ~1.9%, [3]. The hallmark of psoriasis is the appearance of red flaky-crusty patches covered with silvery seals. The cause of psoriasis is unknown. The skin accumulates immune cells that secrete proinflammatory cytokines. Three of them tumor necrosis factor (TNF), interleukin 17 (IL17) and interferon γ (IFN-γ) are the most important for the pathogenesis of the disease. Their accumulation in the skin leads to activation of epidermal keratinocytes, structural remodeling of the epidermis and development of the plaques. It also results in a faster turnover of epidermal keratinocytes and causes their hyperproliferation. [4].

Small interfering RNAs (siRNAs) that destroy protein-encoding mRNAs are present in any viable cell [5]. Targeting mRNAs, siRNAs prevent their translation into proteins by the ribosomes. Respectively, even partial degradation of mRNA by siRNA decreases protein expression. For this reason, the artificially designed siRNAs, known as small hairpin RNAs (shRNAs), are often used in routine experimental practice to knock down disease-associated genes. For instance, shRNA directed to MMP1 could be used to reduce MMP1 expression in cultured mammalian cells.

Matrix metalloproteinases (MMPs) are a group of zinc-containing, calcium-dependent endopeptidases. In psoriasis, MMPs modify the intercellular contacts by degrading the proteins of hemidesmosomes [6] and desmosomes [7-9]. They also change the composition of the extracellular matrix [10], facilitate the penetration of dermal microcapillaries by the immune cells and influence the biological activity of some cytokines [11].

In the lab, our research is focused on matrix metalloproteinases, such as MMP1, and their role in psoriasis. Previously, we have shown changes in MMP1, -9 and -12 expression in lesional psoriatic skin that coincided with exacerbation of the disease and correlated with the disease severity [12]. The aim of this study was to explore whether MMP1 silencing in epidermal keratinocytes could be beneficial for psoriasis.

2. Material and Methods

2.1 Cell lines and cell culturing:

The experiments were performed on human epidermal keratinocytes HaCaT-MMP1 and HaCaT-KTR that expressed MMP1-specific and scrambled (control) shRNA, respectively. The details on selection, design and cloning of the mentioned shRNAs were described earlier [13,14]. The target sequences used to design specific and scrambled shRNA were CAACAATTTCAGAGAGTAC and GTAAAGGGAACCAACTAACAGA, respectively. The specificity of the selected shRNAs to all know protein-encoding mRNA was verified by "Blastn". The cells were obtained by the method lentiviral tranduction in accordance with the previously described protocol [15].

2.2 Purification of total RNA

Total RNA was extracted with TRIzol reagent (ThermoFisher Scientific, USA) as described earlier [16]. Quality of the obtained RNA samples was verified using non -denaturing 1.5 % agarose gel electrophoresis. The RNA concentration was measured using the fluorimetric Qubit RNA BR Assay Kit (ThermoFisher Scientific) according to the manufacturer's protocol.

2.3 qPCR:

Before the experiment, total RNA was converted to cDNA using MMLV RT kit (Evrogen, Russia) according to the manufacturer's protocol. The real-time PCR experiments were carried out in the Eco real-time PCR system (Illumina, USA). The primers used in this study were taken from the database NCBI Probe [17]. The results were analyzed using the software supplied by Illumina. Each probe was run in triplicates. After all, three independent experiments were performed. The ACTB assay was used as an endogenous control.

2.4 Western blot

Before the experiment, whole cell lysates were obtained as described earlier [18] and protein concentration was measured by Bradford assay (Bio-Rad Laboratories; Richmond, CA, USA). Then, equal amounts of protein (10 μg) were added to Laemmli sample buffer (5% SDS, 25% glycerol, 125 mM TRIS, 0.004% bromphenol blue, 10% β-mercaptoethanol, pH 8.2) and subjected to electrophoresis in 12% polyacrylamide gel. Following transfer to PVDF membrane, samples were probed with primary antibodies (Abcam, USA, Cat #ab137332). Signals were captured using X-Omat K film (Eastman Kodak Co., USA). The films were scanned as image files, and the optical densities of the bands in these image files were quantified using the ImageJ software [19].

2.5 Proliferation assay

The cells were seeded in 6-well plates, 40,000 cells per well. At the indicated time points, randomly chosen samples were treated with 0.25% of trypsin-EDTA solution (PanEco). Then, cells were resuspended, stained with trypan blue (0.2%) and counted in hemocytometer. The obtained values were used for plotting the cell growth curves in linear

coordinates. After all, three independent experiments were performed.

2.6 Scratch assay

Scratch assay was used to assess cell migration rates. The cells were cultured until in 6-well plates until they covered the entire growth surface. Before the experiment, the cell monolayer was scratched with a pipette tip to obtain a 1.2–1.3 mm-wide cell-free area across the center of the well. The remained cells were washed with PBS and cultured for 5–6 days. The representative parts of cell-free areas were photographed daily and quantified with ImageJ software [19].

2.7 Statistics

Data were represented as means±SE. The statistical differences between the means were analyzed by one-way ANOVA. If *p*-values were less than 0.05, means were considered to be significantly different.

3. Results

3.1. Quantitative analysis of MMP1 expression

Evaluation of cDNA (Figure 1A) and protein fractions (Figure 1B) isolated from HaCaT-MMP1 and HaCaT-KTR cells discovered that the mentioned cell lines exhibited different expression levels of MMP1 mRNA and protein. In this respect, the expression levels of MMP1 mRNA and fully -processed catalytically active enzyme in HaCaT-MMP1 did not exceed 15.9 and 16.1% of the corresponding values in HaCaT-KTR cells. In cell homogenates, MMP1 protein was represented by two bands that were identified as proenzyme and catalytically active MMP1 (Mw ~63 and 52 kDa, respectively).

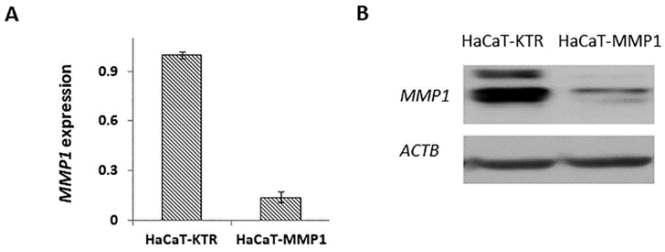

Figure 1 | MMP1 silencing in HaCaT cells. Analysis of gene (A) and protein expression (B) in the cells expressing shRNA directed to MMP1 (HaCaT-MMP1) compared to the cells expressing scrambled shRNA. (HaCaT-KTR). MMP1 expression level in non-stimulated HaCaT cells was referred to as 1. РНК-интерференция MMP1 в эпидермальных кератиноцитах HaCaT. Изменения концентрации мРНК (A) и белка (B) в клетках, экспрессирующих shРНК, специфичную к MMP1 (HaCaT-MMP1) и контрольную, т.н. "scrambled" shRNA (HaCaT-KTR). Соответствующий уровень MMP1 в нетрансдуцированных клетках принимали равным единице

3.2. Changes in cell proliferation

A comparative analysis of cell growth demonstrated that non-stimulated cells as well as the cells stimulated with either TNF or IL17 remained in the active growth phase (Figure 2A-C). The time-dependences of cell growth in linear coordinates suggested that the cells grew monotonously, i.e. the growth curves did not reach saturation for the time of observation. Despite untreated HaCaT-KTR and HaCaT-MMP1 cells did not exhibit significant differences in cell proliferation rate (Figure 2A), the proliferation rates of HaCaT-MMP1 cells treated with the named cytokines were significantly lower compared to HaCaT-KTR cells (Figure 2B and C). In addition, an exposure of HaCaT-MMP1 cells to IFN-γ irreversibly suspended their growth. The cells stopped dividing and shed off the growth surface (Figure 2D and E).

3.3. Analysis of cell migration :

The monitoring of cell migration revelead differences in the migration rates of HaCaT-MMP1 and HaCaT-C cells. Particularly, HaCaT-KTR cells gradually covered the scratch (Figure 3A). Moreover, either tested Th1 cytokine accelerated their migration compared to untreated HaCaT-KTR cells. In the same time, the migration rates of HaCaT-MMP1 cells treated with either IL17 or TNF, only slightly exceeded the migration rate of untreated HaCaT-KTR cells (Figure 3B). Moreover, either untreated HaCaT-MMP1 or HaCaT-MMP1 treated with IFN-γ mostly remained at the scratch edge for the time of experiment.

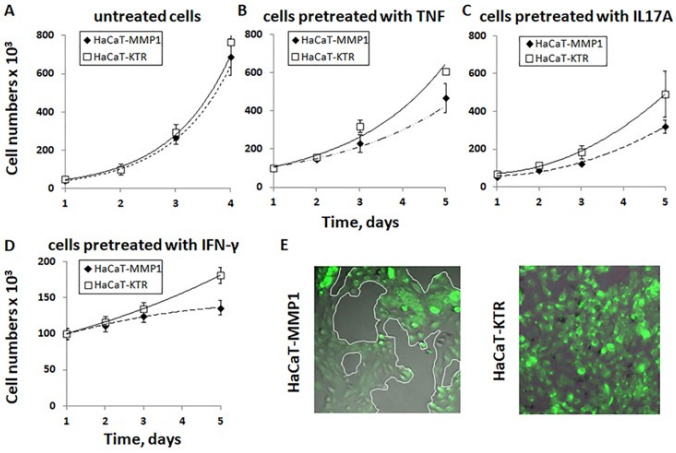

Figure 2 | Proliferation of MMP1-deficient and control HaCaT cells. A – cells not exposed to the cytokines; cells exposed to TNF (B), IL17 (C) and IFN-γ (D); E – Cell survival in the presence of IFN-γ. The cytokines were used at the following concentrations: TNF – 20 ng/mL, IFN-γ – 50 ng/mL; and IL17 – 50 ng/mL. Изменения скорости пролиферации в трансдуцированных эпидермальных кератиноцитах HaCaT. A – клетки, необработанные цитокинами; Клетки, обработанные TNF (B), IL17 (C) и IFN-γ (D); E – гибель клеток при культивировании с IFN-γ. Для проведения экспериментов использовали следующие концентрации цитокинов: TNF – 20 нг/мл, IFN-γ – 50 нг/мл и IL17 – 50 нг/мл

3.4 Analysis of gene expression:

To assess changes in gene expression caused by MMP1 silencing, we selected a pannel of ten genes. Six of these genes were involved into regulation of proliferation (CCNA2, CCND1 and MKI67) and differentiation (IVL, LOR and FLG) of epidermal keratinocytes. The others (KRT17, MMP1, MMP9 and MMP12) were associated with the pathogenesis of disease [12]. Then, we treated HaCaT-KTR and HaCaT-MMP1 cells with one of Th1 cytokines (TNF, IL17 or IFN-γ), obtained cDNA and performed qPCR.

The results of qPCR experiments demonstrated that each cytokine produced a distinct gene expression profile. In HaCaT-MMP1 cells, IFN-γ caused significant changes in expression of all ten genes (Table 1). In the same time, an exposure of these cells to IL17 did not change the expression of IVL and FLG, whereas their treatment with TNF (Table 1) did not cause significant changes in expression of MKI67 and LOR ($p > 0.05$). In addition, the expression of the terminal differentiation markers IVL, LOR and FLG in HaCaT-KTR cells treated with IL17 as well as the expression of CCNA2, MKI67 and KRT17 in HaCaT-KTR cells treated with TNF did not exceed 1.5 times their expression levels in non-stimulated HaCaT cells.

Importantly, some changes in gene expression that we observed were specifically linked to MMP1 silencing. The target gene MMP1 was downregulated in HaCaT-MMP1 cells even when the cells were exposed to high concentrations of proinflammatory cytokines. The expression of the cyclins CCNA2 and CCND1 changed in the opposite direction. Particularly, CCNA2 expression decreased, whereas CCND1 expression increased in HaCaT-MMP1 cells compared to HaCaT-KTR. In turn, the expression of the proliferation marker MKI67 was higher in HaCaT-MMP1 treated with either IFN-γ or IL17. In the same time, treatment of the named cells with TNF did not change MKI67 expression significantly. In addition, IL17 and TNF downregulated KRT17 in HaCaT-MMP1 cells, whereas the differences in KRT17 expression levels between HaCaT-KTR and HaCaT-MMP1 cells treated with IFN-γ were insignificant.

To explain the altered migration and proliferation of HaCaT-MMP1 cells treated with IFN-γ, we also compared the expression of IFN-γ–dependent proapoptotic markers – DAPK1 and the transcription factor IRF8 in both cell lines after their 24h exposure to the named cytokine. We found that both mentioned genes were upregulated in MMP1-deficient cells (Figure 4A). Moreover, HaCaT-MMP1 exhibited higher expression levels of the genes encoding cytokeratins -1, -10 and -14 (Figure 4B), compared to HaCaT-KTR cells.

4. Discussion

In this paper, we explored how MMP1 silencing in epidermal keratinocytes influenced the biological effects of proinflammatory cytokines TNF, IL17 and IFN-γ that play a crucial role in the pathogeneesis of psoriasis. After evaluation of MMP1 expression in HaCaT-MMP1 and HaCaT-KTR cells (Figure 1), we assessed changes in their migration and proliferation rates (Figure 2 and 3,

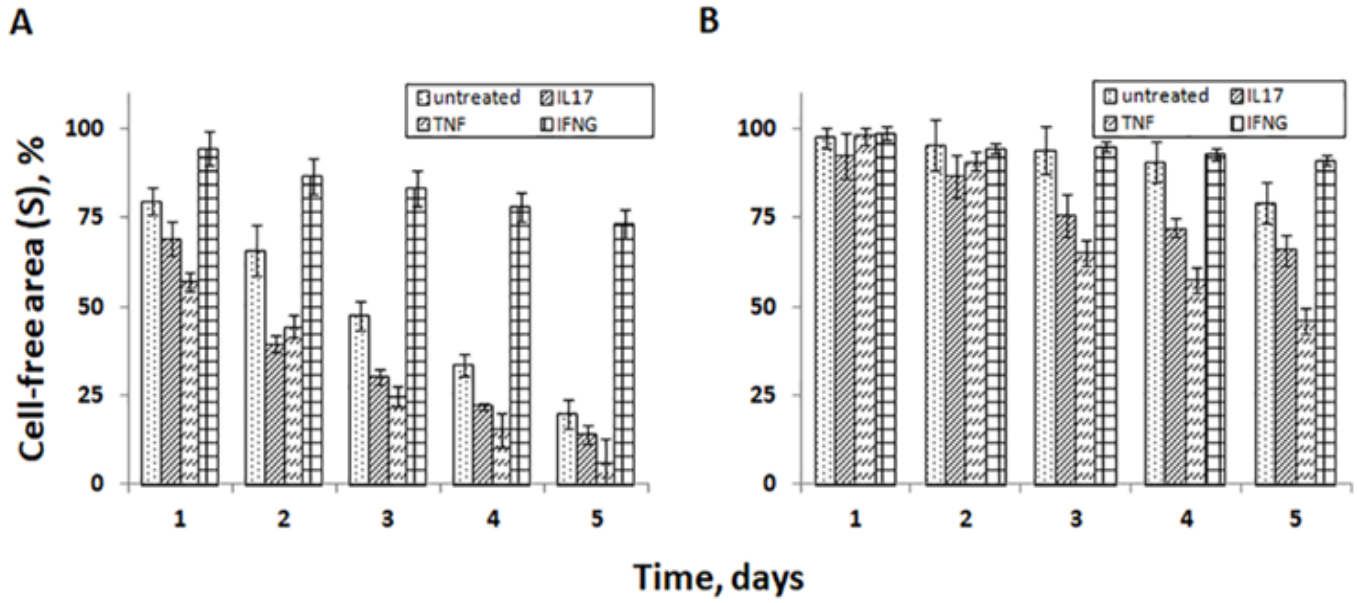

Figure 3 | Migration of MMP1-deficient and control HaCaT cells. Experimental data that reflect the cell migration in real time are represented in linear coordinates: A – HaCaT-KTR; B-HaCaT-MMP1. The cytokines were used at the following concentrations: TNF – 20 ng/mL, IFN-γ – 50 ng/mL; and IL17 – 50 ng/mL. Оценка скоростей миграции в трансдуцированных эпидермальных кератиноцитах HaCaT. Изменения в миграции клеток HaCaT-KTR (A) и HaCaT-MMP1 (B) представлены в линейных координатах. Для проведения экспериментов использовали следующие концентрации цитокинов: TNF – 20 нг/мл, IFN-γ – 50 нг/мл и IL17 – 50 нг/мл.

Table 1 | Gene expression in MMP1-deficient and control cells cultured in the presence of proinflammatory cytokines IFN-γ, TNF and IL17.The cells were treated with one of the mentioned cytokines – IFN-γ (A), IL17 (B) or TNF (C) for 24h. The cytokines were used at the following concentrations: IFN-γ – 50 ng/mL, IL17 – 50 ng/mL or TNF – 20 ng/mL. Gene expression in the parental cell line, i.e. HaCaT cells treated with vehicle control, was referred to as 1-fold relative expression. Изменения экспрессии генов в эпидермальных кератиноцитах HaCaT-MMP1 и HaCaT-MMP1 после их обработки провоспалительными цитокинами IFN-γ, TNF и IL17. Клетки культивировали в присутствии цитокинов IFN-γ (A), IL17 (B) или TNF (C) в течение 24ч. Для проведения экспериментов использовали следующие концентрации цитокинов: TNF – 20 нг/мл, IFN-γ – 50 нг/мл и IL17 – 50 нг/мл.. Уровень экспрессии указанных генов в клетках HaCaT-KTR, обработанных буферным раствором, который не содержал цитокинов, принимали равным единице.

Genes	TNF			IL17			IFN-γ		
	HaCaT-KTR	HaCaT-MMP1	*p*-value	HaCaT-KTR	HaCaT-MMP1	*p*-value	HaCaT-KTR	HaCaT-MMP1	*p*-value
CCNA2	1.11 ± 0.17	0.40 ± 0.06	0.002	0.32 ± 0.05	0.13 ± 0.20	0.020	0.31 ± 0.05	0.24 ± 0.04	0.080
CCND1	0.32 ± 0.05	1.43 ± 0.21	< 0.001	0.13 ±0.02	0.71 ± 0.11	0.107	0.007 ± 0.001	0.02 ± 0.003	< 0.001
MKI67	1.40 ± 0.21	1.07 ± 0.16	0.096	3.80 ± 0.57	5.66 ± 0.89	0.849	1.06 ± 0.16	7.01 ± 1.05	< 0.001
MMP1	1.44 ± 0.01	0.41 ± 0.003	< 0.001	1.02 ± 0.15	0.28 ± 0.04	0.041	3.22 ± 0.48	0.02 ± 0.003	0.003
MMP9	32.15 ± 0.30	25.35 ± 0.24	< 0.001	11.14 ± 1.14	2.29 ± 0.37	0.366	0.57 ± 0.09	1.60 ± 0.24	0.015
MMP12	0.02 ±0.003	0.34 ± 0.05	0.004	7.58 ± 0.65	2.44 ± 0.16	0.161	8.43 ± 1.27	11.10 ±1.67	0.272
KRT17	0.97±0.15	0.35 ± 0.06	0.002	1.64 ± 0.15	0.19 ± 0.02	0.020	2.00 ± .30	2.18 ± 0.33	0.516
IVL	1.83±0.27	1.80 ± 0.27	0.955	1.44 ± 0.24	1.01 ± 0.12	0.115	2.00 ± 0.30	3.98 ± 0.60	0.041
LOR	0.58±0.09	1.35 ± 0.20	0.083	1.15 ± 0.11	1.79 ± 0.17	0.168	0.56 ± 0.08	0.54 ± 0.08	0.898
FLG	0.32±0.02	0.28 ± 0.02	0.372	1.26 ± 0.27	0.89 ± 0.15	0.145	5.77 ± 0.87	13.19 ± 1.98	0.026

respectively). We also compared the expression of genes that are associated with the disease, regulate cell proliferation and the terminal differentiation (Table 1). In addition, we verified the expression of proapoptotic factors DAPK1 and IRF8 and cytokeratins in the cells treated to IFN-γ (Figure 4).

Previously, it was shown that MMP1 silencing changes the morphological characteristics of epidermal keratinocytes [18]. Unlike the cells that expressed scrambled shRNA and preserved a familiar cobblestone-like appearance, MMP1-deficient cells grew in spots, climbed each other and formed layers before they could cover the growth surface. Moreover, the collonies of HaCaT-MMP1 exhibited sharp boundaries, whereas the boundaries of the colonies formed by HaCaT-KTR cells were blurred.

Assuming that MMP1-deficiency influenced the strength of intercellular contacts, we verified how it could affect the cell migration in the presence of proinflammatory cytokines – IL17, TNF and IFN-γ. We found that the ability of MMP1-deficient cells to migrate was impaired and their migration rates did not exceed the migration rate of untreated control cells. For this reason, we assume that MMP1 silencing could be used to suppress structural rearrangements in lesional skin.

Then, we verified how MMP1 silencing could influence the cell proliferation. Surprisingly, when we compared untreated cells we did not see any significant difference between MMP1-deficient and control cells. In contrast, the proliferation rate of MMP1-deficient cells significantly decreased after we treated the cells with either IL-17 or TNF.

Analyzing qPCR data, we found significant changes in MKI67 expression in HaCaT-MMP1 cells treated with IFN-γ. Previously, it was shown that MKI67 is induced in all phases of the cell cycle, except the interphase [20]. In this respect, MKI67 expression level in cultured cells reflects the total number of cells entered the cycle rather than their proliferation rate. For this reason, we also verified whether MMP1-silencing affects the cytokine balance in HaCaT-KTR and HaCaT-MMP1 cells and found that treatment of HaCaT-MMP1 with either TNF or IL17 shifts the balance between CCNA2 and CCND1 in favor of CCND1 (Table 1). To the references, the named cyclins are key regulators of cell cycle. Particularly, CCNA2 controls the transition from G2 to M-phase of cell cycle. In turn, CCND1 is needed for the G1/S transition [21,22]. In this context, we would like to acknowledge that changes in the expression CCNA2 and CCND1 in lesional psoriatic skin are quite opposite to ones that we see in HaCaT-MMP1 cells. Compared to uninvolved skin, the skin samples obtained from lesional skin exhibit a 2-fold decrease in CCND1 [23] and an 8.7-fold increase in CCNA2 [24] expression. Respectively, a shift in the expression of cyclins that we observe in real-time PCR experiments explains why MMP1-deficienct cells exhibit lower proliferation rate.

However, the most dramatic changes we observe in the presence of IFN-γ. Particularly, we see that MMP1-deficient cells stopped proliferating and detached from the growth surface. To explain this phenomenon, we compared the DAPK1 and IRF8 in the cells treated with IFN-γ.

DAPK1 and IRF8 in the cells treated with IFN-γ. Respectively, we found that their expression levels were higher in HaCaT-MMP1 cells. We also discovered a higher expression of the late differentiation markers loricrin and filaggrin (Table 1) as well as the genes encoding KRT1, -5, -10 and -14. The observed changes in gene expression suggested us that MMP1-silencing could potentially trigger apoptosis and shift the balance between differentiation and proliferation in epidermal keratinocytes toward differentiation.

Notably, the changes in the expression of KRT17 that we observe in response to either IL17 or TNF are opposite to ones that occur in lesional psoriatic skin [25]. In the skin of lab animals, suppression of KRT17 that is often referred to as a "key gene" of psoriasis [26,27] prevents hyperplasia, i.e. thickening of the epidermis due to more intensive cell division and lowering the intensity of inflammatory process. In contrast, an induction of KRT17 stimulates the secretion of Th1 chemokines, such as CXCL5, -9, -10, -11 [26]. For this reason, downregulation of KRT17 caused by MMP1 silencing could be beneficial for the psoriasis patients. Particularly, MMP1 silencing in epidermal keratinocytes could attenuate the inflammatory response and suppress hyperplasia in lesional psoriatic skin.

5. Concluding Remarks

In conclusion, we would like to summarize our key findings:

1. In the cultured epidermal keratinocytes, MMP1-deficiency shifted the balance between differentiation and proliferation toward differentiation. Respectively, MMP1-deficiency can be used to stimulate the terminal differentiation of epidermal keratinocytes in lesional skin.

2. Unlike the cells where MMP1 expression was not affected by shRNA, MMP1-deficient cells were susceptible to apoptosis in the presence of IFN-γ. Respectively, MMP1-deficiency can be used to promote apoptosis in lesional epidermis where IFN-γ is elevated.

3. In addition, MMP1 targeting could be beneficial for psoriasis due to its antiproliferative effect in the presence of proinflammatory cytokines. Respectively, MMP1-deficiency can be used to normalize the proliferation rate of epidermal keratinocytes in diseased skin.

We would also acknowledge that delivery of MMP1 shRNA to diseased skin is a challenging task that requires an optimization of existing delivery systems to make the genetic material of interest (shRNA, genetically modified virions etc.) capable of penetrating the skin barrier.

Заключение

В заключение, мы хотели бы обобщить основные результаты нашей работы.

1. «Нокдаун» MMP1 в культивируемых эпидермальных кератиноцитах приводит к смещению баланса между их дифференцировкой и пролиферацией в сторону дифференцировки. По этой причине, РНК-интерференцию MMP1 можно использовать для того, чтобы стимулировать терминальную дифференцировку эпидермальных кератиноцитов в пораженной болезнью коже.

2. В отличие от клеток с нормальным уровнем экспрессии MMP1 эпидермальные кератиноциты с пониженным уровнем экспрессии этого гена подвержены апоптозу в присутствии IFN-γ. В силу

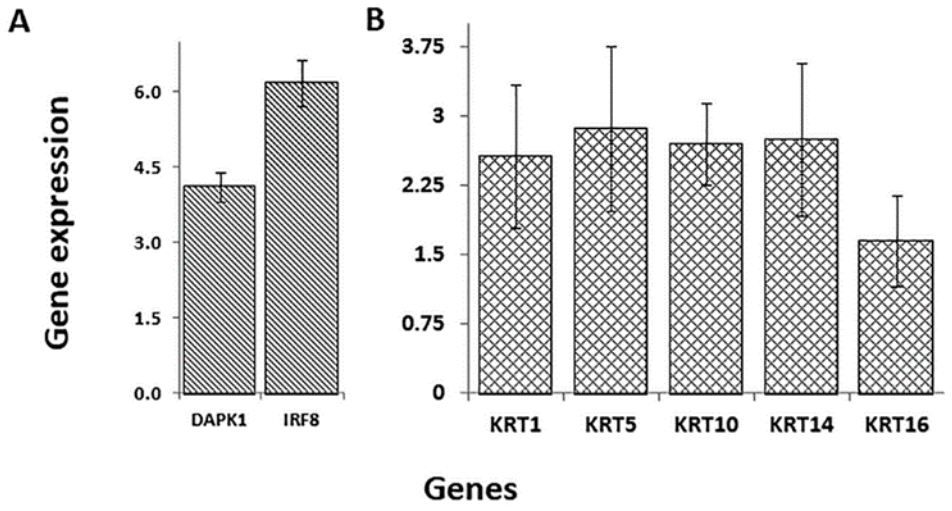

Figure 4 | Migration Expression of proapoptotic factors and cytokeratines in MMP1-deficient cells exposed to IFN-γ. The cells were treated with IFN-γ (50 ng/mL) for 24h. A – expression of proapoptotic factors and B – expression of cytokeratins. Gene expression in HaCaT-KTR cells treated with IFN-γ, was referred to as 1-fold relative expression. Уровень экспрессии маркеров апоптоза и цитокератинов в эпидермальных кератиноцитах HaCaT-MMP1, обработнных IFN-γ. Клетки культивировали в присутствии IFN-γ (50 нг/мл) в течение 24ч. Экспрессия маркеров апоптоза (A) и генов, кодирующих цитокератины (B). Уровень экспрессии указанных генов в клетках HaCaT-KTR, обработанных IFN-γ, принимали равным единице.

этого, снижение уровня экспрессии MMP1 можно использовать для того, чтобы инициировать апоптоз в псориатическом эпидермисе, где концентрация IFN-γ превышает нормальные физиологические значения.

3. Наконец, РНК-интерференция MMP1 может иметь клиническое значение для псориаза, поскольку присутствие провоспалительных цитокинов в культуральной среде приводит к снижению скорости пролиферации клеток с дефицитом MMP1. Соответственно, «нокдаун» MMP1 можно использовать для того, чтобы снизить скорость пролиферации эпидермальных кератиноцитов in vivo.

Мы также хотели бы отметить, что в настоящее время проведение РНК-интерференции в терапевтических целях все еще является трудновыполнимой задачей, поскольку эпидермис, являясь естественным барьером на пути чужеродных биомолекул, эффективно мешает их проникновению в кожу. Решение этой задачи потребует разработки более эффективных способов трансфекции клеток, находящихся в коже больного

Acknowledgements

The authors are grateful to Prof. E.S. Piruzian for critical analysis of the manuscript and fruitful discussion of the obtained results. We also declare no conflict of interest .

References

[1] J.E. Greb, A.M. Goldminz, J.T. Elder, Nat. Rev. Dis. Primers. 2 (2016) 16082. DOI: 10.1038/nrdp.2016.82

[2] I.M. Michalek, B. Loring, S.M. John. J, Eur. Acad. Dermatol. Venerol. 31 (2017) 205–212. DOI: 10.1111/jdv.13854

[3] I.V. Khamaganova, A.A. Almazova, G.A. Lebedeva, A.V. Ermachenko. Klinicheskaya, dermatologiya i venerologiya. 1 (2015) 12-16. DOI: 10.17116/klinderma2015112-16

[4] M. Lebwohl. Ann, Intern. Med. 168 (2018) 49–64. DOI: 10.7326/AITC201804030

[5] N. Agrawal, P.V. Dasaradhi, A. Mohmmed, P. Malhotra, R.K. Bhatnagar, S.K, Mukherjee. Microbiol. (2003) Mol. Biol. Rev. 67 (2003) 657-685. DOI: 10.1128/MMBR.67.4.657-685.2003

[6] N. Kirschner, C. Poetzl, P. von den Driesch, E. Wladykowski, I. Moll, M.J. Behne, J.M. Brandner, Am J Pathol. 175 (2009) 1095-106. DOI: 10.2353/ajpath.2009.080973.

[7] V. Noe, B. Fingleton, K. Jacobs, H.C. Crawford, S. Vermeulen, W. Steelant, E. Bruyneel, L.M. Matrisian, M. Mareel, J. Cell Sci. 114 (2001) 111-118.

[8] N. Cirillo, F. Femiano, F. Gombos, A. Lanza, Oral Dis. 13 (2007) 341-345. DOI: 10.1111/j.1601-0825.2006.01287.x

[9] C. Li., S. Lasse, P. Lee, M. Nakasaki, S.W. Chen, K. Yamasaki, R.L. Gallo, C. Jamora C, Proc. Natl. Acad. Sci. USA. 107 (2010) 22249-22254. DOI: 10.1073/pnas.1009751108

[10] A. Mezentsev, A. Nikolaev, S. Bruskin, Gene 540 (2014) P. 1–10. DOI: 10.1016/j.gene.2014.01.068

[11] L. Nissinen, V.M. Kahari, Biochim. Biophys. Acta. 1840 (2014) 2571–2580. DOI: 10.1016/j.bbagen.2014.03.007

[12] N.L. Starodubtseva, V.V. Sobolev, A.G. Soboleva, A.A. Nikolaev, S.A., Bruskin. Genetika 47 (2011) 1117–1123. DOI: 10.1134/S102279541109016X

[13] J.A. Mogulevtseva, A.V. Mezentsev, Wschodnioeuropejskie czasopismo naukowe 9 (2016) 85–93.

[14] J.A. Mogulevtseva, A.V. Mezentsev, Progress in modern science: theoretical and practical aspects 6 (2016) 70–77.

[15] J.A. Mogulevtseva, A.V. Mezentsev. Progress in modern science: theoretical and practical aspects 13 (2017) 123–134.

[16] V. Ranta, A. Orpana, O. Carpén, U. Turpeinen, O. Ylikorkala, L. Viinikka. Crit. Care Med. 27 (1999) 2184–2187.

[17] NCBI Probe. (2018) https://www.ncbi.nlm.nih.gov/probe/

[18] Y.A. Mogulevtseva, A.V. Mezentsev, S.A. Bruskin. Bulletin of RSMU 3 (2017) 35–42. DOI: 10.24075/brsmu.2017-03-04

[19] C.T. Rueden, J. Schindelin, M.C. Hiner, B.E. DeZonia, A.E. Walter, E.T. Arena, K.W. Eliceiri, BMC Bioinformatics 18 (2017) 529. DOI:10.1186/s12859-017-1934-z.

[20] S. Bruno, Z. Darzynkiewicz. Cell. Prolif. 25 (1992) 31–40.

[21] M. Pagano, R. Pepperkok, F. Verde, W. Ansorge, G. Draetta, EMBO J. 11 (1992) 961–971.

[22] H. Matsushime, M.E. Ewen, D.K. Strom, J.Y. Kato, S.K. Hanks, M.F. Roussel, C.J. Sherr, Cell. 71 (1992) 323–334.

[23] C.P. Prasad, S.D. Gupta, G. Rath, R. Ralhan, Oncology. 73 (2007) 112–117. DOI: 10.1159/000120999

[24] M. Manczinger, L. Kemény, PLoS One. 8 (2013) e80751. DOI: 10.1371/journal.pone.0080751

[25] R.P. Nair, K.C. Duffin, C. Helms, J. Ding, P.E. Stuart, D. Goldgar, J.E. Gudjonsson, Y. Li, T. Tejasvi, B.J. Feng, A. Ruether, S. Schreiber, M. Weichenthal, D. Gladman, P. Rahman, S.J. Schrodi, S. Prahalad, S.L. Guthery, J. Fischer, W. Liao, P.Y. Kwok, A. Menter, G.M. Lathrop, C.A. Wise, A.B. Begovich, J.J. Voorhees, J.T. Elder, G.G. Krueger, A.M. Bowcock, G.R. Abecasis, Nat. Genet. 41 (2009) 199–204. DOI: 10.1038/ng.311.

[26] A.A. Al Robaee, Int. J. Health Sci. (Qassim). 4 (2010) 103–127.

[27] L. Jin, G. Wang. Med. Res. Rev. 34 (2014) 438–454. DOI: 10.1002/med.21291

JOURNAL OF INTEGRATED OMICS
A METHODOLOGICAL JOURNAL
HTTP://WWW.JIOMICS.COM

ORIGINAL ARTICLE | DOI: 10.5584/jiomics.v9i1.272

Thiaminase process is present in the brain of mammals

S. A. Petrov*, A. V. Zaharov, O. I. Stanev , O. K. Budnyak

Department of Biochemistry, Odessa I.I. Mechnikov National University, Odessa, Ukraine.

Received: 09 January 2019 **Accepted:** 03 May 2019 **Available Online**: 14 June 2019

ABSTRACT

The presence of the thiaminase process in the brain of rabbits and bulls has been established. Most intensively this process takes place in the pituitary gland. Production of adrenocorticotropic hormone is significantly reduced as a result of the formation of 4-methyl-5β-oxyethylthiazole in this part of the brain.

Аннотация

Установлено наличие тиаминазного процесса в мозге кроликов и быков. Наиболее интенсивно этот процесс происходит в гипофизе. Продукция адренокортикотропного гормона значительно снижается в результате образования 4-метил-5β-оксиэтилтиазола в этой части мозга.

Keywords: Thiaminase, brain, pituitary gland, 4-methyl-5β-oxyethylthiazole, ACTH, TSH

1. Introduction

Thiaminase is an enzyme that divides thiamine into two parts-4-methyl-5β-oxyethylthiazole and 2,5-dimethyl-4-aminopyrimidine. There are two forms of thiaminase - thiaminase I and thiaminase II.

Thiaminase I catalyzes the cleavage of thiamine with subsequent adherence to the pyrimidine fragment of the nitrogenous base. Tiaminase II carries out the hydrolysis of thiamine into the two above-mentioned components [1].

The presence of thiaminase I is proven in tissues of fish, intestinal cavities, mumps, and some microorganisms [1]. Thiaminase II is present exclusively in microorganisms, in particular *Bac. alvei, Bac. brevis, Bac. firmus, Bac. subtilis* and some others [2].

Until recently, it was generally accepted that in human and other mammals, the thiamine decompositiondown to the thiazole and pyrimidine components was carried out exclusively in the intestines at the expense of its microflora, in particular *Bac. aneurinolyticus* [3], *Clostridium thiaminolyticum* [4], *Bacillus thiaminolyticus* [5] and some others.

However, since the 1960s of the last century, there were single studies that showed the presence of 4-methyl-5β-oxyethylthiazole in the urine of sterile animals [6], which proves the possibility of the thiaminase process existencedirectly in the tissues. In our laboratory, a significant increase in the level of 4-methyl-5β-oxyethylthiazole in the brain of rats after parenteral administration of 14C-thiamine [7] was demonstrated. Linkage of the thiazole with nervous system proteins has been demonstrated in a recently published work [8].

Studies of thiaminase pathways are considered in the works [9-11], however, studies on the functioning of thiaminase and its physiological significance in the brain do not exist.

***Corresponding author:** Sergiy Anatoliyovich Petrov, doctor of biological sciences, professor of Odesa National Mechnykov I. I. University, Department of Biochemistry, 2, Dvoryanska Str., Odesa, 65082, Ukraine.

Table 1 | The content of thiamine and its metabolites in blood taken from the jugular vein, *venae jugularis externa*, after injection of thiamine into the carotid artery (μg/ml of blood) n=8. * – the difference with the control group is significant (p≤0.05). Содержание тиамина и его метаболитов в крови, взятой из яремной вены, *venae jugularis externa*, после введения тиамина в сонную артерию (мкг / мл крови) n = 8. * - различия с контрольной группой достоверны (p≤0,05).

Parameter	Control	1 minute	2 minutes	5 minutes	10 minutes
T-S-S-T	0.070±0.006	0.095±0.010	0.120±0.011*	0.155±0.017*	0.160±0.014*
TPP	0.355±0.037	0.470±0.048	0.595±0.061*	0.590±0.058*	0.590±0.062*
Thiamine	0.795±0.080	0.510±0.040*	0.400±0.038*	0.405±0.041*	0.410±0.039*
4-methyl-5β-oxyethylthiazole	0.030±0.003	0.055±0.004*	0.085±0.007*	0.085±0.009*	0.090±0.009*

2. Material and Methods

All studies were carried out on rabbits of 3-3.5 years old and the brain of bulls. The norms of the European convention on carrying out experiments with vertebrates have been adhered to the current research.

The content of thiamine and TPP was measured by fluorimetric method [12]. The content of 4-methyl-5β-oxyethylthiazole was determined after separation of thiamine and its metabolites using spectrophotometry after column chromatography at 253 nm [13].In this work, DEAE -cellulose was used for the chromatographic separation of thiamine metabolites, since the stability constants of their complexes, which are formed, and, therefore, their adsorption properties at certain pH differ very significantly.

Thiamine disulfide was determined by the fluorimetric method [1].

Determination of adrenocorticotropic (ACTH) and thyroid stimulating (TT) hormones was carried out by immunoassay analysis [14, 15].

The obtained results are processed by methods of variation statistics. The normality of distribution is rechecked using [16]. Values are reported as means ± SE. For further analysis, the Student's t-test was used, or its modification - Newman–Keuls method by Glantz S., 1999 [17]. Statistical significance was considered to be $p \leq 0.05$.

3. Results

We started research on whether the thiaminase process in the brain was present. For this, 1 mg of thiamine was injected into the carotid artery (arteria carotis externa) of rabbit and in 1, 2, 5, and 10 minutes blood samples from the jugular vein (venae jugularis externa) were collected and the content of thiamine, TPP, thiamine disulphide (TSST) and 4 -methyl-5β-oxyethylthiazole were determined.

The results of this study are presented in Table 1.

The obtained results indicate that injections of thiamine into the carotid artery arteria carotis externa lead to its rather rapid metabolism in the brain tissues. So, 1 minute after injection, a significant increase in the content of 4-methyl-5β-oxyethylthiazole was observed due to a decrease in the thiamine content, indicating a rapid decay in the brain. Two minutes after injection, the level of 4-methyl-5β-oxyethylthiazole continued to increase, the amount of TPP and T-S-S-T also increased, while the thiamine level continued to decrease. In 5 and 10 minutes, further significant changes in the level of thiamine and its metabolites in the blood were not observed.

Thus, this part of the research shows that after thiamine entrance into the brain, the transformation of its part first occurs due to thiaminasedecomposition. Later, the remnants of free thiamine are converted into coenzyme (TPP) and into the reserve form T-S-S-T.

The next step of our research was to find out in which part of the brain thiaminase process is most intense. These data are shown in Tables 2 and 3.

To solve this problem, the following parts of the brain of the bull were separated: cortex, pons, cerebellum, pituitary gland, thalamus + hypothalamus and corpus callosum. Each department was perfused with glucose solution with thiamine at a certain concentration for 5 minutes. The content of thiamine, TPP and 4-methyl-5β-oxyethylthiazole was determined before and after perfusion.

The results presented in Table 2 indicate that the highest content of free thiamine was observed in the corpus callosum.

In all other investigated brain departments, except for cortex, it does not differ significantly. In the cortex, this value was more than twice as low. The TPP content was the largest in the corpus callosum, it was slightly lower in the pons, the pituitary gland and thalamus + hypothalamus. The smallest one was registered in the cortex. The level of 4-methyl-5β-oxyethylthiazole was highest in the corpus callosum, and the lowest in thalamus + hypothalamus.

Perfusion with thiamine and glucose increased the level of free thiamine in the corpus callosum, while the level of TPP significantly increased in all of the studied brain departments, but the greatest effect was established in the pons and thalamus + hypothalamus. Under these conditions, the level of 4-methyl-5β-oxyethylthiazole was significantly increased in the pituitary gland and cortex. In the cerebellum this increase was less pronounced.

Thus, relatively high doses of thiamine resulted in its accumulation in the unchanged form in the corpus callosum. Subsequently, its part was converted into the

Table 2 | The content of thiamine, TPP and 4-methyl-5β-oxyethylthiazole in the brain parts of the bull after perfusion with thiamine (1 mg / ml) solution (mg/g of tissue) n=8. * – the difference with the baseline group is significant (p≤0.05). Содержание тиамина, ТПП и 4-метил-5β-оксиэтилтиазола в отделах головного мозга быка после перфузии раствором тиамина (1 мг / мл) (мг / г ткани) n = 8. * - различия с соответствующим контролем достоверны (p≤0,05).

Brain department	Thiamine		TPP		4-methyl-5β-oxyethylthiazole	
	baseline	increase	baseline	increase	baseline	increase
Cortex	0.36±0.02	2.12±0.04*	0.66±0.05	5.54±0.23*	0.64±0.08	4.46±0.05*
Pons	0.78±0.02	2.12±0.07*	0.92±0.04	4.46±0.20*	0.62±0.06	1.40±0.04*
Cerebellum	0.78±0.02	1.76±0.56*	0.80±0.17	1.82±0.45*	0.42±0.07	1.32±0.08*
Pituitary gland	0.64±0.07	2.64±0.24*	0.90±0.06	7.18±0.31*	0.58±0.06	8.62±0.13*
Thalamus + hypothalamus	0.72±0.04	2.78±0.18*	0.92±0.14	4.16±0.13*	0.14±0.02	0.50±0.03*
Corpus callosum	0.88±0.02	6.24±0.10*	1.04±0.11	6.12±0.04*	0.86±0.02	1.20±0.11*

Table 3 | Increase of thiamine, TPP and 4-methyl-5β-oxyethylthiazole content in the bovine brain sections with perfusion of thiamine (0.1 mg/ml) (μg/g of tissue) n=8. Увеличение содержания тиамина, ТПП и 4-метил-5β-оксиэтилтиазола в отделах головного мозга крупного рогатого скота при перфузии тиамина (0,1 мг / мл) (мкг / г ткани) n = 8

Brain department	Thiamine	TPP	4-methyl-5β-oxyethylthiazole
Cortex	1.16±0.05	1.98±0.09	0.92±0.05
Pons	1.10±0.03	2.10±0.08	0.86±0.02
Cerebellum	0.96±0.05	1.76±0.05	0.84±0.04
Pituitary gland	1.06±0.04	1.38±0.24	1.36±0.20
Thalamus + hypothalamus	1.06±0.04	1.98±0.19	0.60±0.10
Corpus callosum	2.16±0.17	1.82±0.05	0.68±0.12

Table 4 | Determination of the concentration of ACTH and TSH in blood taken from the jugular vein after administration of 4-methyl-5β-oxyethylthiazole solution in the carotid artery at a concentration of 1 mg/ml (μM/ml of blood) n=8. * – the difference with the control group is significant (p≤0.05). Определение концентрации АКТГ и ТТГ в крови, взятой из яремной вены, после введения раствора 4-метил-5β-оксиэтилтиазола в сонную артерию в концентрации 1 мг / мл (мкМ / мл крови) n = 8. * - различия с контрольной группой достоверны (p≤0,05).

Time after administration	ACTH	TSH
Control	15.0±0.9	6.0±0.5
5 minutes	10.1±0.8*	5.0±0.5
10 minutes	8.2±0.7*	4.2±0.4*
15 minutes	6.1±0.7*	3.5±0.4*
20 minutes	4.0±0.3*	1.0±0.2*

major coenzyme form of TPP in all parts of the brain, but to a greater extent in the pons and thalamus + hypothalamus. Intensive thiamine decompositionby thiaminase occurred in the pituitary gland and cortex.

A decrease in the thiamine dose to 0.1 mg / ml resulted in the following effects (Table 3).

The results presented in Table 3 indicate that with the use of 0.1 mg/kg of thiamine, the highest amount of free thiamine was present in the corpus callosum, as with after the use of 1 mg / ml. In other parts of the brain its contents did not differ significantly. The content of TPP in all studied brain departments, except for the pituitary gland, was almost similar. In the pituitary glandit was the smallest. As for 4-methyl-5β-oxyethylthiazole, its content was significantly higher in the pituitary gland than in other parts of the brain.

Thus, this part of our study suggests that thiaminase pathway of thiamine decomposition takes place in the brain, resulting in the formation of 4-methyl-5β-oxyethylthiazole. This processis most intensive in the pituitary gland.

To find out the possible specific physiological function of 4-methyl-5β-oxyethylthiazole in the pituitary gland, we conducted the next series of studies.

We injected 4-methyl-5β-oxyethylthiazole solution into the carotid artery of the rabbit, and after 5, 10, 15 and 20 minutes, the blood from the jugular vein was taken out and the content of ACTH and TSH was measured. The control included administration of saline solution. Data for this series are presented in Table 4.

As can be seen from the data presented in Table 4, administration of 4-methyl-5β-oxyethylthiazole in the carotid artery at a concentration of 1 mg/ml resulted in a significant decrease in both ACTH and TSH levels in 20 minutes after administration. The level of ACTH was reduced by almost 4-fold, and SH - 6 times in 20 minutes after injection.

When the concentration of 4-methyl-5β-oxyethylthiazole was reduced by 100 times to a concentration of 10 μg/ml, which corresponds to the physiological concentration in the blood, we obtained the following results (Table 5).

The results presented in Table 5 indicate that physiological concentrations of 4-methyl-5β-oxyethylthiazole can reduce the level of ACTH, while they do not affect the level of TSH.

Table 5 | Determination of the concentration of ACTH and TSH in blood taken from the jugular vein after the introduction of 4-methyl-5β-oxyethylthiazole solution in a carotid artery at a concentration of 10 μg/ml (μM/ml of blood) n=8. * – the difference with the control group is significant (p≤0.05). Определение концентрации АКТГ и ТТГ в крови, взятой из яремной вены, после введения раствора 4-метил-5β-оксиэтилтиазола в сонную артерию в концентрации 10 мкг / мл (мкМ / мл крови) n = 8. * - различия с контрольной группой достоверны (p≤0,05).

Time after administration	ACTH	TSH
Control	15.0±1.1	11.0±1.2
5 minutes	14.0±0.9	11.0±1.0
10 minutes	13.6±1.3	11.0±1.0
15 minutes	11.1±0.9*	10.2±1.1
20 minutes	12.0±0.9*	10.1±1.2

The obtained data confirm the presence of enzymatic degradation of thiamine in the brain. The discovery of this 4-methyl-5β-oxyethylthiazoledegradation product in the body was reported in 1969 [6]. It is important to note that this experiment was conducted on sterile animals, which excluded the participation of microorganisms in this process. In our laboratory, this fact has been confirmed [7].

In 2015, a large international team of researchers reported the interaction of thiazole and its derivatives with proteins of the nervous system [8].

In our study, it was established that the formation of this product of thiaminase reaction in the brain occurs in its different parts, but the most intensively this process is conducted in the pituitary gland. According to our data, the physiological role of this process includes inhibition of adrenocorticotropic hormone adenohypophysis.

This fact agrees well with the observations of several authors on the influence of thiamine on some processes with the regulatory participation of adrenaline, in particular carbohydrates metabolism [18].

In the future, we are going to isolate and purify thiaminase using first classical methods, such as salting out, dialysis, column chromatography on different carriers and electrophoresis to assess the degree of purification of the enzyme.

4. Concluding Remarks

Thus, the materials presented in this study indicate the existence of hormone-mediated non-enzymatic function of the product of the thiaminase process of 4-methyl-5β-oxyethylthiazolemammalian brain.

Заключение

Таким образом, материалы, представленные в этом исследовании, указывают на существование гормон-опосредованной неферментативной функции продукта тиаминазного процесса 4-метил-5β-оксиэтилтиазола мозга млекопитающих.

References

[1] Y. M. Ostrovsky Experimental vitaminology, Minsk: Science and Technology, (1979) 551.

[2] F. Shimomura, J. Ogata, H. Nakayama, R. HayashiJ Vitaminol (Kyoto) 10;3(2) (1957) 96-105.

[3] H. Ikehata J. Vitaminol. 2(3) (1956) 242-244.

[4] R. Kimura, T. H. Liao Proceedings of the Japan Academy 29 (1953) 132-133.

[5] D. Matsukawa, S. Chang, M. Fujimiya, H. MisawaJ Vitaminol (Kyoto) 101(2) (1955) 53-55.

[6] T. Matsuo, Z. Suzuoki J Biochem. 65(6) (1969) 953-60.

[7] S.A. Petrov Fiziol Zh. 38(2) (1992) 79-85.

[8] Garik Mkrtchyan, Vasily Aleshin, Yulia Parkhomenko, Thilo Kaehne, Martino Luigi Di Salvo, Alessia Parroni, RobertoContestabile, Andrey Vovk, Lucien Bettendorff, and Victoria BunikSci Rep. 5 (2015) 12583. doi: 10.1038/srep12583

[9] C. A. Kreinbring, S. P. Remillard, P. Hubbard, H. R. Brodkin, F. J. Leeper, D. Hawksley, E. Y. Lai, C. Fulton, G. A. Petsko, D. Ringe. Proc Natl Acad Sci U S A. 111(1) (2013) 137-42. doi: 10.1073/pnas.1315882110

[10] Amy Haas Jenkins, Ghislain Schyns, Sébastien Potot, Guangxing Sun & Tadhg P Begley Nat. Chem. Biol. 3 (2007) 492–497. DOI:10.1038/nchembio.2007.13

[11] Lucien Bettendorff Nat. Chem. Biol. 3 (2007) 454–455. DOI https://doi.org/10.1038/nchembio0807-454

[12] G. D. Eliseeva Vitamins 1 (1953) 38-57.

[13] O. A. Volkov, M. G. Magla, O. O. Prutyanova, S. A. Petrov Bulletin of the Odessa National University 9(1) (2004) 34-38.

[14] E. Engall, Methods in Enzymology, Academic Press, New York, 70, (1980) 419- 492

[15] Dorothy T. Krieger, Anthony S. Liotta, Toshiro Suda, Abraham Goodgold, Edward Condon The Journal of Clinical Endocrinology & Metabolism48 (4) 1 (1979) 566–571. https://doi.org/10.1210/jcem-48-4-566

[16] S.N. Lapach, A.V. Chubenko, P.N. Babich. Statistical methods in biomedical research using Excel, Kyiv: Morion, (2003) 408

[17] S. Glantz Biomedical statistics. Moscow: Practice, (1999) 460

[18] V.V. Vinogradov Non-enzyme vitaminology. Grodno, (2000) 535

JOURNAL OF INTEGRATED OMICS
A METHODOLOGICAL JOURNAL
HTTP://WWW.JIOMICS.COM

ORIGINAL ARTICLE | DOI: 10.5584/jiomics.v9i1.261

Thiochrome activates DNA polymerase

V. E. Yakimenko, O. K. Budnyak, S. S. Chernadchuk, A. V. Zaharov, S. A. Petrov*

Department of Biochemistry, Odessa I.I. Mechnikov National University, Odessa, Ukraine

Received: 09 January 2019 **Accepted:** 03 May 2019 **Available Online**: 27 June 2019

ABSTRACT

We studied the effect of thiochrome on the activity of DNA polymerase isolated from the liver of white rats. This article shows the possibility of the influence of the most important thiamine metabolite – thiochrome on DNA polymerase activity. Roles of carboxyl groups of the enzyme and hydrophobic and hydrogen bonds in it in the realization of the activating action of thiochrome on the enzyme have been studied. The influence of thiochrome on the activity of DNA polymerase was studied. It was found that thiochrome is capable to activate this enzyme through interaction with the enzyme.

Аннотация

Мы изучали влияние тиохрома на активность ДНК-полимеразы, выделенной из печени белых крыс. В данной статье показана возможность влияния важнейшего метаболита тиамина – тиохрома на активность ДНК-полимеразы. Изучена роль карбоксильных групп фермента и гидрофобных и водородных связей в нем в реализации активирующего действия тиохрома на фермент. Исследовано влияние тиохрома на активность ДНК-полимеразы. Было установлено, что тиохром способен активировать этот фермент путем взаимодействия с ферментом.

Keywords: Thiochrome, DNA polymerase, enzyme

1. Introduction

The most of investigations in the field of biochemistry of thiamine are devoted to its coenzyme form – thiamine pyrophosphate and diseases associated with the deficiency of this vitamin in the body. Studies on non-coenzyme functions of both thiamine and its metabolites have been published during last three years. In particular, the specific role of thiamine triphosphate has been shownin the nervous system [1]. The regulatory role of thiochrome (thiamine catabolite) in the activity of a number of NAD-dependent enzymes [2-5], pyruvate dehydrogenase complex [4] and some proteolytic enzymes were demonstrated in our previous studies [5].

According to the recent findings, thiamine itself and the products of its oxidation and decomposition in the body can affect the activity of many enzymes. So, it is known that thiamine inhibits human saliva amylase at millimolar concentrations[6]. The carbohydrate absorption process depends on the thiazole moiety of thiamine. Thus, in the study of the effect of thiamine and its phosphates on the activity of the purified preparation of succinate dehydrogenase, it was established that thiamine, TMP, and TPF activate this enzyme [4]. In our laboratory the regulatory role of thiamine and its metabolites in the regulation of the activity of tissue and purified alcohol dehydrogenase and lactate dehydrogenase was investigated. In these experiments, it was shown that only thiochrome among all thiamine metabolites, is able to inhibit the activity of both studied enzymes effectively [4, 7]. It is important to note that the cytoplasmic arrangement of these enzymes coincides with that for thiochrome, and its effective

***Corresponding author:** Sergiy Anatoliyovich Petrov, doctor of biological sciences, professor of Odesa National Mechnykov I. I. University, Department of Biochemistry, 2, Dvoryanska Str., Odesa, 65082, Ukraine.

concentrations are actually present in the cytoplasm after loading with thiamine. These results gave us reason to believe that the thiamine metabolite, thiochrome, can act as an inhibitor of some NAD-dependent dehydrogenases [4]. The study of the binding of thiamine and its metabolites with the purified alcohol dehydrogenase preparation in the presence of various concentrations of NAD showed that thiochrome binds to the enzyme 4-5 times stronger than other metabolites of thiamine. In the presence of NAD in an environment of equal or even superior doses to thiamine and its metabolites, the binding of thiochrome remained fairly high. In these studies, it was shown that thiochrome is able to inhibit the activity of alcohol dehydrogenase even at concentrations three times lower than that of NAD, and only a six-fold excess of the concentration of NAD compared to thiochrome removed the inhibitory effect of the latter. The results suggest that inhibition of thiochrome alcohol dehydrogenase is competitive with NAD. Since thiochrome is a compound with pronounced hydrophobic properties, it can be assumed that when it joins the "hydrophobic pocket" of the active center of ADH, it prevents the addition of NAD. This assumption is supported by the same type of shifts to the shortwave region of the NAD and thiochrome absorption maxima when they are added to alcohol dehydrogenase, which we found in special studies [4]. Data on the participation of thiamine in the regulation of RNA synthesis have been obtained [8]. Thanks to these studies, it was found that this effect can be achieved by binding vitamin B1 to certain motifs of DNA, which affects DNA-dependent RNA polymerase [9]. The direct involvement of thiamine in the synthesis of RNA in tumor cells is also shown. In this case, this vitamin should have a potentiating effect on the transcription process [4].

The stimulating role of thiochrome in the reproduction of a number of invertebrate organisms [10] and its effect on the level of DNA and RNA in white rat tissues [7] are shown in our previous studies. The purpose of this work was to study the possibility of the thiochrome effect on the activity of DNA polymerase.

2. Material and Methods

2.1 Method of DNA polymerase isolation

Isolation of DNA polymerase was carried out using the method of isolation of Taq-polymerase [11].

The liver of a rat was homogenized and precipitated by centrifugation at 6000g per 30 minutes. The pellet was resuspended in 100 ml TE-buffer (10 mm Tris-HCl, pH 8.0, 1 mM EDTA), centrifuged for 6000g per 10 minutes. The resulting precipitate was stored at -20°C. To destroy the cells, 3g of the obtained liver pellet was resuspended in 30 ml Tris-HCl buffer with the addition of the necessary components (50 mM Tris-HCl, pH 7.5, 1 mM EDTA, 1.25 mM PMSF, 2 mg/ml lysozyme). After 15 minutes incubation at 20°C, the cells were destroyed in the ultrasonic disintegrator UZDN-A ("sounding", 1 minute with interruptions) in theice bath. This procedure was carried out until the optical density was reduced by a factor of ten at a wavelength of 590 nm. To denature the proteins to the suspension with constant stirring and 4°C, ammonium sulfate was added to the crusts to a concentration of 0.2M.

The suspension of the destroyed cells was centrifuged for 10000g per 1 hour on a Beckman LS-75 centrifuge (T35, Beckman rotor, USA). To denature the proteins, the supernatant was heated at 75°C for 30 minutes. Then polyimine P was added to the solution with constant stirring to a concentration of 0.6% at 4°C. The solution was incubated for 2 hours on ice, and then centrifuged for 10000 gper 1 hour. The supernatant was applied to the column with 6 mL of phenyl sepharose, equilibrated with buffer A (50 mM Tris-HCl, pH 7.5, 1 mM EDTA) containing 0.2 M ammonium sulfate. The column was washed with bufferA containing 20% glycerol (wt/vol.). The bound proteins elution was carried out with 100 ml of a linear gradient of urea concentration (0 – 4 M) on buffer A at a rate of 10 ml/ hr, 5 mlfractions were collected. The optical elution profile was determined from the absorbance at 280 nm on a spectrophotometer. Fractions containing the DNA polymerase were pooled and dialyzed overnight against buffer B (100 mM KCl, 50 mM Tris-HCl, pH 7.5, 0.1 mM EDTA, 0.2% Tween 20). The dialyzed preparation was applied to the column with heparin sepharose equilibrated with buffer B. Elution was carried out with 60 ml of a gradient of 100-700 mM KC1 in buffer B at a rate of 10 ml/ hr. Fractions (3 ml)were collected. Fractions with DNA polymerase were pooled and dialyzed against buffer for preservation (20 mM Tris-HCl, pH 7.5, 100 mM KCl, 0.1 mM EDTA, 1 mM dithiothreitol, 0.2% Tween 20, 50% glycerol). Dialysis preparation stored at -20°C.

2.2 Determination of the DNA polymerase activity

Determination of DNA-dependent DNA polymerase activity was carried out in A_1 and A_2 systems.

System A_1: 3 mM $MgCl_2$, 0.07 M KCl, 0.05 M tris-HCl buffer (pH = 8.5), 2mM dithiothreitol, 40 mg of bovine serum albumin, 10 μg of active DNA and 100 μM of each of the four deoxyribonucleotides (dNTP).

System A_2: 8 mM $MgCl_2$, 0.12 M KCl, 0.05 M Tris-HCl buffer (pH = 8.5), 2 mM dithiothreitol, 40 μg bovine serum albumin, 10 μg of active DNA, and 100 μM of each of the four deoxyribonucleotides (dNTP).

0.1 ml of DNA polymerase was added to each system, the control groups were incubated for 30 minutes at 37°C. During the pre-incubation tests, thiochrome was added with concentrations: 1 nM, 10 nM, 100 nM, 1 μM.

Then, the reaction was stopped by the addition of 40 μl of the mixture consisting of 0.2 M EDTA and a saturated solution of $Na_4P_2O_7$ (1:1). 1 ml of 30% TCA was added to each system in which 1/10 volume of $Na_4P_2O_7$ was dissolved. It was centrifuged for 3000g per 10 minutes. The

supernatant and sediment were separated.

The pellet was resuspended in the same volume as the supernatant, centrifuged for 3000g per 10 minutes, and the precipitates were determinedfor the DNA content

2.3 Determination of the binding rate of thiochrome to DNA polymerase

Determination of the thiochrome binding rate to DNA polymerase was carried out in two systems.

System A_1: 3 mM $MgCl_2$, 0.07 M KCl, 0.05 M Tris-HCl buffer (pH = 8.5), 2 mM dithiothreitol, 40 mg of bovine serum albumin, and 100 mM each of the four deoxyribonucleotides (dNTP).

System A_2: 8 mM $MgCl_2$, 0.12 M KCl, 0.05 M Tris-HCl-buffer (pH = 8.5), 2 mM dithiothreitol, 40 μg bovine serum albumin, and 100 μM each of four deoxyribonucleotides (dNTP).

DNA polymerase was added in a concentration of 100 μg/ml and thiochrome in a concentration of 1 μm. Then inhibitors were introduced in the test samples: ether, urea, formaldehyde, lead chloride in concentrations of 1, 2, 5, 10 μm ($PbCl_2$ for blocking sulfhydryl groups, formaldehyde for blocking amino groups, diethyl ether for blocking the carboxylgroups, urea for partial destruction of hydrophobic and hydrogen bonds). The samples were incubated in a thermostat at 30°C for 30 minutes, then the samples were centrifuged at 20000g per 30 minutes, the supernatants were merged. The precipitates were washed twice with incubation medium and the thiochrome content was determined by the fluorimetric method.

All obtained data were processed statistically. All data were analyzed by statistical data processing using the non-parametric parameter Mann-Whitney [12]. Statistical significance was considered to be $p \leq 0.05$[13].

The bulk of used reagents meet the high purity requirements (Reanal, Fluka, Sigma, Orion, Beloris), others are Reahim production, with a characteristic of not less than chemically pure, which, if necessary, are further refined.

3. Results

In our work, DNA polymerase of rat Rattus norvegicus was used.

Inour previous studies [5, 14, 15] it was shown that thiochrome is a thiamine metabolite that responsible for activation of the process of reproduction in the mammals and some invertebrates tissues. To find out the mechanism of this action of thiochrome we studied the effect of this metabolite on the activity of DNA polymerase isolated from the liver of white rats. The results of these studies showed (Figure 1) that thiochrome even at a concentration of 1 nm is able to activate DNA polymerase in the A_2 system, and at a concentration of 10 nm it activates the enzyme in both systems. The greatest effect was observed at a concentration of 1 μm.t

Next it was necessary to establish which groups in the DNA polymerase molecule participate in interaction with thiochrome and are responsible for the activation of this enzyme. To that case we used the inhibitor analysis method, in which the following compounds were added to pre-incubation medium.To block the sulfhydryl groups of the enzyme, we used $PbCl_2$, formaldehyde blocked the amino groups, diethyl ether blocked the carboxyl groups, urea partially destroyed the hydrophobic and hydrogen bonds.

These inhibitors have been used in micromolar concentrations in order to avoid a nonspecific effect on the enzyme (Table 1).

The data in Table 1 indicate that when the $PbCl_2$ inhibitor was introduced into the incubation medium, the activity of the DNA polymerase decreased significantly in the A_1 system. At the same time, the introduction of only

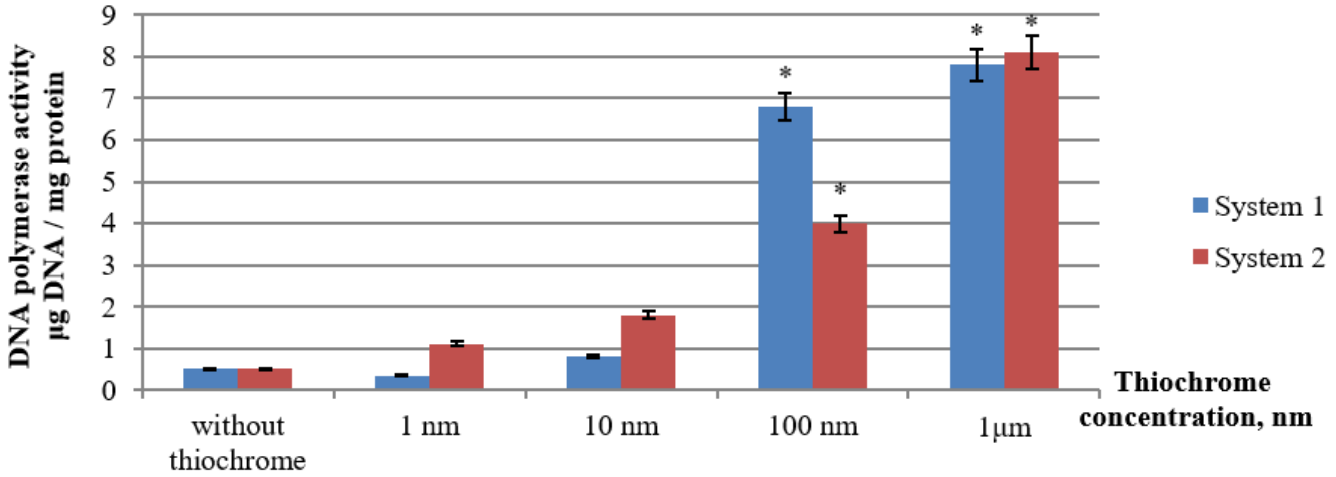

Figure 1 | The DNA polymerase activity in the presence of various thiochrome concentrations (μg DNA / mg protein)(n=8) *p<0.05 in comparison with control. ДНК-полимеразная активность в присутствии различных концентраций тиохрома (мкг ДНК / мг белка) (n = 8) * p<0,05 по сравнению с контролем

Table 1 | The activity of DNA polymerase in the presence of thiochrome and functional groups blockers (μgt hiochrome /mg protein) (n=8).* - p=0.05 in comparison with control. ** - p=0.05 in comparison with thiochrome. Активность ДНК-полимеразы в присутствии тиохрома и функциональных групп (мкг тиохрома / мг белка) (n = 8) * - p = 0,05 по сравнению с контролем. ** - p = 0,05 по сравнению с тиохромом.

$PbCl_2$							
	Control	$PbCl_2$ 1 μm	Thiochrome 1 μm	$PbCl_2$+thiochrome			
				1 μm $PbCl_2$	2 μm $PbCl_2$	5 μm $PbCl_2$	10 μm $PbCl_2$
SystemA_1	0,065	0,038*	0,115*	0,100*	0,110*	0,096*	0,110*
SystemA_2	0,070	0,041	0,110*	0,095*,**	0,105*	0,100*	0,110*
Formaldehyde							
	Control group	Formaldehyde 1 μm	Thiochrome 1 μm	Formaldehyde +thiochrome			
				1 μm formaldehyde	2 μm formaldehyde	5 μm formaldehyde	10 μm formaldehyde
SystemA_1	0,065	0,085	0,115*	0,110*	0,100*	0,111*	0,118*
SystemA_2	0,070	0,041*	0,110*	0,120*	0,116*	0,128	0,118*
Ether							
	Control group	Either 1 μm	Thiochrome 1 μm	Ether +thiochrome			
				1 μm ether	2 μm ether	5 μm ether	10 μm ether
SystemA_1	0,065	0,030*	0,115*	0,048*,**	0,042*,**	0,033*,**	0,030*,**
SystemA_2	0,070	0,032*	0,110*	0,05**	0,044*,**	0,039**	0,039**
Urea							
	Control group	Urea 1 μm	Thiochrome 1 μm	Urea +thiochrome			
				1 μm urea	2 μm urea	5 μm urea	10 μm urea
SystemA_1	0,065	0,040*	0,115*	0,055*,**	0,050*,**	0,048*,**	0,033*,**
SystemA_2	0,070	0,041	0,110*	0,058*,**	0,054*,**	0,049*,**	0,032*,**

thiochrome led to the activation of this enzyme in both systems. The most interesting results were obtained when $PbCl_2$ was introduced into the incubation medium together with thiochrome. This inhibitor in concentrations from 1 μm to 10 μm did not reduce the activating effect of thiochrome, except at the concentration of 1 μm in system A_2.

When using formaldehyde, it was found that this inhibitor reduced the activity of DNA polymerase only in the A_2 system. The introduction of only thiochrome into the incubation medium increased the activity of the enzyme in both systems. The combined use of formaldehyde and thiochrome did not reduce the activating effect of thiochrome.

The addition of diethyl ether to the incubation medium as well as in the previous cases led to the decrease in activity of the enzyme, and the addition of thiochrome led to its activation. However, unlike previous inhibitors, diethyl ether inhibited the activity of DNA polymerase even in the presence of thiochrome.

A similar pattern was observed when using urea, which reduced the activity of the enzyme under study. The introduction of thiochrome into the incubation medium did not prevent this effect.

Proceeding from the data given in the table, it should be noted that both $PbCl_2$ and formaldehyde at concentrations from 1 to 10 μm did not decrease the activating effect of thiochrome on DNA polymerase. Diethyl ether and urea already at a concentration of 1 μm removed the activation effect of thiochrome on DNA polymerase. Higher concentrations of these two compounds exerted a greater inhibitory effect. Thus, these data indicate the role of carboxyl groups of the enzyme, hydrophobic and hydrogen bonds in the realization of the activating effect of thiochrome on this enzyme. To clarify the obtained data, we studied the binding of thiochrome to DNA polymerase in the presence of the above inhibitors at the same concentrations.

So, from Table 2 it can be seen that diethyl ether caused a tendency to decrease for the registered parameters already at its introduction in the concentration of 1 and 2 μm in comparison with the control. Higher concentrations, such as 5 and 10 μm, caused a significant decrease in these parameters by an average of 40.1% in the A_1 and A_2 systems at 5 μm, and at 10 μm this average was lower by 49.8% in both systems compared with the control option.

It is noted that when added to the medium, urea at all concentrations is capable of reliable reduction of the binding of thiochrome to the DNA polymerase. Thus, from Table 2 it can be seen that even with the introduction of urea at a concentration of 1 μm, the recorded value on average in the two systems was reduced by 39.2% with respect to the control, and at urea concentration of 2 μm, the value was on average 53.4% lower than in the control version. Introduction of the investigated blocker into the medium at a concentration of 5 μm led to the decrease in the indices in

Table 2 | Thiochrome binding to DNA polymerase in the presence of different functional groups blockers (μg thiochrome/mg protein) (n=8). * - p=0.05 in comparison with control. Связывание тиохрома с ДНК-полимеразой в присутствии блокаторов различных функциональных групп (мкг тиохрома / мг белка) (n = 8). * - p = 0,05 по сравнению с контролем).

System	Control	Ether			
		1 μm	2 μm	5 μm	10 μm
A_1	0,90	0,70	0,65	0,58*	0,32*
A_2	0,94	0,74	0,69	0,52*	0,61*
System	Control	Urea			
		1 μm	2 μm	5 μm	10 μm
A_1	0,90	0,54*	0,44*	0,32*	0,21*
A_2	0,94	0,58*	0,42*	0,29*	0,19*
System	Control	$PbCl_2$			
		1 μm	2 μm	5 μm	10 μm
A_1	0,90	0,99	0,85	0,86	0,78
A_2	0,94	0,93	0,87	0,83	0,85
System	Control	Formaldehyde			
		1 μm	2 μm	5 μm	10 μm
A_1	0,90	1,11	0,94	0,88	0,83
A_2	0,94	0,92	0,99	1,02	0,95

systems A1 and A2 below the control by 66.8% on average. When urea was introduced at a concentration of 10 μm, a similar pattern was observed. So, in systems A_1 and A_2, on average, the binding intensity decreased by 78.3% in relation to the control.

Table 2 shows the data on the binding of thiochrome to DNA polymerase. After the analysis of data, it was determined that their concentrations fully correspond to the content of thiochrome in animal tissues [4].

4. Concluding Remarks

It can be assumed that the binding of thiochrome to certain sites of DNA polymerase is carried out using hydrophobic interactions.

In this way, probably, thiochrome is capable of activating the DNA polymerase through interaction with specific sites of the enzyme containing amino acids with hydrophobic radicals.

Заключение

Можно предположить, что связывание тиохрома с определёнными сайтами ДНК-полимеразы осуществляется с использованием гидрофобных взаимодействий.

Таким образом, вероятно, тиохром способен активировать ДНК-полимеразу путем взаимодействия с конкретными сайтами фермента, содержащего аминокислоты с гидрофобными радикалами.

References

[1] S. Bergink, W. Toussaint, M. S. Luijsterburg, Ch. Dinant, S. Alekseev, J.H.J. Hoeijmakers, N.P. Dantuma, A.B. Houtsmuller, W.Vermeulen, The Journal of Cell Biology, 196 (6), 2012 681–688. doi:10.1083/jcb.201107050

[2] L. Bettendorf, P. Wins, E. Schoffenels, Arch. Int. Physiol. et Biochim., 97 (1989) 127.

[3] F. C. Lawyer, S. Stoffel, R K. Saiki, Sh.-Yu. Chang, Ph. A. Landre, R. D. Abrarnson, D. H. Gelfand, Genome Res., 2 (1993) 275-287.

[4] S.A. Petrov, Biomed Khim. 52(4) (2006) 335-345.

[5] V. Ye. Yakimenko, S. A. Petrov, Odesa National University Herald. Biology, 20 (2015) 23-25.

[6] M.F. Merezhynskyy Mekhanizm diyi biolohichna rol vitaminiv. Mynsk: Hosyzdat BSSR, (1959) 110-111.

[7] S.A. Petrov Regulation of the formation and exchange of amino acids and keto acids in the body by thiamine and its metabolites. Author's abstract. Dis. Doct. Biol. Sciences., Minsk. (1992) 1- 42 .

[8] A.M. Khokha RNA biosynthesis in the nuclei of the liver of animals with vitamin B1 deficiency Author's abstract. Dis. Cand. Biol. Sciences., Moscow. (1984) 1-18.

[9] B.P. Komarova Thiamine-2. Grodno: Editorial and Publishing Council of the Academy of Sciences of the BSSR, (1972) 48–50.

[10] A. N. Shiyan Bioorganic chemistry 2 (1976) 950-957.

[11] V. Devyatnin Methods of chemical analysis in the production of vitamins (2013) 94-96.

[12] L. O. Atramentova, O. M. Ytevskaya Statisticheskiye metodiki v biologii: Pídruchnik. – KH.: KHNU ímení V. N. Karazína. 2007. – 288.

[13] S. Glantz Medico-biological statistics. Trans. with English. - Moscow, Practice (1999) 459.

[14] V. Yakimenko, O. Bytlan, S. Petrov, Visnyk of the Lviv University. Series Biology, 73 (2016) 352–355

[15] V. Ye Yakimenko, S. A. Petrov, ScienceRise 8 (1(25)) (2016) 26-31.

JOURNAL OF INTEGRATED OMICS
A METHODOLOGICAL JOURNAL
HTTP://WWW.JIOMICS.COM

ORIGINAL ARTICLE | DOI: 10.5584/jiomics.v9i1.273

Molecular mechanisms of adaptation to the habitat depth in visual pigments of *A. subulata* and *L. forbesi* squids: on the role of the S270F substitution

Dmitrii M. Nikolaev [1], Demid E. Osipov [2], Daniil M. Strashkov [1], Sergey Yu. Vyazmin [1], Vasily E. Akulov [1], Denis V. Kravtcov [3], Oleg B. Chakchir [1], Maxim S. Panov [3], Mikhail N. Ryazantsev [3*]

[1] Department Nanotechnology Research and Education Centre RAS, Saint-Petersburg Academic University, 8/3 Khlopina Street, St. Petersburg 194021, Russia; [2] Peter the Great St. Petersburg Polytechnic University, Polytekhnicheskaya Str. 29, St. Petersburg, 195251, Russia; [3] St. Petersburg State University, Institute of Chemistry, Universitetskiy Ave. 26, St. Petersburg, Petergof, 198504, Russia

Received: 09 January 2019 **Accepted:** 03 May 2019 **Available Online**: 27 June 2019

Abstract

Revealing the mechanisms of animal adaptation to different habitats is one of the central tasks of evolutionary physiology. A particular case of such adaptation is the visual adaptation of marine species to different depth ranges. Because water absorbs more intensively longer wavelengths than shorter wavelengths, the increase of habitat depth shifts the visual perception of marine species towards the blue region. In this study, we investigated the molecular mechanisms of such visual adaptation for two squid species – *Alloteuthis subulata* and *Loligo forbesi.* These species live at different depths (200 m and 360 m, respectively) and the absorption maximum of *A. subulata* visual rhodopsin is slightly red-shifted compared to *L. forbesi* rhodopsin (499 and 494 nm, respectively). Previously, the amino acid sequences of these two species were found to differ in 22 sites with only seven of them being non-neutral substitutions, and the S270F substitution was proposed as a possible candidate responsible for the spectral shift. In this study, we constructed computational models of visual rhodopsins of these two squid species and determined the main factors that cause the 5 nm spectral shift between the two proteins. We find that the origin of this spectral shift is a consequence of a complex reorganization of the protein caused by at least two mutations including S270F. Moreover, the direct electrostatic effect of polar hydroxyl-bearing serine that replaces non-polar phenylalanine is negligible due to the relatively long distance to the chromophore.

Аннотация

Определение механизмов адаптации животных к различным условиям среды является одной из центральных задач эволюционной физиологии. Частным случаем такой адаптации является зрительная адаптация морских животных к различным глубинам. Так как вода поглощает длинноволной свет более интенсивно, чем коротковолновой, то с увеличением глубины обитания происходит сдвиг видимой части спектра морских животных в синюю область. В данном исследовании мы изучили молекулярные механизмы, обеспечивающие зрительную адаптацию двух кальмаров — *Alloteuthis subulata* и *Loligo forbesi.* Эти кальмары живут на разных глубинах (200 м и 360 м соответственно), и максимум поглощения зрительного родопсина *A. subulata* слегка сдвинут в длинноволновую область относительно родопсина *L. forbesi* (499 и 494 нм соответственно). В более ранней работе уже проводился анализ аминокислотных последовательностей этих двух видов, который показал наличие 22 аминокислотных замен, только семь из которых были неконсервативными. Было выдвинуто предположение, что аминокислотная замена S270F является возможной причиной наблюдаемого спектрального сдвига. В данной работе мы сгенерировали компьютерные модели визуальных родопсинов двух кальмаров и определили основные факторы, которые отвечают за 5 нм спектральный сдвиг между белками. Мы обнаружили, что причиной спектрального сдвига является сложная реорганизация белка, вызванная как минимум двумя мутациями, включая S270F. Более того, мы показали, что прямой электростатический эффект полярного серина, который заменяется неполярным фениланином, незначителен, так как данная аминокислота находится на значительном расстоянии от хромофорора.

Keywords: Visual adaptation; squid rhodopsins; molecular mechanisms of visual adaptation; *L. forbesi* vision; *A. subulata* vision; non-direct tuning in rhodopsins; spectral tuning in rhodopsins

***Corresponding author:** Mikhail N. Ryazantsev, candidate of chemical sciences, associate professor of Saint-Petersburg State University, Institute of Chemistry, Universitetskiy Ave. 26, St. Petersburg, Petergof, 198504, Russia.

1. Introduction

Understanding the molecular mechanisms of visual adaptation is an essential problem of evolutionary physiology that allows for deriving general patterns of rhodopsin alterations during the evolution of vision. A prime example is the visual adaptation of marine species to the habitat depth. An increase of habitat depth correlates with a blue-shifting of visual range of marine animals, which can be rationalized by the fact that longer wavelengths are more intensively absorbed by water. For example, the rod pigments of a majority of deep-sea fish exhibit λ_{max} around 480 nm close to the maximum of oceanic water light transmission. A similar blue shift has been found both in the rod and cone pigments of cottoid fish species that live in fresh-water Lake Baikal, in visual pigments of rockfishes and crustacean.[1-3]

In this study, we consider a particular case of such visual adaptation by comparing the visual rhodopsins of two squid species. While *Alloteuthis subulata* squid lives at the depth range around 200 m and its rhodopsin demonstrates an absorption maximum at 499 nm, *Loligo forbesi* lives at the depth around 360 m and the absorption maximum value of its rhodopsin is 494 nm. The origin of this shift has already been studied experimentally.[4] According to this study, the amino acid sequences of these two rhodopsins differ only in 22 sites, and only seven of them are non-neutral substitutions. The substitution S270F was attributed as a possible candidate responsible for the 5 nm difference. The S270F substitution was singled out as a reasonable candidate because it is the only substitution of a polar hydroxyl-bearing serine located relatively close to the chromophore with the non-polar phenylalanine. In this study, we constructed a series of computational Quantum Mechanics/ Molecular Mechanics (QM/MM) models for rhodopsins of *A. subulata* and *L. forbesi* and their mutants.

We found that direct electrostatic effect of the S270F substitution cannot lead to any spectral shift due to the relatively long distance from the chromophore. However, the S270F substitution, along with other substitutions, is responsible for the significant reorganization of the hydrogen bond network in the protein that leads to change in the position of the polar and charged residues including the counterion E180. Thus, the spectral shift between *A. subulata* and *L. forbesi* rhodopsins is an example of complex non-direct spectral tuning rather than a direct electrostatic effect of substituted residues. In addition, the spectral shift between *A. subulata* and *L. forbesi* rhodopsins cannot be explained completely by a single S270F substitution, and other non-neutral substitutions are involved in the tuning of the spectral shift.

2. Material and Methods

The structures of *A. subulata* and *L. forbesi* visual rhodopsins were generated using a homology modeling approach on the basis of their primary sequences (UniProt codes Q17094 and P24603, respectively).[4, 5] The X-ray structure of *Todarodes Pacificus* visual rhodopsin (RCSB code 2Z73) was used as a template.[6] To align primary sequences we used AlignMe program package.[7] The obtained values of sequence identity between target proteins and the template (83% and 85% for *A. subulata* and *L. forbesi*, respectively) were very high, i.e. the structures of all three proteins are very similar. To generate the three-dimensional structures of target rhodopsins we applied the I -TASSER program package.[8] Because I-TASSER can generate several structures based on its scoring functions and does not take into consideration the membrane environment, we used visual inspection to sort out the structure(s) with the correct fold. For each of the studied rhodopsins and mutants, all structures except a single one folded incorrectly, i.e. they could not exist in the membrane environment. The final structures were subjected to additional processing and optimization. We inserted the retinal chromophore in rhodopsin models bound to the K305 residue. Proteins were hydrated with Dowser++ program.[9] Then we used pdb2pqr (version 2.1.1)[10] and propka (version 3.0)[11] programs to calculate pKa values for the titratable amino acids in proteins, assign their protonation states (pH=7.0) and add hydrogen atoms. These complete models were subjected to geometry optimization first at the MM level (AMBER force field)[12] and then applying a hybrid quantum-mechanics/molecular-mechanics approach [QM:MM (SORCI+Q//B3LYP/6-31g (d):AMBER-96)] implemented in Gaussian09 program package.[13] To calculate absorption maxima values of the retinal chromophore in protein environment we applied SORCI+Q/6-31G* level of theory implemented in ORCA 4.0 program package.[14] The same methodology was applied to perform all other spectral calculations performed in the current work. All applied protocols have been successfully tested in a number of previous studies.[15-24]

For both proteins amino acid numbering is in accordance with the published *L. forbesi* amino acid sequence.[5] .

3. Results

The absorption maxima values calculated for the generated three-dimensional rhodopsin models were in good agreement with experimental values and reproduced the experimentally observed spectral red shift of *A. subulata*

Table 1 | The comparison of calculated and experimental absorption wavelengths of rhodopsins from *A. subulata* and *L. forbesi.*
Сравнение рассчитанных и экспериментальных значений λ_{max} для родопсинов кальмаров *A. subulata* и *L. forbesi.*

	***A. subulata* λ_{max}, nm**	***L. forbesi* λ_{max}, nm**
experimental	499	494
calculated	473	467

Table 2 | Absorption maxima values for several computational models of visual rhodopsins from *A. subulata, L. forbesi, A. subulata* S270F mutant and *L. forbesi* rhodopsin F270S mutant. a) Model 2 is the retinal chromophore with geometry optimized in corresponding protein environment of rhodopsin in the absence of external charges. b) Model 3 is the retinal chromophore in the presence of charges corresponding to the E180 residue, the rest of AMBER charges of protein atoms are set to zero. c) Model 4 is the retinal chromophore in the presence of charges corresponing to the E180 residue, polar residues and water molecules located within 5 Å from the retinal chromophore. d) Model 5 is the model that contains all residues of the protein. Значения λ_{max} для нескольких вычислительных моделей изучаемых белков: зрительных родопсинов кальмаров *A. subulata, L. forbesi*, мутанта родопсина *A. subulata* S270F и мутанта родопсина *L. forbesi* F270S. a) Модель 2 представляет собой ретинальный хромофор, геометрия которого была оптимизирована в соответствующей белковой среде родопсина. b) Модель 3 представляет собой ретинальный хромофор и заряды, соответствующие аминокислоте E180, остальные AMBER заряды на атомах белка приравнены нулю. c) Модель 4 представляет собой ретинальный хромофор и заряды, соответствующие аминокислоте E180, а также полярным аминокислотам и молекулам воды, расположенным в пределах 5 Å от ретинального хромофора. d) Модель 5 представляет собой ретинальный хромофор и заряды всех аминокислот белка.

Model	*A. subulata* λ_{max}, nm	*L. fobesi* λ_{max}, nm	*A. subulata* S270F λ_{max}, nm	*L. forbesi* F270S λ_{max}, nm
Model 2[a]	603	601	596	603
Model 3[b]	525	501	524	532
Model 4[c]	487	467	487	501
Model 5[d]	473	467	476	485
full protein with charges of S270/F270 set to zero	471	465		

rhodopsin relative to *L. forbesi* rhodopsin (Table 1). To analyze the origin of this spectral shift we performed a series of additional calculations for each rhodopsin model (Table 2).

Eq. 1 $$\Delta\lambda_{max}^{A-L} = \lambda_{max}^{A.subulata} - \lambda_{max}^{L.forbesi}$$

To discern the impact of different factors to the 5 nm spectral shift between two proteins (Equation 1), we performed the following analysis (see Figure 1). First, we calculated λ_{max} for the gas-phase chromophore (11-cis protonated Schiff base, PSB11) (Model 1). After that, we evaluated the spectral shift caused by the retinal geometry modification by a protein environment. To accomplish this task, we calculated the absorption maxima of retinal chromophores (with geometries optimized in corresponding protein environments of two rhodopsins) in the absence of external charges (Model 2). These calculations provide the +2 nm absorption red shift of retinal from *A. subulata* rhodopsin compared to retinal from *L. forbesi* rhodopsin.

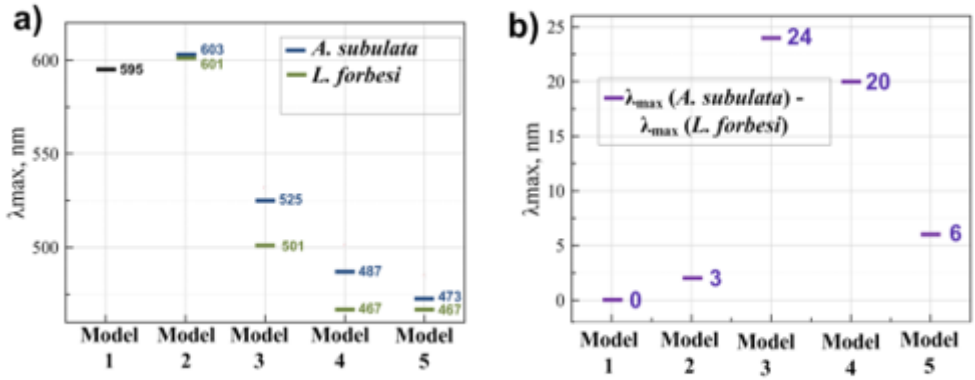

Figure 1 | a) λ_{max} of the investigated computational models of rhodopsins from *A. subulata* (blue) and *L. forbesi* (green). b) The values for the models. Model 1 is the gas-phase chromophore (11-cis protonated Schiff base, PSB11). Model 2 is the retinal chromophore with geometry optimized in corresponding protein environment of rhodopsin in the absence of external charges. Model 3 is the retinal chromophore in the presence of charges corresponding to the E180 residue, the rest of AMBER charges of protein atoms are set to zero. Model 4 is the retinal chromophore in the presence of charges corresponding to the E180 residue, polar residues and water molecules located within 5 Å from the retinal chromophore. Model 5 is the model that contains all residues of the protein. a) Рассчитанные значения λ_{max} для изученных моделей родопсинов *A. subulata* (синий) and *L. forbesi* (зеленый). b) Спектральные сдвиги между моделями. Модель 1 представляет собой хромофор (11-цис протонированное основание Шиффа), геометрия которого была оптимизирована в отсутствии зарядов. Модель 2 представляет собой ретинальный хромофор, геометрия которого была оптимизирована в соответствующей белковой среде родопсина. Модель 3 представляет собой ретинальный хромофор и заряды, соответствующие аминокислоте E180, остальные AMBER заряды на атомах белка приравнены нулю. Модель 4 представляет собой ретинальный хромофор и заряды, соответствующие аминокислоте E180, а также полярным аминокислотам и молекулам воды, расположенным в пределах 5 Å от ретинального хромофора. Модель 5 представляет собой ретинальный хромофор и заряды всех аминокислот белка.

Next, we evaluated the effect of a negatively charged residue located in the retinal-binding pocket (counterion E180). We calculated the absorption maxima of retinal chromophores in the presence of charges corresponding to the E180 residue, setting the rest of AMBER charges of protein atoms to zero (Model 3). The results showed that, in *A. subulata* rhodopsin, the counterion causes a smaller spectral blue shift than in *L. forbesi* rhodopsin (-78 and -100 nm relative to absorption of the retinal model without external charges). Analysis of rhodopsin structure reveals that E180 of *A. subulata* rhodopsin is located further from the NH part of the chromophore than E180 of *L. forbesi* rhodopsin. The distance measured from the closest oxygen atom of E180 to the carbon atom C15 of the chromophore is 6.03 Å vs 3.99 Å for *A. subulata* and *L. forbesi*, respectively (see Figure 2). This trend is in full agreement with previous studies[19,25,26] that state the importance of the counterion distance to NH moiety for spectral tuning. Adding polar residues and water molecules located within 5 Å from the retinal chromophore to the model containing only E180 residue (Model 4) gives the total +20 nm spectral shift of *A. subulata* model relative to *L. forbesi* model. Thus, all residues and water molecules in the retinal-binding pocket except the counterion only slightly decrease the spectral red shift between *A. subulata* and *L. forbesi* rhodopsins caused by the change of the distance from NH moiety to the E180 counterion. In the Figure 3 we show some of the polar residues in the binding pocket with most prominent reorganization. The impact of these residues on λ_{max} is estimated by setting the charges of the corresponding residues to zero. The calculated λ_{max} shifts are given in the Table 3. It worth mentioning that total 4 nm effect for the polar residues reorganization is due to the complex reorganization of many residues, and each of them is responsible for much larger shift than 4 nm. For example, the impact of N87 residue, which is connected to the -N-H part of the chromophore through the hydrogen bond, is -49 nm and -33 nm for *A. subulata* and *L. forbesi* models, respectively. This $\Delta\lambda_{max}$ difference can be explained by the change in the orientation of the $-C(O)NH_2$ part of the N87 residue relative to the –N-H part of the chromophore (see Figure 2 a,b). Another striking example is the reorganization of the –OH part of the S187 residue: due to the change of the dipole moment orientation, the $\Delta\lambda_{max}$ sign changes from positive to negative for *A. subulata* and *L. forbesi* models, respectively. Similarly, a flip of the $-C(O)NH_2$ part of the N185 residue leads to the change of the $\Delta\lambda_{max}$ sign. The above-described effect of polar residues reorganization is also well-known and it has been reported before.[19, 27]

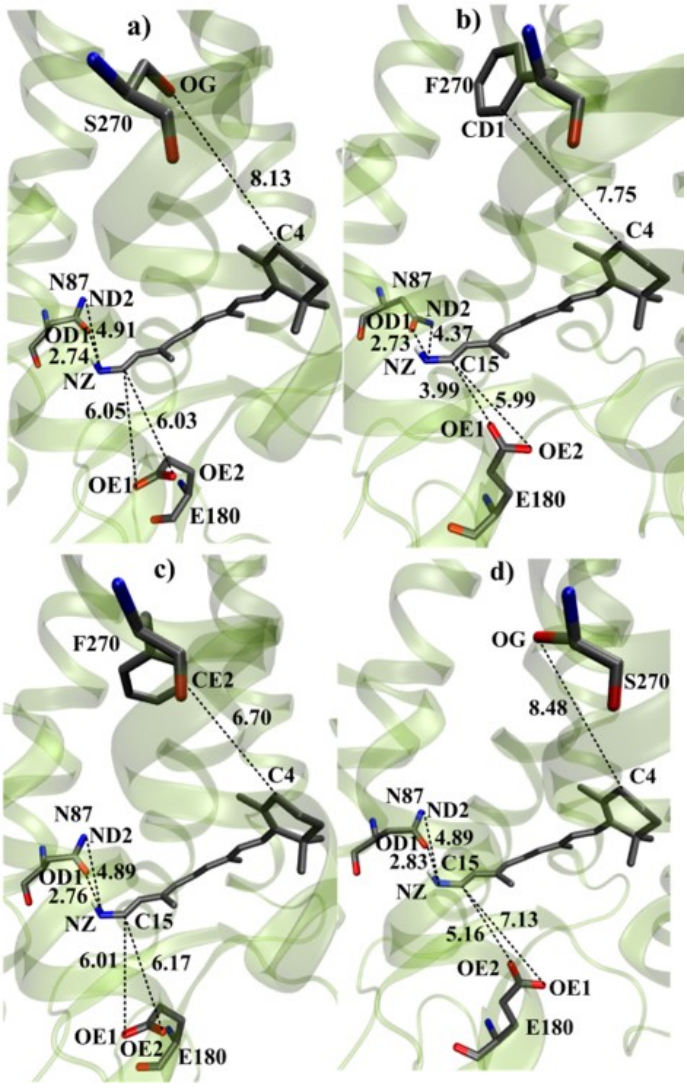

Figure 2 | The comparison of structural differences between four investigated proteins: visual rhodopsins from *A. subulata* (a), *L. forbesi* (b), *A. subulata* rhodopsin S270F mutant(c) and *L. forbesi* rhodopsin F270S mutant (d). All distances are given in Å. Сравнение структур четырех изученных моделей белков: зрительного родопсина *A. subulata* (a), *L. forbesi* (b), мутанта *A. subulata* S270F (c) и мутанта *L. forbesi* F270S (d). Все расстояния приведены в Å.

Table 3 | The impact of polar residues in the retinal-binding cavity of *A. subulata* and *L. forbesi* rhodopsins that show the most prominent reorganization (see Figure 3) on λ_{max}. The effect was estimated by setting the charges of the corresponding residues to zero. Эффект полярных аминокислот в хромофорной полости родопсинов из *A. subulata* и *L. forbesi*, которые демонстрируют наиболее сильную реорганизацию (см. Рисунок 3), на значения λmax. Для расчета эффекта заряды, соответствующие целевой аминокислоте, были приравнены нулю.

Residue	A. subulata $\Delta\lambda_{max}$, nm	L. forbesi $\Delta\lambda_{max}$,
N87	-49	-33
N185	-19	13
C186	-16	-7
S187	16	-12
Y190	17	6

Eq. 2 $$\Delta\lambda_{max}^{A-L}$$

The Model 5 is the model that contains all residues of the

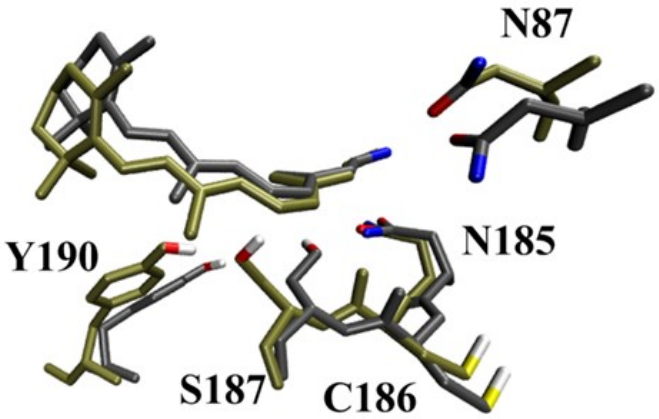

Figure 3 | Polar residues in the binding pocket of A. *subulata* (tan) and *L. forbesi* (gray) rhodopsins that demonstrate the most prominent reorganization. Наиболее сильно реорганизованные полярные аминокислоты в хромофорной полости родопсинов *A. subulata* (желто-коричневый) and *L. forbesi* (серый).

protein. The difference in the (Equation 2) values between models containing the 5 Å cavity and the complete protein models (i.e. -14 nm) can be explained by the reorganization of the charged residues outside the binding pocket.

We also tested the hypothesis proposed in a previous experimental study[4] that the spectral shift is caused by S270F substitution. First, we analyzed the direct electrostatic effect of S270 and F270 residues on the absorption maximum value of retinal chromophore in *A. subulata* and *L. forbesi* rhodopsins, respectively. To perform this task, we constructed new models by setting to zero charges of S270 and F270 in our models of *A. subulata* and *L. forbesi* rhodopsins, and recalculated the absorption maxima without preliminary geometry optimization. The results are given in Table 2. One can see that the above-described elimination of charges does not lead to any change of (Equation 2) value. Moreover, the charges on these residues have a negligible effect on the absorption maxima of the corresponding rhodopsins. The analysis of the predicted rhodopsin structures showed that S270 and F270 residues are located too far from the retinal chromophore (8.13 Å and 7.75 Å, see Figure 2 a,b) to produce a detectable direct electrostatic effect.

As the next step, we investigated if the F270S substitution in *L. forbesi* rhodopsin or S270F substitution in *A. subulata* rhodopsin lead to notable structural reorganization and, consequently, to a spectral shift for the absorption band of *L. forbesi* and *A. subulata* rhodopsins. To address this issue, we predicted a three-dimensional model of F270S and S270F mutants of *L. forbesi* and *A. subulata* rhodopsins respectively starting from their amino acid sequences following the protocol described in the "Materials and methods" section.

The analysis of the obtained structures reveals that the F270S substitution causes the structural reorganization of the *L. forbesi* rhodopsin binding pocket including counterion. The distance from the oxygen atom of the counterion E180 to the C15 atom is 5.16 Å (Figure 2d) that is between 6.03 Å and 3.99 Å found for *A. subulata* rhodopsins and *L. forbesi* rhodopsin, respectively. On the contrary, the S270F substitution in the *A. subulata* rhodopsin does not change the distance from the oxygen atom of the counterion E180 to the C15 atom of the chromophore that is 6.01 Å comparing to 6.03 Å (see Figure 2c). Additional analysis of the obtained structures reveals (see Figure 4) that in the *A. subulata* rhodopsin, the M126 residue located in the α-helix III (shown in orange in Figure 4a) is connected by a hydrogen bond network through a water molecule to the S270 residue located in the α-helix VI (shown in green in Figure 4a) and, finally, to the counterion E180, which is located on the relatively flexible β-sheet (shown in red in Figure 4a). For the *L. forbesi* rhodopsin and both studied mutants, M126 does not make a hydrogen bond that is connected the α-helix III and the counterion through the residues of the α-helix VI (Figure 4b). For the *L. forbesi* rhodopsin and the S270F mutant of the *A. subulata* rhodopsin, the F270 residue does not have a part to make a hydrogen bond (Figures 4b, c). For the F270S mutant of the *L. forbesi* rhodopsin, M126 is H-bonded to another residue but not to S270 (Figure 4d). Thus, one of the roles of the S270 residue is an adjustment of the counterion position and, therefore, its distance to the chromophore through an H-bond network.

To summarize, a comparative analysis of the spectral tuning mechanism for the F270S and S270F mutants, *L.*

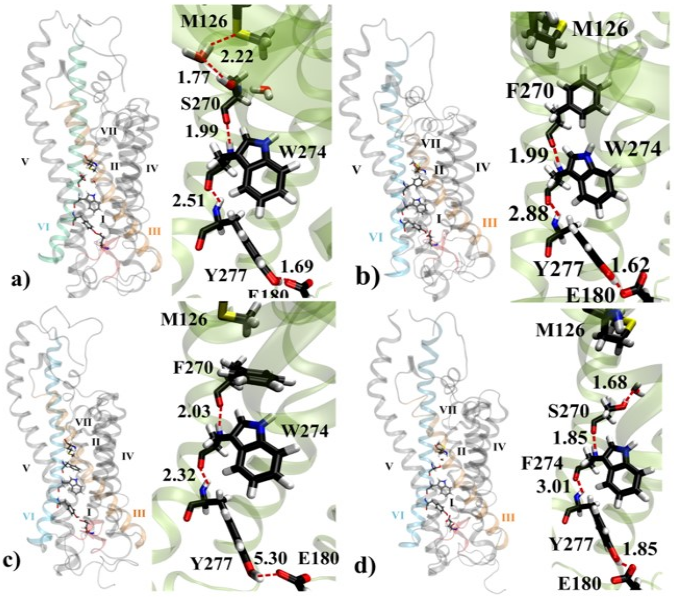

Figure 4 | The differences in hydrogen-bond network that is related to the orientation of E180 counterion in four investigated proteins: visual rhodopsins from *A. subulata* (a), *L. forbesi* (b), *A. subulata* rhodopsin S270F mutant (c) and *L. forbesi* rhodopsin F270S mutant (d). All distances are given in Å. Сравнение сетей водородных связей, которые вызывают реориентацию контриона E180 в четырех изученных белках: зрительных родопсинов *A. subulata* (a), *L. forbesi* (b), мутанта родопсина из *A. subulata* S270F (c) и мутанта родопсина из *L. forbesi* F270S (d). Все расстояния приведены в Å.

tuning mechanism for the F270S and S270F mutants, *L. forbesi* and *A. subulata* rhodopsins shows that the reorganization of the charged and polar residues in the binding pocket, which is caused by F270S substitution, is responsible only for a part of the spectral shift between *L. forbesi* and *A. subulata* rhodopsins. The rest of the spectral shift is due to the reorganization of residues located outside of the binding pocket. According to our models, this reorganization is caused by other substitution/substitutions than F270S. Additional computational/experimental work has to be performed to locate these mutations.

4. Concluding Remarks

In this study we investigated the origin of a spectral shift between visual rhodopsins from two squid species – *A. subulata* and *L. forbesi* that live at different depths in the ocean. To accomplish this task, we constructed a series of QM/MM models for these two rhodopsins, the F270S mutant of *L. forbesi* rhodopsin and the S270F mutant of *A. subulata* rhodopsin. We calculated λ_{max} values for these proteins, and performed an extensive analysis of their spectral tuning mechanisms. We showed that the origin of the 5 nm spectral shift between rhodopsins from *A. subulata* and *L. forbesi* is the consequence of the protein reorganization (non-direct tuning) caused by at least two mutations including S270F rather than an effect of a single specific amino acid substitution. Also, we find that the effect of the S270F substitution cannot be explained by the direct electrostatic effect of polar hydroxyl-bearing serine that replaces non-polar phenylalanine due to its far location from the chromophore.

Generally, these two squid rhodopins provide a striking example of non-direct tuning mechanism. The obtained results can be useful for the rational design of modern rhodopsin-based tools with altered optical properties that can be used in the fields of optogenetics and molecular visualization.[28,29] .

Заключение

В данной работе мы изучили причину спектрального сдвига между зрительными родопсинами двух кальмаров — *A. subulata* и *L. forbesi*, которые живут на различной глубине в океане. Для решения данной задачи мы сгенерировали ряд квантово-механических/молекулярно-механических моделей для этих двух родопсинов, а также мутанта родопсина из *L. forbesi* (F270S), рассчитали для них значения λ_{max} и провели детальный анализ механизмов, отвечающих за их спектральные свойства. Мы показали, что причиной 5 нм спектрального сдвига между родопсинами *A. subulata* и *L. forbesi* является реорганизация белка (непрямая регуляция спектральных свойств), вызванная как минимум двумя мутациями, включая замену S270F, а не определенная одиночная мутация. Также мы показали, что эффект аминокислотной замены S270F не является прямым электростатическим эффектом замены полярного серина, содержащего гидроксильную группу, на неполярный фениланин, так как данная аминокислота находится далеко от хромофора.

Таким образом, изученные родопсины кальмаров представляют собой показательный пример непрямой регуляции спектральных свойств. Полученные результаты могут быть использованы для рационального дизайна современных устройств оптогенетики и молекулярной визуализации на основе родопсинов с модифицированными оптическими свойствами

Acknowledgements

The work was supported by the SPbAU RAS state order, project 16.9790.2017/Bch. The research was carried out using equipment of the shared research facilities of HPC computing resources at the Lomonosov Moscow State University. The research was carried out using computational resources provided by Resource Center “Computer Center of SPbU”. The authors also express their gratitude to the SPbSU Centre for Molecular and Cell Technologies, Magnetic Resonance Research Centre, Chemical Analysis and Materials Research Centre, Centre for Optical and Laser Materials Research.

References

[1] D.M. Hunt, J. Fitzgibbon, S.J. Slobodyanyuk, J.K. Bowmaker, Vis. Res., 36 (1996) 1217-1224.
[2] A. Sivasundar, S.R. Palumbi, J. Evol. Biol., 23 (2010) 1159-1169.
[3] P.A. Jutte, T.W. Cronin, R.L. Caldwell, Mar. Freshw. Behav. Phy., 31 (1998) 231-250.
[4] A. Morris, J.K. Bowmaker, D.M. Hunt, Proc. R. Soc. Lond. B Biol. Sci., 254 (1993) 233-240.
[5] M. Hall, M. Hoon, N. Ryba, J. Pottinger, J. Keen, H. Saibil, J. Findlay, Biochem. J., 274 (1991) 35-40.
[6] M. Murakami, T. Kouyama, Nature, 453 (2008) 363.
[7] M. Stamm, R. Staritzbichler, K. Khafizov, L.R. Forrest, Nucleic Acids Res., 42 (2014) W246-W251.
[8] J. Yang, R. Yan, A. Roy, D. Xu, J. Poisson, Y. Zhang, Nat. Methods, 12 (2015) 7.
[9] A. Morozenko, A. Stuchebrukhov, Proteins, 84 (2016) 1347-1357.
[10] T.J. Dolinsky, P. Czodrowski, H. Li, J.E. Nielsen, J.H. Jensen, G. Klebe, N.A. Baker, Nucleic Acids Res., 35 (2007) W522-W525.
[11] M.H. Olsson, C.R. Søndergaard, M. Rostkowski, J.H. Jensen, J. Chem. Theory Comput., 7 (2011) 525-537.
[12] W.D. Cornell, P. Cieplak, C.I. Bayly, I.R. Gould, K.M. Merz, D.M. Ferguson, D.C. Spellmeyer, T. Fox, J.W. Caldwell, P.A. Kollman, J. Am. Chem. Soc., 117 (1995) 5179-5197.
[13] M. Frisch, G. Trucks, H.B. Schlegel, G.E. Scuseria, M.A. Robb, J.R. Cheeseman, G. Scalmani, V. Barone, B. Mennucci, G. Petersson, in, Gaussian, Inc., Wallingford CT, 2009.

[14] F. Neese, Wiley Interdiscip. Rev. Comput. Mol. Sci., 2 (2012) 73-78.
[15] D.M. Nikolaev, A.A. Shtyrov, M.S. Panov, A. Jamal, O.B. Chakchir, V.A. Kochemirovsky, M. Olivucci, M.N. Ryazantsev, ACS omega, 3 (2018) 7555-7566.
[16] M. Sumita, M.N. Ryazantsev, K. Saito, Phys. Chem. Chem. Phys., 11 (2009) 6406-6414.
[17] A.V. Struts, M.N. Ryazantsev, X. Xu, T.R. Molugu, S.M. Perera, C. Guruge, S. Faylough, C. Nascimento, N. Nesnas, M.F. Brown, Biophys. J., 116 (2019) 204a.
[18] P.Z. El-Khoury, A.N. Tarnovsky, I. Schapiro, M.N. Ryazantsev, M. Olivucci, J. Phys. Chem. A, 113 (2009) 10767-10771.
[19] M.N. Ryazantsev, A. Altun, K. Morokuma, J. Am. Chem. Soc., 134 (2012) 5520-5523.
[20] A. Filatov, N. Knyazev, M. Ryazantsev, V. Suslonov, A. Larina, A. Molchanov, R. Kostikov, V. Boitsov, A. Stepakov, Org. Chem. Front., 5 (2018) 595-605.
[21] D.M. Nikolaev, A. Emelyanov, V.M. Boitsov, M.S. Panov, M.N. Ryazantsev, F1000Research, 6 (2017).
[22] I. Schapiro, M.N. Ryazantsev, W.J. Ding, M.M. Huntress, F. Melaccio, T. Andruniow, M. Olivucci, Aust. J. Chem., 63 (2010) 413-429.
[23] D.S. Parker, B.B. Dangi, R.I. Kaiser, A. Jamal, M. Ryazantsev, K. Morokuma, J. Phys. Chem. A, 118 (2014) 12111-12119.
[24] M.N. Ryazantsev, A. Jamal, S. Maeda, K. Morokuma, Phys. Chem. Chem. Phys., 17 (2015) 27789-27805.
[25] A. Altun, S. Yokoyama, K. Morokuma, J. Phys. Chem. B, 112 (2008) 6814-6827.
[26] A. Altun, S. Yokoyama, K. Morokuma, J. Phys. Chem. B, 112 (2008) 16883-16890.
[27] T. Chan, M. Lee, T. Sakmar, J. Biol. Chem., 267 (1992) 9478-9480.
[28] D.M. Nikolaev, M.S. Panov, A.A. Shtyrov, V.M. Boitsov, S.Y. Vyazmin, O.B. Chakchir, I.P. Yakovlev, M.N. Ryazantsev, in: Progress in Photon Science, Springer, 2019, pp. 139-172.
[29] A.Y. Rotov, L.A. Astakhova, V.S. Sitnikova, A.A. Evdokimov, V.M. Boitsov, M.V. Dubina, M.N. Ryazantsev, M.L. Firsov, Acta naturae, 10 (2018) 75-84.

JOURNAL OF INTEGRATED OMICS
A METHODOLOGICAL JOURNAL
HTTP://WWW.JIOMICS.COM

REVIEW | DOI: 10.5584/jiomics.v9i1.265

Long non-coding RNA in regulation of vascular smooth muscle cells plasticity

Veronika Myasoedova [1], Dongwei Zhang [2], Andrey V. Grechko [3], Alexander N. Orekhov [1,4,5*]

[1]Laboratory of Angiopathology, Institute of General Pathology and Pathophysiology, 125315 Moscow, Russia; [2]Diabetes Research Center, Traditional Chinese Medicine School, Beijing University of Chinese Medicine, Beijing 100029, China; [3]Federal Research and Clinical Center of Intensive Care Medicine and Rehabilitology, 109240 Moscow, Russia; [4]Institute for Atherosclerosis Research, Skolkovo Innovative Center, 121609 Moscow, Russia; [5] Centre of Collective Use, Institute of Gene Biology, Russian Academy of Sciences, Moscow 121552, Russia

Received: 29 October 2018 **Accepted:** 31 December 2018 **Available Online**: 15 March 2019

Abstract

Phenotypic plasticity of vascular smooth muscle cells (VSMCs) is a functional property that is essential for vascular remodeling in vessel injury healing. During phenotypic switch, quiescent VSMCs loss contractile capacity but acquire ability to proliferate and migrate to the injured site where they differentiate again to the quiescent state. However, in pathological conditions such as endothelial dysfunction or atherosclerosis, phenotypic changes in arterial VSMCs become deregulated leading to elevated VSMC dedifferentiation, proliferation, excessive extracellular matrix deposits, and intimal thickening. VSMC hyperplasia is a complex mechanism that is coordinated by a network of various regulatory factors. Long non-coding (lnc)RNAs represent an important part of this regulatory network. Some of lncRNAs are involved in VSMC differentiation, apoptosis, and maintenance of quiescence, while other lncRNAs promote VSMC dedifferentiation, proliferation, and motility. In this review, we characterize these lncRNAs and their function in the context of possible involvement in atherosclerosis.

Аннотация

Гладкомышечные клетки кровеносных сосудов характеризуются пластическим фенотипом, который играет важную роль в восстановительных процессах. Эти клетки могут менять свой фенотип, теряя сократительные свойства и приобретая способность пролиферировать и мигрировать к поврежденным участкам ткани, где они снова дифференцируются и приходят в состояние покоя. Однако, при развитии различных патологий, в том числе, атеросклероза, регуляция фенотипической пластичности гладкомышечных клеток сосудов нарушается, что приводит к неконтролируемой и избыточной пролиферации, отложению межклеточного матрикса и, в конечном итоге, утолщению стенки сосуда. В этом сложном процессе принимают участие различные факторы. Длинные некодирующие РНК (длнкРНК) являются одним из таких факторов. Некоторые длнкРНК участвуют в дифференциации гладкомышечных клеток, апоптозе и поддержании фенотипа покоя, в то время как другие способствуют дедифференциации клеток, их пролиферации и миграции. В этом обзоре обсуждаются различные виды длнкРНК, возможно играющие важную роль в развитии атеросклероза.

Keywords: long non-coding RNA; VSMC; phenotype switch; proliferation; hyperplasia; atherosclerosis

1. Introduction

Vascular smooth muscle cells (VSMCs) reside in the arterial wall, in the layer called tunica media. These cells produce a variety of contractile proteins, ion carriers, and intracellular signaling components all involved in the regulation of vascular tone. Under normal conditions, VSMCs exhibit a quiescent phenotype characterized by contractility and a lack of proliferation and motility. However, adult VSMCs can acquire proliferative phenotype through the mechanism of hyperplasia under specific conditions such as vascular injury or hypoxia. Under stress, VSMCs are able to dedifferentiate to non-contractile cells that have a capacity to proliferate and migrate [1]. Dedifferentiated cells are also characterized by higher

***Corresponding author:** Alexander N. Orekhov; a.h.opexob@gmail.com; +7 903 169 08 66; Laboratory of Angiopathology, Institute of General Pathology and Pathophysiology, Moscow 125315, Russia

production of extracellular matrix (ECM) proteins and lower expression of contractile proteins, such as smooth muscle myosin heavy chain (SM-MHC), smooth muscle actin-α (SMA-α), sm-22α, calponin, caldesmon, i.e. typical markers of differentiated SMCs [2].

During vascular tissue repair, dedifferentiated VSMCs undergo several rounds of proliferation and participate in vascular remodeling. This process is characterized by neointima formation, medial stiffening, and intimal thickening, a phenomenon observed in vascular pathologies, such as atherosclerosis or pulmonary hypertension [3, 4]. In atherosclerosis, the phenotypic switch of VSMCs is a frequent event that may involve over 80% of plaque VSMCs [5]. Several studies aimed to understand the abundance of VSMC hyperplasia and identify molecular factors that drive both SMC-specific gene expression and differentiation. This work resulted in the discovery of a complex network of regulatory proteins and non-coding RNAs controlling the phenotypic switch of VSMCs [6-8]. However, precise molecular mechanisms that prime phenotypic changes in VSMCs during vascular remodeling remain to be elucidated. Long non-coding RNA (lncRNA) is a very diverse group of non-protein coding RNA molecules that are present in different organisms, from viruses to mammals [9]. However, it was noted that the abundance of lncRNA increases with the organism's complexity, even exceeding that of protein-coding genes [10]. According to current understanding, lncRNAs perform important regulatory and other functions that are only partly known to date. In this review, we will focus on the role of lncRNA in the control of the VSMCs phenotypic switch.

Origin and functions of long non-coding RNAs

Non-protein-coding lncRNAs are transcripts with a length over 200 nucleotides that are distinct from small non-coding RNA, such as microRNAs that are less than 25 nucleotides long. So far, over 167K and 130K lncRNA genes were identified in human and mouse respectively (NONCODE database version 6.0, http://www.noncode.org) [11]. These numbers exceed greatly the number of human protein-coding genes (circa 20K according to the GENCODE database version 19, http://www.gencodegenes.org/stats.html). However, it is unclear whether all these RNA sequences have a biological function because of the lack of categorizing and validating data about lncRNAs. Current criteria for categorization of lncRNAs are based on association with adjacent protein-coding genes (Figure 1).

The origin of lncRNA remains obscure, largely because of the elusive definition of this RNA class and its remarkable variety [9]. However, a recent hyporthesis proposed a possibility of an evolutionary path between enhancer-derived RNAs (eRNAs), which are short, unspliced and cis-acting, and lncRNAs that are much longer, undergo splicing and can be trans-acting [12]. Examples of intermediate forms were found, such as Lockd [13] and Bloodlinc [14] that support this suggestion. More details on eRNA functions are given below.

The localization of lncRNA genes can vary within the genome. Sense lncRNAs overlap with protein-coding genes and usually share the same promoter. Anti-sense lncRNAs are localized on the opposite strands to protein-coding genes. Intronic and intergenic (linc) RNAs reside in introns of protein-coding genes or between protein-coding genes respectively. Enhancer RNAs (eRNAs) span the enhancer regions of protein-coding genes. Circular RNAs (circRNAs) represent covalently enclosed RNAs that are usually originated from splicing of protein-coding genes. However, this classification does not reflect lncRNA function since only a few lncRNAs were functionally characterized so far. In general, lncRNA functions can be divided into four categories: imprinting, activation of enhancer, molecular sponges, and serving as scaffold/guide for epigenetic/transcription factors.

Imprinting

Imprinting can be generally defined as parental-specific gene expression in diploid cells when only one allele is active, and the other allele is epigenetically silenced [15]. The first lncRNA discovered was X-inactive specific transcript (XIST) [16]. The XIST sequences literally cover a whole chromosome X and perform X-inactivation mainly through interaction with polycomb-repressive complex 2 (PRC2) [17]. Other examples of well-studied lncRNAs involved in imprinting are Airn [18], KCNQ1OT1 [19, 20], and H19 [21]. Generally, imprinting-associated lncRNAs inhibit the expression of neighboring genes, acting as cis-regulators. Imprinting is of great importance for embryogenesis (as in the case of murine Xist) [22]. Therefore, imprinting lncRNAs are functionally significant in the developmental processes.

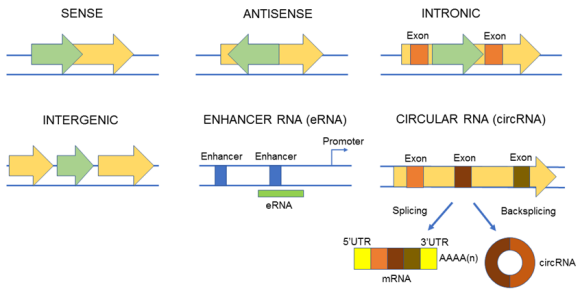

Figure 1 | Nomenclature of non-coding RNAs. Green and orange indicate non-coding RNA and protein-coding genes respectively. UTR, untranslated region. Номенклатура длнкРНК. Зелёным и оранжевым отмечены длнкРНК и кодирующие белок гены, соответственно. UTR – нетранслируемый участок.

Enhancer activation

eRNAs have a compact size that does not exceed 2000 nucleotides. They are transcribed in association with the regulated gene. For eRNAs, several possible mechanisms of action were suggested, including serving as decoys for major transcription factors or their binding sites, facilitating the interaction between the promoter and the enhancer through loop formation, and nucleosome depletion at the promoter region [23]. eRNAs are widely distributed across the genome. For example, in a primary mouse neuronal culture, about 12,000 activity-regulated enhancers were found [24]. Expression levels of these enhancers correlated with expression of adjacent protein-coding genes indicating the presence of enhancer-promoter interaction. Another study showed that 60% of transcribed enhancers are polyadenylated whereas the rest is transcribed without polyadenylation [25]. Similar situation was described for other types of lncRNAs. Polyadenylated eRNAs are unidirectly transcribed to the enhancer and therefore called 1d-eRNAs. By contrast, non-polyadenylated eRNAs (or 2d-eRNAs) are bidirectionally transcribed [26].

The so-called super-enhancer regions of the genome contain enhancer clusters marked by the presence of key tissue-specific transcription factors and mediators. For example, in embryonic stem cells, most genes that control the pluripotent state, have enhancer elements for binding Oct4, Sox2 and Nanog. These transcription factors are responsible for maintenance of the characteristic stem cell properties. After binding to an enhancer, these factors recruit Mediator, a transcriptional coactivator, to induce the expression of target genes [27]. For instance, PR (PRD1-BF1 -RIZ1 homologous) domain-containing 16 (PRDM16), a transcriptional coregulator, recruits MED1, a component of the Mediator complex, to super-enhancers at brown fat-selective genes to initiate a brown fat differentiation program [28].

Molecular sponges

circRNAs can originate from introns or exons (ecircRNAs) of coding genes. Circular intronic RNAs are predominantly present in the nucleus, while those originating from the exons are preferentially cytoplasmic [29]. In human fibroblasts, more than 25000 distinct circRNA species were found, that contained non-colinear exons and increased in numbers after exonuclease degradation of linear RNA [30]. CircRNAs are abundant, stable and evolutionary conserved (especially ecircRNAs), however, their function remains largely unknown. Some ecircRNAs may serve as RNA-binding proteins and contribute to miRNA regulation, and, presumably, to the control of parental gene expression and cell proliferation [31].

The detection of miRNA-binding sites in circRNAs allowed suggesting that circRNAs may act as molecular sponges for miRNAs, regulating their function by sequestration [32]. Circular RNA sponges for miR-7 (ciRS-7, also known as CDR1as) may serve as an example of miRNA-binding circRNA [33]. Linear lncRNAs can also act as sponges for miRNA. A muscle-specific linc-MD1 catches miR-133 and miR-135 to induce a differentiation switch in myoblasts [34, 35]. lncRNAs highly up-regulated in liver cancer (HULC) promote tumorigenesis by sequestering miR -372 [36]. Imprinting lncRNA H19 binds let-7 family of miRNAs, which in turn increases invasiveness of many cancers [37]. Protein-coding transcripts termed competing endogenous RNAs (ceRNAs), which are able to compete with miRNAs, also exist. These transcripts express concordantly with PTEN and possess regulatory properties by suppressing or supporting tumor growth [38].

Scaffolds for epigenetic/transcription factors

Scaffolding function of nuclear lncRNAs was first described in a study focusing on two histone modification complexes and polycomb repressive complex 2 (PRC2) and the LSD1/CoREST/REST complex binding to chromatin [39]. In mouse embryonic cells, the expression of lncRNAs is controlled by key transcription factors including stem cell markers Oct4 and Nanog while lincRNAs transcripts interact with numerous chromatin regulatory proteins to influence shared gene expression programs [40]. Inactivation of dozen of lincRNAs caused either loss of the pluripotent state or induction of alternative differentiation programs. These data indicated the importance of lncRNAs in the processes directing pluripotency and lineage commitment programs [41, 42]. A model was proposed, in which lincRNAs act as cell-type–specific flexible scaffolds to bear protein complexes (i.e. epigenetic factors) to induce specific transcriptional programs [40].

Other functions

Small conserved open-reading frames that encode micropeptides were found in annotated lncRNAs. For example, a putative skeletal muscle-specific lncRNA encodes a functional micropeptide termed myoregulin, which regulates muscle contractility by interaction with the endoplasmic reticulum Ca^{2+}-ATPase (SERCA) and inhibition of Ca^{2+} uptake into the sarcoplasmic reticulum [43]. Later, another micropeptide called DWORF was discovered, encoded by a putative skeletal muscle-specific lncRNA. Compared with myoregulin, DWORF possesses opposite functional properties by activating SERCA and enhancing Ca^{2+} load to the endoplasmic reticulum. These findings suggest that many annotated lncRNAs are 'hidden' mRNAs. Finally, lncRNAs may be involved in protein translocation between the nucleus and the cytosol and in the regulation of the stability of protein-coding genes [44].

Long non-coding RNAs that promote vascular smooth muscle cell proliferation and migration

H19

The gene encoding this imprinted lncRNA resides on chromosome 11p15.5, immediately downstream of the IGF2 gene encoding the insulin-like growth factor II (IGF2) [45]. H19 and IGF2 are imprinted in a mutual way. In the maternal chromosome, H19 is expressed but IGF2 is not. In the paternal chromosome, IGF2 is expressed, while H19 is not [21]. While IGF2 supports cell growth and proliferation, H19 exhibits anti-proliferative activity. The IGF2-H19 locus is involved in the regulation of embryogenesis. Hypomethylation of the IGF2-H19 locus on both chromosomes leads to the abolishment of imprinting accompanied by activation of H19 expression and decrease of IGF2 expression. This phenomenon is essential for the maintenance of quiescence of adult pluripotent stem cells. At the same time, hypermethylation of the IGF2-H19 locus on both chromosomes (i.e. loss of imprinting) results in IGF2 overproduction and is associated with tumorigenesis [46].

Expression of H19 was found at highest levels in the fetal muscle, in aortic smooth muscle, and at almost undetectable levels in adult VSMCs [47]. Up-regulation of this lncRNA was observed in the arterial neointima after acute vascular damage [48] and in atherosclerotic lesions [49]. In cell culture, H19 transcripts were undetectable in proliferating neointimal cells, but were highly abundant in differentiated neointimal cells. The first exon of H19 contains miR-675-encoding gene [50]. H19 regulates the processing of miR-675 and cooperates with this miRNA in physiological effects. For example, in the fetus, H19/miR-675 limits the prenatal placenta growth by inhibiting insulin-like growth factor 1 receptor (Igf1r) gene, a target for miR-675 [50]. However, overexpression of H19/miR-675 was shown to enhance proliferation and invasiveness of breast cancer cells by down-regulating members of ubiquitin ligase E3 family (c-Cbl and Cbl-b) and thereby increasing the stability of pro-oncogenic receptors EGFR and HGFR [51]. In the neointima of balloon-injured artery, both regulatory RNAs are overexpressed and promote neointimal formation and arterial restenosis by inhibition of phosphatase and tensin homolog (PTEN), a suppressor of cell growth and proliferation [52]. It seems that pathologic conditions such as vascular proliferative disorders (like atherosclerosis) and cancer, induce global epigenetic reprogramming accompanied by a loss of imprinting at the IGF2-H19 locus. In such conditions, this locus supports VSMC proliferation. In normal conditions, IGF2-H19 imprinting exists that is associated with suppression of VSMC proliferation.

ANRIL

The antisense noncoding RNA in the INK4 locus (ANRIL; also known as CDKN2BAS) is located on chromosome 9p21.3. This lncRNA shares the promoter with the CDKN2A (p14ARF) gene. The first ANRIL exon overlaps with two exons of the CDKN2B (p15INK4B) gene. Both CDKN2A and CDKN2B encode negative cell cycle regulators that target cyclin-dependent kinases CDK4 and CDK6 respectively. This disrupts binding of CDK4/CDK6 to D-cyclins and leads to the cell cycle arrest [53]. In addition, CDKN2A interacts with the E3 ubiquitin-protein ligase MDM2 that results in MDM2 degradation and derepression of p53 [54]. Expression of ANRIL and CDKN2A is coordinated both in steady-state and pathological conditions [55]. ANRIL silences the expression of CDKN2A by recruiting the polycomb repressive complex-2 (PRC2), a chromatin-modifying complex, to the shared promoter thereby permitting the cell cycle progression and cell proliferation [56].

The results of early studies suggested that ANRIL acts as a scaffold for PRC1 and PRC2 mediating the repression of the CDKN2B/ CDKN2A/CDKN1B locus in a cis manner [56, 57]. However, ANRIL exhibits a more complicated regulatory pattern displaying the ability to regulate gene expression in a trans manner as well. Genome-wide association studies showed a strong association of the ANRIL locus with coronary artery disease (CAD), type 2 diabetes, cancer, and intracranial aneurisms [58]. Association between ANRIL and cardiovascular diseases is complex and mediated by extended haplotypes located in the 58-kb region (so called CAD interval) that lacks any known protein-coding gene [40]. Disease-associated ANRIL variants were shown to influence the expression of this lncRNA. It was found that the association between ANRIL and atherosclerosis can be modulated in trans by Alu elements located in ANRIL and the promoters of its target genes [59].

Another study showed that the C/C genotype of single nucleotide polymorphism (SNP) rs1333049, a CAD risk ANRIL variant, was associated with the lowest expression of this lncRNA in VSMCs, increased VSMC proliferation, and the highest content of VSMCs in atherosclerotic plaques [60]. The risk allele C of rs1333049 can decrease the expression of the long ANRIL transcript but increase that of short transcripts, which in turn leads to CDKN2A/B down-regulation and VSMC proliferation [61]. The significance of this genomic region in the pathogenesis of vascular diseases was confirmed by the experiments, in which the orthologous 70-kb non-coding CAD interval was deleted from murine chromosome 4. That led to increased proliferation of VSMCs, reduction of cardiac expression of Cdkn2a/b [62], and vascular aneurism progression [63]. Loss of the CAD interval also resulted in reduced transforming growth factor (TGF)-β-dependent canonical Smad2 signaling [63]. This is consistent with recent observations that alterations in Tgf-β signaling in Cdkn2b-deficient VSMCs due to down-regulation of the inhibitor Smad7 impairs vessel maturation and VSMC recruitment to neovessels under hypoxic

conditions. However, inhibition of CDKN2B in hypoxic VSMCs leads to up-regulation of Tgf-β itself [64]. These findings suggest that overexpression of ANRIL in VSMCs promotes dedifferentiation, growth, proliferation, and profibrotic activity in a TGF-β-dependent manner.

Up-regulation of ANRIL contributes to atherogenesis. It was demonstrated that knockdown of ANRIL in VSMCs correlated with reduction of cell growth [65]. However, while linear forms of ANRIL appear to promote VSMC proliferation, a recently identified atheroprotective circular ANRIL (circANRIL) isoform exhibits opposite effects by inducing VSMC apoptosis and inhibiting proliferation. Mechanistically, circANRIL binds to pescadillo homologue 1 (PES1), an essential 60S-preribosomal assembly factor, that leads to the abnormalities in exonuclease-mediated pre-rRNA processing and ribosome biogenesis in VSMCs and macrophages. As a result, this circular RNA induces nucleolar stress and p53 activation with subsequent apoptosis [66]. In summary, ANRIL exerts complex effects on VSMC behavior and function. In human aortic SMCs, different ANRIL splice variants may have distinct roles by influencing the expression of genes involved in cell proliferation, apoptosis, vascular remodeling, and inflammation.

SMILR

The intergenic lncRNA (chromosome 8q24.13) has been recently identified in VSMCs stimulated with interleukin (IL)-1α and platelet-derived growth factor (PDGF) [67]. Followed stimulation, levels of this RNA called smooth muscle-induced lncRNA enhances replication (SMILR). SMILR activates VSMC proliferation. Interestingly, SMILR depletion led to down-regulation of hyaluronan synthase 2 (HAS2), an enzyme involved in the extracellular matrix synthesis during neointimal formation [68]. High levels of SMILR were observed in vulnerable atherosclerotic plaques suggesting for a possible proatherogenic role.

HAS2-AS1

Hyaluronan synthase 2 antisense RNA1 (HAS2-AS1) is located on chromosome 8q24.13, in the vicinity to the HAS2 gene, but seems to have a distinct promoter [69]. Expression of this antisense RNA is coordinated with that of HAS2. In renal proximal tubular epithelial cells, expression of both genes can be induced by IL-1β or TGF-β. Furthermore, for HAS2-AS1 and HAS2, the possibility to form a heterodimer was shown in silico [69]. O-GlcNAcylation modulates HAS2 -AS1 promoter up-regulation through mobilization of the NF-κB subunit p65, while HAS2-AS1 itself performs cis-regulation of HAS2 expression by chromatin remodeling about the proximal HAT2 promoter via O-GlcNAcylation and acetylation [70]. Overactivity of HAS2/HAS2-AS1 may contribute to diabetic macrovascular complications by stimulating dedifferentiation and proliferation of VSMCs since diabetic vessels are rich of matrix hyaluronan, a stimulator of HAS2 synthesis.

MIR222HG

The non-coding miR-222 host gene (MIR222HG; also known as Lnc-Ang362) is located on chromosome Xp11.3 and serves as a host transcript for miR-221 and miR-222, two RNAs that stimulate proliferation of VSMCs. In VSMCs, MIR222HG expression can be induced by angiotensin II. MIR222HG knockdown reduces VSMC proliferation thereby suggesting that this lncRNA possesses proproliferative properties [71].

Long non-coding RNAs that promote vascular smooth muscle differentiation or inhibit proliferation

SENCR

The gene encoding this cytoplasmic lncRNA is located on chromosome 11q24.3. SENCR (Smooth muscle and Endothelial cell-enriched migration/differentiation-associated long non-coding RNA) is transcribed antisense at 5'end of the Friend leukemia integration 1 transcription factor (FLI1) and contains two splice variants [72]. This lncRNA is enriched in vascular cells such as VSMCs and the endothelial cells. Despite the overlap with the FLI gene, little or no cis-effect of SENCR to FLI1 or neighboring gene expression was observed [72]. SENCR knock-down was accompanied with significant down-regulation of the expression of myocardin and multiple smooth muscle contractile genes. Accordingly, down-regulation of SENCR also led to the activation of VSMC proliferation and migration mediated through up-regulation of the transcription factor Forkhead box protein O1 (FoxO1) and transient receptor potential cation channel C6 (TRPC6) [73]. These data indicate that this SMC-enriched RNA is involved in the regulation of SMC differentiation program. Overexpression of SENCR could reverse proproliferative effects of high glucose on VSMC suggesting for a potential vasculoprotective function in diabetes. Recently, it was reported that expression of SENCR significantly correlated with left ventricular (LV) mass to LV end-diastolic volume ratio, a marker of cardiac remodeling, in type 2 diabetic patients [74]. This indeed indicates a role of SENCR as an independent predictor of remodeling in diabetes. In summary, SENCR supports VSMC differentiation and is expected to play an anti-atherosclerotic role. Further studies are required to identify the molecular targets and signaling pathways regulated by this lncRNA.

MYOSLID

Recently, a new SMC-specific lncRNA was identified, named MYOcardin-induced Smooth muscle LncRNA, Inducer of Differentiation (MYOSLID) [75]. The MYOSLID

gene is situated on chromosome 2q33.3, upstream the LINC01802 gene that encodes long intergenic non-protein coding RNA 1802. Myocardin drives the transcription of MYOSLID. In VSMCs, this RNA is involved in propagation of the VSMC differentiation and inhibition of proliferation. MYOSLID did not influence expression of any transcription factors. However, knock-down of this RNA in VSMCs abolished formation of actin stress fibers and prevented the translocation of MYOCD-related transcription factor A (MKL1) to the nucleus. In addition, down-regulation of MYOSLID inhibited TGF-β-mediated activation of SMAD2, an intracellular effector that mediates the effects of this growth factor on cell differentiation [75].

LincRNA-p21

LincRNA-p21 (also known as tumor protein p53 pathway corepressor 1, TRP53COR1) is a p53-induced intergenic lncRNA located on chromosome 6p21.2. By binding to MDM2, lincRNA-p21 derepresses p53 and stimulates p53 interaction with p300. P53/p300 complex then binds to the promoters or enhancers of target genes to promote their expression [76]. LincRNA-p21 inhibits VSMC proliferation and induces apoptosis of cultured VSMCs and macrophages. Expression of this RNA is decreased in CAD patients. In in a murine carotid artery injury model, lincRNA-p21 knockdown promoted neointima formation [77]. Together, these data indicate that lincRNA-p21 suppresses neointimal hyperplasia of VSMCs and may therefore have anti-atherosclerotic properties.

HIF1A-AS1

This lncRNA spans the 5' region of the hypoxia-inducible factor-1α-encoding HIF1A gene in the antisense direction (chromosome 14q23.2). It is unknown whether HIF1A-AS1 influences HIF1A expression in cis. In VSMCs, this RNA is induced by Brahma-related gene 1 (BRG1), a transcription factor. Both BRG1 and HIF1A-AS1 are overexpressed in the aortic media of patients with thoracic aortic aneurysms that leads to increased apoptosis and suppressed proliferation of aortic SMCs in a p53-dependent manner and finally to aortic dissection [78]. It was found that inhibition of HIF1A-AS1 in VSMCs resulted in suppression of caspase-3 and caspase-8, both are proapoptotic proteins, and stimulation Bcl2, an anti-apoptotic protein [79]. It is likely that HIF1A-AS1 plays a pathogenic role in aortic aneurism by suppressing proliferation and activating apoptosis of VSMCs.

GAS5

LncRNA Growth arrest specific 5 (GAS5) is located on chromosome 1q25.1 within the cluster of 11 small nucleolar (sno)RNAs. According to current understanding, snoRNAs act as guide non-coding RNAs, which are involved in biogenesis (modifications) of other small nuclear RNAs [80]. GAS5 and the cluster of GAS5 resides between two protein-coding genes, namely DARS2 (encodes aspartyl-tRNA synthetase 2, mitochondrial) and ZBTB37 (encodes zinc finger and BTB domain containing 37, a transcriptional regulator). However, it is unknown whether GAS5 controls the expression of ZBTB37 and DARS2 in a cis manner. The cluster also contains a gene encoding GAS5-AS1 RNA that may potentially be responsible for the control of GAS5 expression. GAS5 exhibits multiple functions. The most prominent role of this RNA is to serve as a tumor suppressor, since GAS5 blocks the growth and spreading of tumor cells in many cancer types [81]. Overexpression of GAS5 is able to suppress the proliferation of non-cancer cells, for example, vein SMCs. It was found that GAS5 overproduction inhibited proliferation and migration, but also reduced apoptosis of human saphenous vein SMCs [82]. However, when expressed at low levels, this RNA contributes to the formation of primary varicose great saphenous veins by stimulating VSMC proliferation and motility. In the vascular wall, GAS5 is expressed in the endothelial cells and VSMCs, and can contribute to controlling functional activity of these cells. In hypertension, vascular expression of GAS5 was shown to be reduced [83]. GAS5 plays a vasculoprotective role by repressing neointimal hyperplasia of VSMCs. Hypertension-induced down-regulation of GAS5 leads to microvascular dysfunction associated with the vessel leakage and retinal neovascularization. In hypertension, GAS5 regulates vascular remodeling by controlling function of endothelial cells and VSMCs through β-catenin-dependent pathway [83].

Other lncRNAs

Recently, at least three lncRNAs (i.e. ADCY5, ARHGEF12, and FGF12) were found to influence the expression of myocardin, a key transcription factor in launching SMC-specific differentiation program [84]. Depletion of these competitive endogenous RNAs resulted in down-regulation of myocardin and phenotypic transformation of VSMCs from contractile cells to undifferentiated cells characterized by advanced proliferation, enhanced ECM production, and mural thrombi formation. These characteristics may cause an abnormal tissue repair and chronical maintenance of intracranial aneurysms. Therefore, these lncRNAs appear to be involved in the regulation of mature SMC contractility.

Long non-coding RNA detection and use

Numerous studies have identified particular lncRNAs as clinically useful biomarkers, mostly, for detection of various cancers [85, 86], but also for other human diseases, such as ischemic stroke [87] and other cardiovascular disorders [88]. Correspondingly, the interest in improved methods of lncRNA detection is growing. To date, the two most commonly used methods for lncRNA detection are

microarrays that were first developed to detect protein-coding RNAs, and RNA sequencing (RNA-seq) [89]. Microarrays are well-characterized and powerful tools for detection of particular lncRNA with previously known sequences. RNA-seq approach requires a more complicated analysis, but has a broader coverage of lncRNA transcriptome than microarrays. Libraries for RNA-seq can be created using oligo dT beads to enrich and detect polyadenylated lncRNAs (together with mRNAs) or via depletion of rRNA to analyze all other lncRNAs, including circRNAs. The methodological difference between the two methods naturally suggests using RNA-seq approach mostly for screening for novel lncRNAs associated with various human diseases, and microarrays – for robust detection of established lncRNA biomarkers.

The discovery of new lncRNAs and better characterization of the known ones increases the number of novel biomarkers and potential therapeutic targets for treatment of cardiovascular diseases, including atherosclerosis. The lncRNAs discussed in this review likely represent only the beginning of the long list of lncRNAs implicated in cardiovascular diseases that remains to be established. Recently, the diagnostic and therapeutic potential of circRNAs for treatment of cardiovascular diseases has been discussed [88]. Silencing disease-associated lncRNAs that promote cell proliferation appears to be an attractive therapeutic possibility, which has already been explored in animal models of some cancers. Inhibition of lncRNAs can be achieved by different modern methods, such as the use of small interfering RNA (siRNAs) or short hairpin RNAs (shRNAs) and knock-down via CRISPR/Cas9 editing. Some of these methods have already been employed at pre-clinical level and are described in a recent review [90]. More studies are needed, however, to translate the accumulating knowledge of regulatory lncRNAs into clinical applications.

5. Concluding Remarks

Phenotypic switch of VSMCs followed by hyperplasia and neointima formation is an essential stage of pro-atherosclerotic vascular remodeling. LncRNAs play an essential role in controlling this process. Some RNAs suppress proliferation/migration of VSMCs thereby preventing phenotype changes, while others up-regulate VSMC proliferation and hence support VSMC dedifferentiation and neointimal formation. Expression of proproliferative VSMCs can be up-regulated in atherosclerotic plaques and therefore inhibition of their expression may have therapeutic interest in order to target aberrant arterial wall remodeling in atherosclerosis. However, at present, using lncRNAs for clinical purposes is not yet considered. Only a few lncRNA are functionally characterized so far. In VSMCs, lncRNAs form a complex regulatory network that controls VSMC function and behavior. This network becomes even more complex since lncRNAs interacts with miRNAs and regulatory proteins. In addition, not all lncRNAs exclusively expressed or enriched in VSMCs. Therefore, targeting widely distributed lncRNAs may increase risk of target-off effects and adverse influences on other cells. Using cell-type specific delivery approaches may reduce off-target effects since quiescent and hyperplastic VSMCs express distinct sets of biomarkers. Circulating lncRNAs can probably be also used as diagnostic and prognostic biomarkers, and this possibility is already being explored in some studies. In conclusion, although lncRNAs have promising therapeutic potential, they have not attained the stage that would provide an option of easy clinical application.

Заключение

Смена фенотипа гладкомышечных клеток кровеносных сосудов, сопровождающаяся гиперплащией и утолщением сосудистой стенки является важным этапом в развитии атеросклеротической бляшки, и длнкРНК играют важную роль в этом процессе. Отдельные виды длнкРНК подавляют пролиферацию и миграцию гладкомышечных клеток, таким образом, препятствуя смере фенотипа, в то время как другие виды наоборот, способствуют пролиферации и миграции и, тем самым, формированию неоинтимы. Пролиферация гладкомышечных клеток наблюдается в атеросклеротических бляшках, и подавление этого процесса может иметь важное терапевтическое значение. Однако, в настоящее время еще рано говорить о терапевтическом применении длнкРНК. Лишь несколько длнкРНК были функционально охарактеризованы к настоящему моменту. В то же время, в гладкомышечных клетках сосудов может существовать развитая регулирующая сеть, включающия различные длнкРНК, которые также могут взаимодействовать с малыми интерферирующими РНК и регуляторными белками. Кроме того, не все описанные длнкРНК экспрессируются преимущественно в гладкомышечных клетках, что создает риск побочных эффектов при применении этих длнкРНК. Решением этой проблемы может стать разработка методов направленной доставки терапевтических молекул в гладкомышечные клетки атеросклеротических бляшек, так как эти клетки имеют некоторые характерные биомаркеры, которые позволяют различать клетки, находящиеся в состоянии покоя от пролиферирующих клеток. длнкРНК, присутствующие в системе кровообращения, могут также служить в качестве диагностических и прогностических факторов, и эта возможность в настоящее время активно исследуется. Таким образом, длнкРНК обладают интересным потенциалом для диагностики и лечения атеросклероза, который, однако, в настоящий момент еще не достаточно исследован.

Acknowledgements

This work was supported by the Russian Science Foundation (Grant # 18-15-00254).

References

[1] G.K. Owens, M.S. Kumar, B.R. Wamhoff, Physiol Rev 84 (2004) 767–801. doi:10.1152/physrev.00041.2003.

[2] G.K. Owens, Novartis Found Symp 283 (2007) 174-91; discussion 191-3, 238-41.

[3] L.A. Shimoda, S.S. Laurie, J Mol Med (Berl) 91 (2013) 297-309. doi: 10.1007/s00109-013-0998-0.

[4] B.P. Herring, A.M. Hoggatt, C. Burlak, S. Offermanns, Vasc Cell 6 (2014) 21. doi: 10.1186/2045-824X-6-21.

[5] L.S. Shankman, D. Gomez, O.A. Cherepanova, M. Salmon, G.F. Alencar, R.M. Haskins, P. Swiatlowska, A.A. Newman, E.S. Greene, A.C. Straub, B. Isakson, G.J. Randolph, G.K. Owens, Nat Med 21 (2015) 628-37. doi: 10.1038/nm.3866.

[6] M.S. Kumar, G.K. Owens, Arterioscler Thromb Vasc Biol 23 (2003) 737-47. doi: 10.1161/01.ATV.0000065197.07635.BA.

[7] B.N. Davis-Dusenbery, C. Wu, A. Hata, Arterioscler Thromb Vasc Biol 31 (2011) 2370-7. doi: 10.1161/ATVBAHA.111.226670.

[8] H. Kang, A. Hata, Curr Opin Hematol 19 (2012) 224-31. doi: 10.1097/MOH.0b013e3283523e57.

[9] J.J. Quinn, H.Y. Chang, Nat Rev Genet 17 (2016) 47-62. doi: 10.1038/nrg.2015.10.

[10] A. Necsulea, M. Soumillon, M. Warnefors, A. Liechti, T. Daish, U. Zeller, J.C. Baker, F. Grutzner, H. Kaessmann, Nature 505 (2014) 635-640. doi: 10.1038/nature12943.

[11] Y. Zhao, H. Li, S. Fang, Y. Kang, W. Wu, Y. Hao, Z. Li, D. Bu, N. Sun, M.Q. Zhang, R. Chen, Nucleic Acids Res 44 (2016) D203-8. doi: 10.1093/nar/gkv1252.

[12] J.M. Espinosa, Trends Genet 33 (2017) 660-662. doi: 10.1016/j.tig.2017.07.005.

[13] V.R. Paralkar, C.C. Taborda, P. Huang, Y. Yao, A.V. Kossenkov, R. Prasad, J. Luan, J.O.J. Davies, J.R. Hughes, R.C. Hardison, G.A. Blobel, M.J. Weiss, Mol Cell 62 (2016) 104-110. doi: 10.1016/j.molcel.2016.02.029.

[14] J.R. Alvarez-Dominguez, M. Knoll, A.A. Gromatzky, H.F. Lodish, Cell Rep 19 (2017) 2503-2514. doi: 10.1016/j.celrep.2017.05.082.

[15] D.P. Barlow, M.S. Bartolomei, Cold Spring Harb Perspect Biol 6 (2014). pii: a018382. doi:10.1101/cshperspect.a018382.

[16] L.B. Herzing, J.T. Romer, J.M. Horn, A. Ashworth, Nature 386 (1997) 272–5. doi:10.1038/386272a0.

[17] M.D. Simon, S.F. Pinter, R. Fang, K. Sarma, M. Rutenberg-Schoenberg, S.K. Bowman, B.A. Kesner, V.K. Maier, R.E. Kingston, J.T. Lee, Nature 504 (2013) 465–9. doi: 10.1038/nature12719.

[18] F. Sleutels, R. Zwart, D.P. Barlow, Nature 415 (2002) 810–13. doi:10.1038/415810a.

[19] R.R. Pandey, M. Ceribelli, P.B. Singh, J. Ericsson, R. Mantovani, C. Kanduri, J Biol Chem 179 (2004) 52685-93. doi: 10.1074/jbc.M408084200.

[20] N. Thakur, V.K. Tiwari, H. Thomassin, R.R. Pandey, M. Kanduri, A. Gondor, T. Grange, R. Ohlsson, C. Kanduri, Mol Cell Biol 24 (2004) 7855–62. doi:10.1128/MCB.24.18.7855-7862.2004.

[21] M.S. Bartolomei, S. Zemel, S.M. Tilghman, Nature 351 (1991) 153–5. doi:10.1038/351153a0.

[22] G.F. Kay, G.D. Penny, D. Patel, A. Ashworth, N. Brockdorff, S. Rastan, Cell 72 (1993) 171–82. doi: 10.1016/0092-8674(93)90658-D.

[23] R. Bonasio, R. Shiekhattar, Annu Rev Genet 48 (2014) 433–55. doi:10.1146/annurev-genet-120213-092323.

[24] T.K. Kim, M. Hemberg, J.M. Gray, A.M. Costa, D.M. Bear, J. Wu, D.A. Harmin, M. Laptewicz, K. Barbara-Haley, S. Kuersten, E. Markenscoff-Papadimitriou, D. Kuhl, H. Bito, P.F. Worley, G. Kreiman, M.E. Greenberg, Nature 465 (2010) 182-7. doi: 10.1038/nature09033.

[25] F. Koch, R. Fenouil, M. Gut, P. Cauchy, T.K. Albert, J. Zacarias-Cabeza, S. Spicuglia, A.L. de la Chapelle, M. Heidemann, C. Hintermair, D. Eick, I. Gut, P. Ferrier, J.C. Andrau, Nat Struct Mol Biol 18 (2011) 956-63. doi: 10.1038/nsmb.2085.

[26] G. Natoli, J.C. Andrau, Annu Rev Genet 46 (2012) 1-19. doi: 10.1146/annurev-genet-110711-155459.

[27] W.A. Whyte, D.A. Orlando, D. Hnisz, B.J. Abraham, C.Y. Lin, M.H. Kagey, P.B. Rahl, T.I. Lee, R.A. Young, Cell 153 (2013) 307-19. doi: 10.1016/j.cell.2013.03.035.

[28] M.J. Harms, H.W. Lim, Y. Ho, S.N. Shapira, J. Ishibashi, S. Rajakumari, D.J. Steger, M.A. Lazar, K.J. Won, P. Seale, Genes Dev 29 (2015) 298-307. doi: 10.1101/gad.252734.114.

[29] Y. Zhang, X.O. Zhang, T. Chen, J.F. Xiang, Q.F. Yin, Y.H. Xing, S. Zhu, L. Yang, L.L. Chen, Mol Cell 51 (2013) 792–806. doi: 10.1016/j.molcel.2013.08.017.

[30] W.R. Jeck, J.A. Sorrentino, K. Wang, M.K. Slevin, C.E. Burd, J. Liu, W.F. Marzluff, N.E. Sharpless, RNA 19 (2013) 141-57. doi: 10.1261/rna.035667.112.

[31] I. Chen, C.Y. Chen, T.J. Chuang, Wiley Interdiscip Rev RNA 6 (2015) 563-79. doi: 10.1002/wrna.1294.

[32] T.B. Hansen, T.I. Jensen, B.H. Clausen, J.B. Bramsen, B. Finsen, C.K. Damgaard, J. Kjems, Nature 495 (2013) 384–8. doi: 10.1038/nature11993.

[33] H. Xu, S. Guo, W. Li, P. Yu, Sci Rep 5 (2015) 12453. doi: 10.1038/srep12453.

[34] M. Cesana, D. Cacchiarelli, I. Legnini, T. Santini, O. Sthandier, M. Chinappi, A. Tramontano, I. Bozzoni, Cell 147 (2011) 358-69. doi: 10.1016/j.cell.2011.09.028.

[35] I. Legnini, M. Morlando, A. Mangiavacchi, A. Fatica, I. Bozzoni, Mol Cell 53 (2014) 506-14. doi: 10.1016/j.molcel.2013.12.012.

[36] J. Wang, X. Liu, H. Wu, P. Ni, Z. Gu, Y. Qiao, N. Chen, F. Sun, Q. Fan, Nucleic Acids Res 38 (2010) 5366-83. doi: 10.1093/nar/gkq285.

[37] A.N. Kallen, X.B. Zhou, J. Xu, C. Qiao, J. Ma, L. Yan, L. Lu, C. Liu, J.S. Yi, H. Zhang, W. Min, A.M. Bennett, R.I. Gregory, Y. Ding, Y. Huang, Mol Cell 52 (2013) 101-12. doi: 10.1016/j.molcel.2013.08.027.

[38] Y. Tay, L. Kats, L. Salmena, D. Weiss, S.M. Tan, U. Ala, F. Karreth, L. Poliseno, P. Provero, F. Di Cunto, J. Lieberman, I. Rigoutsos, P.P. Pandolfi, Cell 147 (2011) 344-57. doi: 10.1016/j.cell.2011.09.029.

[39] M.C. Tsai, O. Manor, Y. Wan, N. Mosammaparast, J.K. Wang, F. Lan, Y. Shi, E. Segal, H.Y. Chang, Science 329 (2010) 689-93. doi: 10.1126/science.1192002.

[40] M. Guttman, I. Amit, M. Garber, C. French, M.F. Lin, D. Feldser, M. Huarte, O. Zuk, B.W. Carey, J.P. Cassady, M.N. Cabili, R. Jaenisch, T.S. Mikkelsen, T. Jacks, N. Hacohen, B.E. Bernstein, M. Kellis, A. Regev, J.L. Rinn, E.S. Lander, Nature 458 (2009) 223-7. doi: 10.1038/nature07672.

[41] M.E. Dinger, P.P. Amaral, T.R. Mercer, K.C. Pang, S.J. Bruce, B.B. Gardiner, M.E. Askarian-Amiri, K. Ru, G. Soldà, C. Simons, S.M. Sunkin, M.L. Crowe, S.M. Grimmond, A.C. Perkins, J.S. Mattick, Genome Res 18 (2008) 1433-45. doi: 10.1101/gr.078378.108.

[42] J. Sheik Mohamed, P.M. Gaughwin, B. Lim, P. Robson, L. Lipovich, RNA 16 (2010) 324-37. doi: 10.1261/rna.1441510.

[43] D.M. Anderson, K.M. Anderson, C.L. Chang, C.A. Makarewich, B.R. Nelson, J.R. McAnally, P. Kasaragod, J.M. Shelton, J. Liou, R. Bassel-Duby, E.N. Olson, Cell 160 (2015) 595-606. doi: 10.1016/j.cell.2015.01.009.

[44] A.T. Willingham, A.P. Orth, S. Batalov, E.C. Peters, B.G. Wen, P. Aza-Blanc, J.B. Hogenesch, P.G. Schultz, Science 309 (2005) 1570–1573. doi:10.1126/science.1115901.

[45] S. Zemel, M.S. Bartolomei, S.M. Tilghman, Nat Genet 2 (1992) 61-5. doi:10.1038/ng0992-61.

[46] M.Z. Ratajczak, Folia Histochem Cytobiol 50 (2012) 171-9. doi: 10.5603/FHC.2012.0026.

[47] D.K. Han, G. Liau, Circ Res 71 (1992) 711-9. doi: 10.1161/01.RES.71.3.711.

[48] D.K. Kim, L. Zhang, V.J. Dzau, R.E. Pratt, J Clin Invest 93 (1994) 355-60.

[49] D.K. Han, Z.Z. Khaing, R.A. Pollock, C.C. Haudenschild, G. Liau, J Clin Invest 97 (1996) 1276-85. doi: 10.1172/JCI118543.

[50] A. Keniry, D. Oxley, P. Monnier, M. Kyba, L. Dandolo, G. Smits, W. Reik, Nat Cell Biol 14 (2012) 659-65. doi: 10.1038/ncb2521.

[51] C. Vennin, N. Spruyt, F. Dahmani, S. Julien, F. Bertucci, P. Finetti, T. Chassat, R.P. Bourette, X. Le Bourhis, E. Adriaenssens, Oncotarget 6 (2015) 29209-23. doi: 10.18632/oncotarget.4976.

[52] J. Lv, L. Wang, J. Zhang, R. Lin, L. Wang, W. Sun, H. Wu, S. Xin, Biochem Biophys Res Commun 497 (2017) 1154-61. doi: 10.1016/j.bbrc.2017.01.011.

[53] J. Gil, G. Peters, Nat Rev Mol Cell Biol 7 (2006) 667-77. doi:10.1038/nrm1987.

[54] N. Popov, J. Gil, Epigenetics 5 (2010) 685-90. doi: 10.4161/epi.5.8.12996.

[55] E. Pasmant, I. Laurendeau, D. Héron, M. Vidaud, D. Vidaud, I. Bièche, Cancer Res 67 (2007) 3963-9. doi: 10.1158/0008-5472.CAN-06-2004.

[56] Y. Kotake, T. Nakagawa, K. Kitagawa, S. Suzuki, N. Liu, M. Kitagawa, Y. Xiong, Oncogene 30 (2011) 1956-62. doi: 10.1038/onc.2010.568.

[57] K.L. Yap, S. Li, A.M. Muñoz-Cabello, S. Raguz, L. Zeng, S. Mujtaba, J. Gil, M.J. Walsh, M.M. Zhou, Mol Cell 38 (2010) 662-74. doi: 10.1016/j.molcel.2010.03.021.

[58] F. Aguilo, S. Di Cecilia, M.J. Walsh, Curr Top Microbiol Immunol 394 (2016) 29-39. doi: 10.1007/82_2015_455.

[59] L.M. Holdt, S. Hoffmann, K. Sass, D. Langenberger, M. Scholz, K. Krohn, K. Finstermeier, A. Stahringer, W. Wilfert, F. Beutner, S. Gielen, G. Schuler, G. Gäbel, H. Bergert, I. Bechmann, P.F. Stadler, J. Thiery, D. Teupser, PLoS Genet 9 (2013) e1003588. doi: 10.1371/journal.pgen.1003588.

[60] A. Motterle, X. Pu, H. Wood, Q. Xiao, S. Gor, F.L. Ng, K. Chan, F. Cross, B. Shohreh, R.N. Poston, A.T. Tucker, M.J. Caulfield, S. Ye, Hum Mol Genet 21 (2012) 4021-9. doi: 10.1093/hmg/dds224.

[61] O. Jarinova, A.F. Stewart, R. Roberts, G. Wells, P. Lau, T. Naing, C. Buerki, B.W. McLean, R.C. Cook, J.S. Parker, R. McPherson, Arterioscler Thromb Vasc Biol 29 (2009) 1671-7. doi: 10.1161/ATVBAHA.109.189522.

[62] A. Visel, Y. Zhu, D. May, V. Afzal, E. Gong, C. Attanasio, M.J. Blow, J.C. Cohen, E.M. Rubin, L.A. Pennacchio, Nature 464 (2010) 409-12. doi: 10.1038/nature08801.

[63] C. Loinard, G. Basatemur, L. Masters, L. Baker, J. Harrison, N. Figg, J. Vilar, A.P. Sage, Z. Mallat, Circ Cardiovasc Genet 7 (2014) 799-805. doi: 10.1161/CIRCGENETICS.114.000696.

[64] V. Nanda, K.P. Downing, J. Ye, S. Xiao, Y. Kojima, J.M. Spin, D. DiRenzo, K.T. Nead, A.J. Connolly, S. Dandona, L. Perisic, U. Hedin, L. Maegdefessel, J. Dalman, L. Guo, X. Zhao, F.D. Kolodgie, R. Virmani, H.R. Davis, N.J. Leeper, Circ Res 118 (2016) 230-40. doi: 10.1161/CIRCRESAHA.115.307906.

[65] A. Congrains, K. Kamide, R. Oguro, O. Yasuda, K. Miyata, E. Yamamoto, T. Kawai, H. Kusunoki, H. Yamamoto, Y. Takeya, K. Yamamoto, M. Onishi, K. Sugimoto, T. Katsuya, N. Awata, K. Ikebe, Y. Gondo, Y. Oike, M. Ohishi, H. Rakugi, Atherosclerosis 220 (2012) 449-55. doi: 10.1016/j.atherosclerosis.2011.11.017.

[66] L.M. Holdt, A. Stahringer, K. Sass, G. Pichler, N.A. Kulak, W. Wilfert, A. Kohlmaier, A. Herbst, B.H. Northoff, A. Nicolaou, G. Gäbel, F. Beutner, M. Scholz, J. Thiery, K. Musunuru, K. Krohn, M. Mann, D. Teupser, Nat Commun 7 (2016) 12429. doi: 10.1038/ncomms12429.

[67] M.D. Ballantyne, K. Pinel, R. Dakin, A.T. Vesey, L. Diver, R. Mackenzie, R. Garcia, P. Welsh, N. Sattar, G. Hamilton, N. Joshi, M.R. Dweck, J.M. Miano, M.W. McBride, D.E. Newby, R.A. McDonald, A.H. Baker, Circulation 133 (2016) 2050-65. doi: 10.1161/CIRCULATIONAHA.115.021019.

[68] Y. Kashima, M. Takahashi, Y. Shiba, N. Itano, A. Izawa, J. Koyama, J. Nakayama, S. Taniguchi, K. Kimata, U. Ikeda, PLoS One 8 (2013) e58760. doi: 10.1371/journal.pone.0058760.

[69] D.R. Michael, A.O. Phillips, A. Krupa, J. Martin, J.E. Redman, A. Altaher, R.D. Neville, J. Webber, M.Y. Kim, T. Bowen, J Biol Chem 286 (2011) 19523-32. doi: 10.1074/jbc.M111.233916.

[70] D. Vigetti, S. Deleonibus, P. Moretto, T. Bowen, J.W. Fischer, M. Grandoch, A. Oberhuber, D.C. Love, J.A. Hanover, R. Cinquetti, E. Karousou, M. Viola, M.L. D'Angelo, V.C. Hascall, G. De Luca, A. Passi, J Biol Chem 289 (2014) 28816-26. doi: 10.1074/jbc.M114.597401.

[71] A. Leung, C. Trac, W. Jin, L. Lanting, A. Akbany, P. Sætrom, D.E. Schones, R. Natarajan, Circ Res 113 (2013) 266-78. doi: 10.1161/CIRCRESAHA.112.300849.

[72] R.D. Bell, X. Long, M. Lin, J.H. Bergmann, V. Nanda, S.L. Cowan, Q. Zhou, Y. Han, D.L. Spector, D. Zheng, J.M. Miano, Arterioscler Thromb Vasc Biol 34 (2014) 1249-59. doi: 10.1161/ATVBAHA.114.303240.

[73] Z.Q. Zou, J. Xu, L. Li, Y.S. Han, Biomed Pharmacother 74 (2015) 35-41. doi: 10.1016/j.biopha.2015.06.009.

[74] D. de Gonzalo-Calvo, F. Kenneweg, C. Bang, R. Toro, R.W. van der Meer, L.J. Rijzewijk, J.W. Smit, H.J. Lamb, V. Llorente-Cortes, T. Thum, Sci Rep 6 (2016) 37354. doi: 10.1038/srep37354.

[75] J. Zhao, W. Zhang, M. Lin, W. Wu, P. Jiang, E. Tou, M. Xue, A. Richards, D. Jourd'heuil, A. Asif, D. Zheng, H.A. Singer, J.M. Miano, X. Long, Arterioscler Thromb Vasc Biol 36 (2016) 2088-99. doi: 10.1161/ATVBAHA.116.307879.

[76] M. Huarte, M. Guttman, D. Feldser, M. Garber, M.J. Koziol, D. Kenzelmann-Broz, A.M. Khalil, O. Zuk, I. Amit, M. Rabani, L.D. Attardi, A. Regev, E.S. Lander, T. Jacks, J.L. Rinn, Cell 142 (2010) 409-19. doi: 10.1016/j.cell.2010.06.040.

[77] G. Wu, J. Cai, Y. Han, J. Chen, Z.P. Huang, C. Chen, Y. Cai, H. Huang, Y. Yang, Y. Liu, Z. Xu, D. He, X. Zhang, X. Hu, L. Pinello, D. Zhong, F. He, G.C. Yuan, D.Z. Wang, C. Zeng, Circulation 130 (2014) 1452-65. doi: 10.1161/CIRCULATIONAHA.114.011675.

[78] Y. Zhao, G. Feng, Y. Wang, Y. Yue, W. Zhao, Int J Clin Exp Pathol 7 (2014) 7643-52.

[79] Q. He, J. Tan, B. Yu, W. Shi, K. Liang, Pharmazie 70 (2015) 310-5.

[80] N. Thorenoor, O. Slaby, Tumour Biol 36 (2015) 41-53. doi:

10.1007/s13277-014-2818-8.
[81] C. Ma, X. Shi, Q. Zhu, Q. Li, Y. Liu, Y. Yao, Y. Song, Tumour Biol 37 (2016) 1437-44. doi: 10.1007/s13277-015-4521-9.
[82] L. Li, X. Li, E. The, L.J. Wang, T.Y. Yuan, S.Y. Wang, J. Feng, J. Wang, Y. Liu, Y.H. Wu, X.E. Ma, J. Ge, Y.Y. Cui, X.Y. Jiang, PLoS One 10 (2015) e0120550. doi: 10.1371/journal.pone.0120550.
[83] Y.N. Wang, K. Shan, M.D. Yao, J. Yao, J.J. Wang, X. Li, B. Liu, Y.Y. Zhang, Y. Ji, Q. Jiang, B. Yan, Hypertension 68 (2016) 736-48. doi: 10.1161/HYPERTENSIONAHA.116.07259.
[84] M. Zhang, Y. Ren, Y. Wang, R. Wang, Q. Zhou, Y. Peng, Q. Li, M. Yu, Y. Jiang, J Neuropathol Exp Neurol 74 (2015) 411-24. doi: 10.1097/NEN.0000000000000185.
[85] S.P. Dai, J. Jin, W.M. Li, Postgrad Med J 94 (2018) 578-587. doi: 10.1136/postgradmedj-2018-135862.
[86] G. Yu, W. Zhang, L. Zhu, L. Xia, Onco Targets Ther 11 (2018) 1491-1499. doi: 10.2147/OTT.S152241.
[87] Q.W. Deng, S. Li, H. Wang, H.L. Sun, L. Zuo, Z.T. Gu, G. Lu, C.Z. Sun, H.Q. Zhang, F.L. Yan, Clin Sci (Lond) 132 (2018) 1597-1614. doi: 10.1042/CS20180411.
[88] A.S. Bayoumi, T. Aonuma, J.P. Teoh, Y.L. Tang, I.M. Kim, Acta Pharmacol Sin 39 (2018) 1100-1109. doi: 10.1038/aps.2017.196.
[89] S. Uchida, High Throughput 6 (2017) pii: e12. doi: 10.3390/ht6030012.
[90] J. Hung, V. Miscianinov, J.C. Sluimer, D.E. Newby, A.H. Baker, Front Physiol 9 (2018) 1655. doi: 10.3389/fphys.2018.01655.

Original Articles

JOURNAL OF INTEGRATED OMICS
A METHODOLOGICAL JOURNAL
HTTP://WWW.JIOMICS.COM

ORIGINAL ARTICLE | DOI: 10.5584/jiomics.v9i1.250

Comparative proteomic analysis in microdissected renal vessels from hypertensive SHR and WKY normotensive rats

Georgios Barkas [1,2], Manousos Makridakis [1], Rafael Stroggylos [1], Jerome Zoidakis [1*], Antonia Vlahou [1], Aristidis Charonis [1], Demetrios V. Vlahakos [1,2]

[1] Biomedical Research Foundation of the Academy of Athens, Greece; [2] National and Kapodistrian University of Athens, Medical School, Greece.

Received: 11 July 2018 **Accepted:** 11 January 2019 **Available Online**: 18 March 2019

ABSTRACT

Systemic hypertension leads to renal damage known as hypertensive nephrosclerosis without obvious clinical symptoms in the initial stages and it has a profound impact on the renal vascular physiology. Despite its major role in End Stage Renal Disease, many aspects of hypertensive nephrosclerosis remain unknown. In order to elucidate the biological pathways and macromolecules deregulated by hypertension, renal vessels were obtained by Laser Capture Microdissection (LCM) from Spontaneously Hypertensive Rats (SHR) and age-matched controls (20 weeks). Proteomic analysis was performed aiming to detect molecular alterations associated with hypertension at the renal vessels before the onset of vascular damage. This analysis identified 688 proteins, of which 58 were differentially expressed (15 up-regulated and 43 down-regulated) in SHR. Many of these proteins are involved in vascular tone regulation by modulating the activity of endothelial Nitric Oxide Synthase (eNOS) (Xaa-Pro aminopeptidase 1 (XPP1), N(G) N(G)-dimethylarginine dimethylaminohydrolase 1 (DDAH1), Dehydropteridine reductase (DHPR)) or in blood pressure control by regulating the renin-angiotensin system (Glutamyl aminopeptidase/Aminopeptidase A (AMPE), Aminopeptidase N (AMPN)). Moreover, pathway enrichment analysis revealed that the eNOS activation pathway is deregulated only in SHR. Our study demonstrates that hypertension causes early proteomic changes in the renal vessels of SHR. These changes are relevant to vascular tone regulation and consequently may be involved in the development of vascular damage and hypertensive nephrosclerosis. Further validation and interference studies to investigate potential therapeutic impact of these findings are warranted.

Keywords: Laser Capture Microdissection; Vascular proteomics; essential hypertension; Endothelial dysfunction; Spontaneously hypertensive rats.

1. Introduction

Chronic hypertension is the second leading cause of End Stage Renal Disease (ESRD) [1]. It leads to renal damage known as hypertensive nephrosclerosis without specific clinical presentation in the initial stages. Despite its major role in ESRD, many aspects of hypertensive nephrosclerosis remain unknown. For instance, alterations in the vascular wall may be involved in the pathogenesis of hypertension at an early stage, while at the same time may be considered a consequence of hypertension at a late stage [2]. Endothelial function is impaired in hypertensive individuals in several arterial beds, including the renal arteries and their branches. Whether endothelial dysfunction is a cause or consequence of hypertension has been the subject of many studies [3]. The mechanisms that lead to endothelial dysfunction may be associated with a decrease of endothelium-derived relaxing factors (EDRFs) (mainly nitric oxide) and/or an increase of various endothelium-derived constricting factors (EDCFs).

Spontaneously Hypertensive Rat (SHR) is a well-established animal model of hypertension [4]. The importance of this model has been attributed to the similarity of its pathophysiology with essential hypertension in humans [2,5]. In a recent publication, we used proteomic analysis of renal parenchyma to identify processes and organelles affected from the early stages of the development of hypertension. Among many molecules and pathways identified, we showed over-expression of the chloride channel CLIC4 in the brush border of proximal tubules and

***Corresponding author:** Jerome Zoidakis, Biomedical Research Foundation, Academy of Athens, Department of Biotechnology, Soranou Efessiou 4, 11527 Athens. tel. +30-210-6597485, email: izoidakis@bioacademy.gr .

we suggested that this molecule could be involved in the pathogenesis of hypertension and could be used as a useful early marker jof renal tubular alterations during hypertension [6]. Other investigators have focused their attention in vascular wall of SHR and found inconsistent results regarding the role of nitric oxide (NO) and endothelial dysfunction in the development of hypertension. Despite hypertension, endothelium-dependent vasodilatory responses were similar or even augmented in SHR compared with the control normotensive animals [7]. Age, gender, the vascular type studied and methodological aspects may all contribute to the variability among various reports.

In this communication we focused our attention to the arterial wall in the kidney of SHR at an early stage of hypertension before the development of hypertensive nephrosclerosis. To this end, we combined Laser Capture Microdissection (LCM) technology and high resolution GeLC-MS/MS proteomic analysis followed by a bioinformatics approach to compare the arterial wall between SHR and their normotensive counterparts Wistar-Kyoto (WKY) rats [8]. Our results demonstrate that significant proteomic changes occur in the renal vessels of SHR compared to WKY prior to the development of structural damage and that these changes are relevant to vascular tone regulation, which eventually lead to the development of hypertensive nephrosclerosis.

2. Material and Methods

2.1. Experimental animals:

The Male WKY and SHR rats were purchased from Charles River Laboratories (Germany) and housed in the animal facility of the National Center for Scientific Research Demokritos (EL25 BIO 019020022). Male SHR rats were outbred WKY rats with marked elevation of blood pressure (Charles River from NIH in 1973). The animals were maintained in polycarbonate cages and were fed with standard rodent diet with free access to water and with a 12 h light-dark cycle. Mean blood pressure was measured using a computerized rat tail-cuff technique (Kent Scientific co, USA) as described previously [6]. Following blood pressure measurements, the animals were deeply anesthetized with ether and the kidneys were removed as reported in our previous study [6]. The experimental protocols were approved by the Institutional Animal Care and were carried out in agreement with the ethical recommendations of the European Communities Council Directive of 22 September 2010 (2010/63/EU).

2.2 Laser Capture Microdissection

Laser Capture Microdissection was performed using a PALM MicroBeam Laser System (Carl Zeiss Microscopy GmbH, Germany). The laser capture system is equipped with an UV-A laser and a computer. Frozen unfixed renal tissue samples from 20 weeks of age SHR and WKY rats (N=4 for each group) were cut into 14 μm cryosections, mounted on glass slides coated with a biochemically inert membrane (PALM Membrane slides NF 1.0 PEN, Carl Zeiss Microscopy, Germany) and lightly stained with Gill's hematoxylin according to standard procedures. Renal vessels and a limited number of glomeruli which exhibited prominent afferent and efferent arterioles were outlined with the drawing tool on the computer view of the field. The laser cut the selected area of renal parenchyma, following the drawn outline, and blew the microdissected sections off the slide by a higher energy laser pulse, to be captured onto 500-μl AdhesiveCap Touch opaque tube (Carl Zeiss Microscopy, Germany) placed over the sample area. Approximately 10,000,000 – 14,000,000 μm2 of microdissected segments were collected from each sample.

2.3. GeLC-MS analysis:

2.3.1. Sample preparation for LC-MS/MS (Liquid Chromatography coupled with tandem Mass Spectrometry):

Microdissected segments of renal parenchyma were homogenized and proteins were extracted in sample buffer (7M Urea, 2M Thiurea, 4% CHAPS, 1% DTE). Protein concentration was determined by the Bradford assay. Equal amounts of protein from each sample (6 μg) were analyzed by SDS PAGE. The electrophoresis was terminated when the samples just entered into the separating gel. In this way each sample was represented by a single band including its total protein content and processed for LC-MS/MS analysis. In brief, Coomassie Colloidal Blue-stained bands were excised from the gels and cut in small pieces (1-2 mm). Gel pieces were destained in 40% Acetonitrile, 50 mM NH4HCO3, reduced in 10 mM DTE, 100 mM NH4HCO3, and alkylated in 50 mM IAA, 100 mM NH4HCO3. Samples were dried and trypsinized overnight with 600 ng trypsin in 10 mM NH4HCO3. Peptide extraction was performed with one wash of the trypsinized gel pieces with 50 mM NH4HCO3, followed by two washes with 50% acetonitrile, 5% formic acid for 15 min at room temperature. Extracted peptides were dried and kept at -80oC.[9]

2.3.2. LC-MS/MS

Dried peptides were solubilized in 10 μL mobile phase A (0.1% formic acid) and separated on a nano HPLC Dionex Ultimate 3000 RSLS system (Dionex™, Camberly, UK). Five μL of each sample were loaded on a Dionex 0.1×20 mm, 5 μm C18 nanotrap column at a flow rate of 5 μL/min in 98% mobile phase A (0,1% formic acid) and 2% mobile phase B (100% acetonitrile, 0,1% formic acid). At a next step the sample was injected into an Acclaim PepMap C18 nanocolumn 75 μm×50 cm (Dionex™, Sunnyvale, CA, USA), at a flow rate of 0,3 μL/min. The samples were eluted with a gradient of solvent B: 2% B-80% B within 120 min LC run

time. The eluted peptides were ionized using a Proxeon nanospray ESI source, operating in positive ion mode, and injected into an Orbitrap Elite FTMS (ThermoFinnigan, Bremen, Germany). The mass-spectrometer was operated in MS/MS mode scanning from 380 to 2000 amu. The resolution of ions in MS1 was 60,000 and 15,000 for HCD MS2. The top 10 multiply-charged ions were selected from each scan for MS/MS analysis using HCD at 35% collision energy. Data analysis was performed with Proteome Discoverer 1.4 software package (ThermoScientific, Hemel Hempstead, UK), using the SEQUEST search engine and the Uniprot rat reviewed database including 7,928 entries. The search was performed using carbamidomethylation of cysteine as static and oxidation of methionine as dynamic modifications. Two missed cleavage sites, a precursor mass tolerance of 10 ppm and fragment mass tolerance of 0.05 Da were allowed. SEQUEST results were filtered for false-positive identifications.

2.3.3. Quantification and statistical analysis

Reliable protein identifications (e.g. based on at least one high confidence peptide, FDR <1%) which were present in at least 3 of the available 4 samples were retained for quantification analysis performed at the peptide level. The intensity for each protein in each sample was normalized in ppm (quotient of intensity for the particular protein to the sum of all intensities of all proteins of the specific sample multiplied with 106). The average normalized intensity for each protein was then determined for all the samples of the two groups (SHR and WKY).

As differentially expressed proteins selected for further analysis, were considered those with a fold change of > 1.5 (up-regulated in SHR compared to WKY) or < 0.66 (down-regulated in SHR compared to WKY), and a p-value of ≤ 0.05 (Mann Whitney).

A comparison of all identified proteins with the online available Rat IMCD Proteome database (https://hpcwebapps.cit.nih.gov/ESBL/Database/IMCD_Proteome_Dev/) was performed.

A heat map of differentially expressed proteins was generated using the online tool available in the link: http://www.heatmapper.ca/. The Row Z-score was calculated for each row using the formula:

$$z_i = (x_i - \bar{x})/s$$

2.4. Bioinformatics analysis

In order to unveil the pathways that may be associated with the identified proteins in both SHR and WKY animals, Kyoto Encyclopedia of Genes and Genomes (KEGG) pathway analysis was performed using Cytoscape software [10] with the ClueGO plugin [11] using Rattus Norvegicus as organism. P-value (corrected with Bonferroni) ≤ 0.05 was set as the threshold.

3. Results

In the present study, we used LCM technology and GeLC-MS/MS analysis in order to characterize the proteomic profile of renal vessels in the SHR model compared to control. Detailed information on the experimental animals, such as blood pressure measurements and histopathology are described in our previous study [6]. The experimental approach we followed is outlined in Figure 1.

3.1. GeLC-MS/MS analysis reveals differentially expressed proteins in renal vessels of hypertensive rats compared to control

Proteomics techniques were applied to investigate the differences in the proteomic profiles of the renal vessels between SHR and WKY rats. 688 proteins were identified based on at least one high confidence peptide; of these, 550 proteins were detected in both SHR and WKY rats, 71 proteins were found exclusively in WKY and 67 exclusively in SHR rats. We refer to exclusively identified proteins as those identified in at least three biological replicates of one condition and in no replicates of the other. A comprehensive list of the identified proteins including the fold change is shown in the Supplementary Table 1. A comparison of all 688 identified proteins in renal vessels with the available Rat IMCD Proteome database revealed 517 overlapping proteins.

Of the 550 proteins identified in both SHR and WKY samples, 58 proteins were differentially expressed, of which 15 proteins were up-regulated and 43 were down-regulated in SHR (listed in Supplementary Table 2). A volcano plot representing the distribution of identified proteins according to p-value and fold change is shown in Figure 2a. Plotting the negative log10 function of the unadjusted p-value against the log2 function of fold change, visualizes all the identified

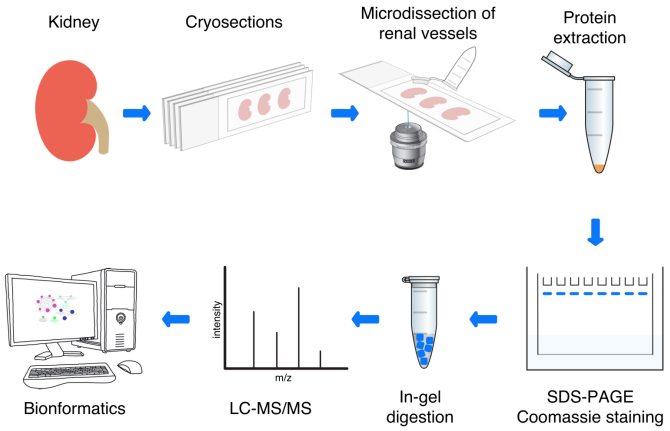

Figure 1 | A. Graphical overview of the experimental approach. Renal vessels were microdissected from kidney tissue cryosections using an UV-A laser. Extracted proteins were analyzed by SDS-PAGE and the resulting single bands were stained with Coomassie Colloidal Blue and excised from the gel. Proteins were in-gel digested and the resulting peptides were analyzed by LC-MS/MS. Identified molecules were used for further bioinformatics analysis.

proteins and the statistically significant up-regulated and down-regulated proteins. Figure 2 (b) presents a heat map of the statistically significant differentially expressed proteins.

3.2. Bioinformatics pathway analysis

Pathway enrichment analysis was performed for all proteins identified in each group in order to uncover significant biological processes relevant for blood vessels functions. 114 and 111 KEGG pathways were identified in WKY and SHR respectively and 106 pathways were common in both groups. Among the common pathways identified were pathways associated with normal functions of vascular cells e.g metabolism, oxidation, signaling, membrane trafficking, detoxification of Reactive Oxygen Species (ROS), VEGFR2 mediated cell proliferation and smooth muscle contraction. These data are presented in Supplementary Figures 1 and 2 for SHR and WKY respectively and a comprehensive list is given in the Supplementary Tables 4 and 5. It is worth mentioning that the eNOS (endothelial nitric oxide synthase) activation pathway was identified only in SHR samples. eNOS is an enzyme responsible for the generation of nitric oxide (NO) in the vascular endothelium, a key player in the regulation of the vascular tone [12].

3.3. Prominent proteomics findings:

GeLC-MS/MS analysis revealed a large number of identified proteins in renal vessels of SHR and WKY animals. The most prominent findings relevant to vascular tone and blood pressure regulation, along with the corresponding P-value and fold change are presented in Table 1. These proteins may play significant roles in the context of vascular physiology.

4. Discussion

Our study aimed to identify early proteomic changes in the renal vessels of SHR involved with pathogenesis of hypertension. The applied protocol consisted of LCM coupled to high resolution GeLC-MS/MS analysis. The high number of identified proteins verifies that this method was highly efficient and capable of identifying canonical proteomic alterations in microdissected renal parenchyma segments of SHR animals compared to controls. Furthermore, a comparison of our data with the available Rat IMCD Proteome database revealed 75% (517 out of 688 proteins of our dataset) overlap of identified proteins in renal vessels with the IMCD database. A recent report on LCM coupled with LC-MS/MS in the study of mouse brain sections following a protocol comparable to our approach resulted in the identification of a similar number of proteins (on average 322 proteins) in the microdissected tissue samples [13]. However, the application of the SP3 method (single-pot solid-phase-enhanced sample preparation) yielded a significantly higher number of protein identifications, on average 5744.

In the SHR model, alterations in vascular structure and

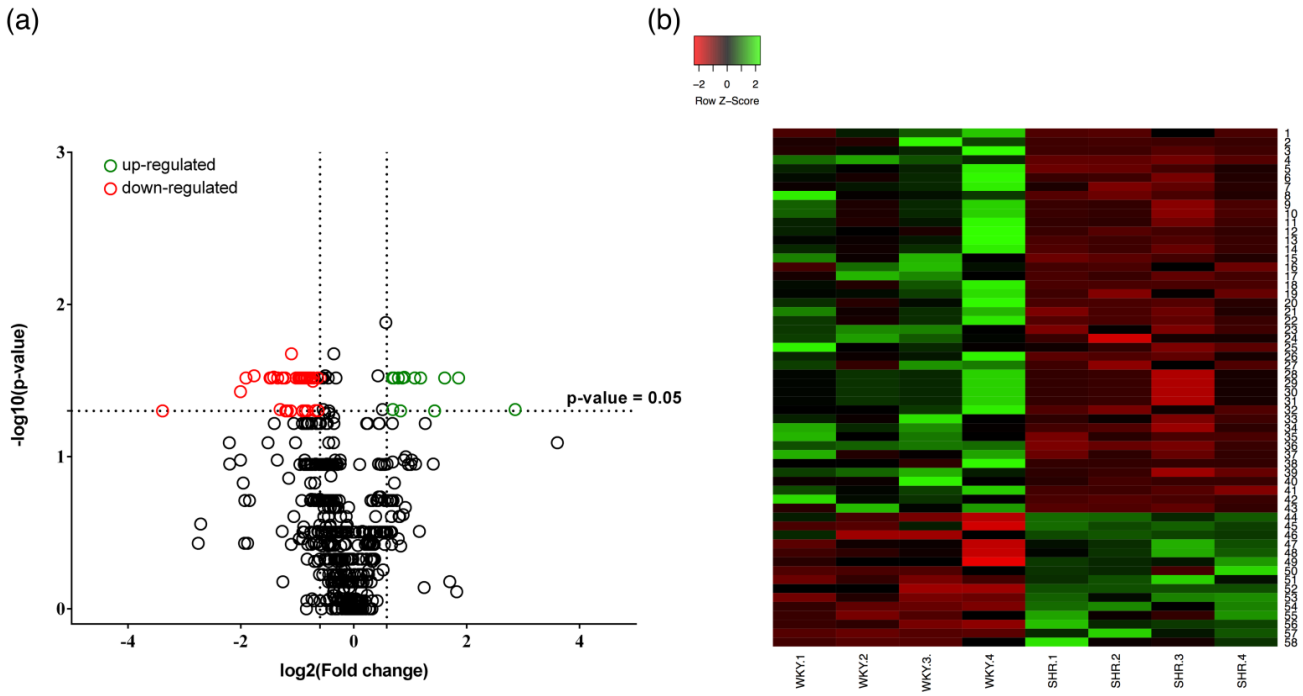

Figure 2 | (a) Volcano plot of proteomic data, presenting the negative log10 of P-value against the log2 of the fold change. All the proteins with fold change <1 have negative X-values and the proteins with fold change >1 have positive X-values. The proteins with fold change > 1.5 and P-value ≤ 0.05 are considered significantly up-regulated in SHR in comparison to controls. The proteins with fold change < 0.66 and P-value ≤ 0.05 are considered significantly down-regulated in SHR. (b) Heat map of 58 differentially expressed proteins. A list of proteins along with their normalized area and the corresponding protein name used in the heat map is presented in the Supplementary Table 3.

Table 1 | Differentially expressed proteins relevant to vascular tone and blood pressure regulation.

Gene	Protein	p-value	Fold change (SHR/WKY)	Function	Reference
Qdpr	Dihydropteridine reductase	0.03	3.05	BH4 regeneration	[32,33]
Ddah1	N(G), N(G)-dimethylarginine dimethylaminohydrolase 1	0.05	1.77	ADMA hydrolase	[34]
Cfl1	Cofilin-1	0.03	1.6	Cytoskeletal remodeling	[35]
Xpnpep1	Xaa-Pro aminopeptidase 1	0.05	0.64	Bradykinin degradation	[23,24]
Pah	Phenylalanine-4-hydroxylase	0.04	0.62	Tyrosine generation	[36]
Enpep	Glutamyl aminopeptidase/ Aminopeptidase A	0.05	0.53	Metabolism of AngII	[20]
Anpep	Aminopeptidase N	0.03	0.37	Metabolism of AngIII	[19]
Calb1	Calbindin	0.05	0.46	Calcium-binding protein	[37]
Calb2	Calretinin	0.05	0.55	Calcium-binding protein	[38]
Phb	Prohibitin	0.03	0.24	ROS formation	[39,40]
Phb2	Prohibitin-2	0.03	0.43	Mitochondrial function	[41]

functions related to hypertension are not present in young animals but are observed in adult animals (older than 25 weeks) [7]. In the present study, focusing on an early interval, we provide evidence that early molecular changes occur in the renal vessels of SHR animals at 20 weeks of age. The proteomic analysis yielded 58 proteins differentially expressed between SHR and WKY animals that play important roles in the context of vascular dysfunction.

Many of the interesting differentially expressed proteins identified in our study are relevant to vascular tone regulation. Thus, proteins involved with NO and vasodilation and affecting eNOS include Xaa-Pro aminopeptidase 1 (XPP1), N(G) N(G)-dimethylarginine dimethylaminohydrolase 1 (DDAH1), Dehydropteridine reductase (DHPR), whereas proteins affecting vasoconstriction and blood pressure regulation by renin-angiotensin system [14] include Glutamyl aminopeptidase/ Aminopeptidase A (AMPE), Aminopeptidase N (AMPN). These molecules may be involved in the pathogenesis of hypertensive nephropathy.

Angiotensin metabolism is critical for blood pressure regulation since in addition to Ang II, peptide fragments derived from this hormone also have diverse and important physiological roles. Ang III has been shown to be a major effector peptide; in the intrarenal Renin–Angiotensin system it has been reported to increase angiotensinogen levels and TGF-β, fibronectin and monocyte chemoattractant protein-1 gene expression [15,16]. Furthermore, Ang III formation is critical for the AT2 receptor-mediated natriuresis in rats contributing in reduction of blood pressure [17] and endothelial metabolism of Ang II to Ang III boosts the vasorelaxation response in adrenal cortical arteries [18]. In our analysis, both AMPE and AMPN responsible for Ang III and Ang IV formation respectively [19,20], were down-regulated in SHR most likely enhancing the vasoconstrictor effect of Ang II, decreasing the Ang III-induced sodium excretion [17], and thus inducing hypertension. These results are consistent with the high mean blood pressure (160 - 170 mmHg) measured in SHR animals used in our study [6].

Nevertheless, despite the established high blood pressure, our analysis revealed several differentially expressed molecules that may have a protective role against hypertension. In other words, defensive mechanisms may be activated in the renal vessels of SHR at an early phase of the development of hypertension, possibly to counteract the vasoconstricting effects of Ang II and other constricting substances. In this regard, other investigators have studied the role of NO in hypertension and kidney damage in SHR and found elevated levels of iNOS in SHR, but not in WKY rats [21,22]. Molecules such as XPP1, DDAH1 and DHPR may affect the synthesis of endothelium-derived relaxing factors (EDRFs) increasing NO levels and vasodilatation. In this regard, XPP1 was found to be down-regulated in SHR compared to WKY reducing the degradation of bradykinin which stimulates endothelial cells to produce and release EDRFs that cause blood vessels to dilate and therefore reduce blood pressure [23,24]. Other protective molecules, such as DDAH1 and DHPR appear to be up-regulated in SHR presumably as a defense mechanism to hypertension.

DDAH 1 is a methylarginine-metabolizing enzyme that reduces asymmetric dimethylarginine (ADMA) levels. ADMA is an endogenous compound derived from the proteolysis of proteins containing methylated arginine residues that inhibits nitric oxide synthase (NOS) catalytic activity. Moreover, ADMA is accumulated in plasma during CKD [25] and reduced renal tubular ADMA synthesis protects against progressive kidney function decline [26]. DHPR is an enzyme that catalyzes the regeneration of tetrahydrobiopterin (BH4). BH4 is a cofactor of a set of enzymes including NOS and plays an essential role in neurovascular homeostasis and has anti-inflammatory activity [27]. DHPR converts BH2 to BH4 which is necessary for NO production by NOS. If BH4 is insufficient, NOS becomes uncoupled and generates superoxide [28,29]. The up-regulated DHPR in SHR model favors the regeneration of BH4 allowing the enzymatic synthesis of NO.

Collectively, the validity of our proteomic results is supported by the relevance of the proteins identified as differentially expressed in the context of hypertension. The trend observed for the differentially expressed proteins is supported by related literature and existing knowledge on regulatory mechanisms of blood pressure (e.g. renin-angiotensin system [14-17]). An overview of these molecules and their putative action on vascular tone and consequently blood pressure regulation is presented in Figures 3 and 4.

Using LCM for renal research provides an important advantage. It gives us the ability to separate different compartments and sub-compartments of renal parenchyma to almost total purity. This is not the case with already described methods that employ different types of sieves in order to separate glomeruli from tubules [30]. In addition, these methodologies are expensive and cannot discriminate between different types of tubular compartments (e.g. proximal vs. distal) [31]. LCM has been used in our study for proteomic analysis but it can also be useful for in depth transcriptomic analysis of different renal compartments in the future. Therefore, use of LCM material in future studies will lead to a more in depth understanding of renal pathophysiology.

5. Concluding Remarks

In summary, combining LCM technology and high resolution GeLC-MS/MS analysis in the renal blood vessels of SHR, a well-established model of hypertension, we offer insights on proteomic profiles of renal vessels with regard to hypertension. Significant early proteomic changes occur in the renal blood vessels of SHR compared to WKY before the onset of vascular dysfunction and structural damage. Whether these changes are of decisive importance in the development of hypertensive nephropathy and endothelial dysfunction due to hypertension needs to be investigated further. Moreover, our data suggest that AMPE, AMPN, XPP1, DDAH1, DHPR are moderators and mediators of renal vascular tone modulation contributing in blood pressure regulation. These molecules may be potentially important therapeutic targets for the hypertensive nephropathy and should be studied further.

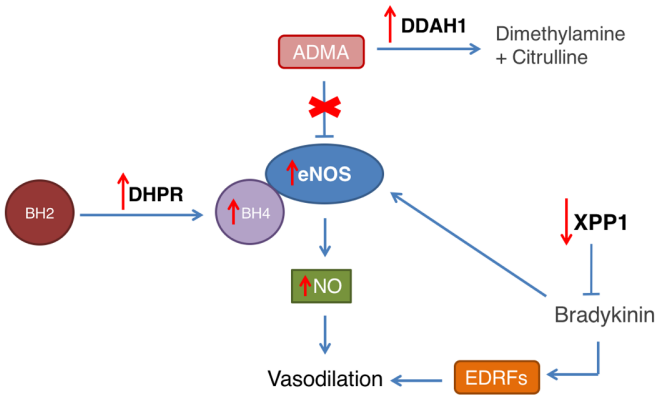

Figure 3 | Putative activation of vasodilation mechanisms via NO and EDRFs production. ADMA: asymmetric dimethylarginine, BH2: dihydrobiopterin, BH4: tetrahydrobiopterin, DDAH1: dimethylarginine dimethylaminohydrolase 1, DHPR: dehydropteridine reductase, EDRFs: endothelium-derived relaxing factors, eNOS: endothelial nitric oxide synthase, NO: nitric oxide, XPP1: Xaa-Pro aminopeptidase 1.

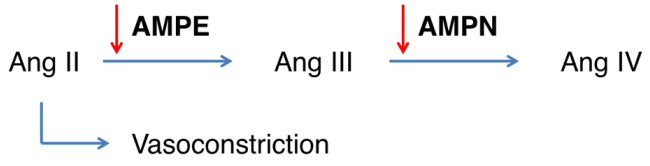

Figure 4 | Putative activation of vasoconstriction mechanism via Angiotensin II (AngII). Down-regulated Aminopeptidases A (AMPE) and N (AMPN) in SHR lead to impaired Ang II and Ang III degradation respectively, enhancing possibly the levels and the vasoconstrictor effect of Ang II.

6. Supplementary material

Supplemetary Figure 1: Pathway analysis of all identified proteins in SHR

Supplementary Figure 2: Pathway analysis of all identified proteins in WKY

Supplementary Table 1: List of all identified proteins

Supplementary Table 2: List of statistically significant differentially expressed proteins in renal vessels of SHR compared to WKY

Supplementary Table 3: List of differentially expressed proteins presented in Figure 2 (b) along with their normalized area per sample and the corresponding ascending number.

Supplementary Table 4: SHR pathway analysis

Supplementary Table 5: WKY pathway analysis

The mass spectrometry proteomics data have been deposited to the ProteomeXchange Consortium via the PRIDE [40] partner repository with the dataset identifier PXD008792.

Acknowledgements

This research is co-financed by Greece and the European Union (European Social Fund- ESF) through the Operational Programme «Human Resources Development, Education and Lifelong Learning» in the context of the project "Strengthening Human Resources Research Potential via Doctorate Research" (MIS-5000432), implemented by the State Scholarships Foundation (IKY). It was also supported from an ARISTEIA II grant (number 4045) to D. Vlahakos from the General Secretariat of Research and Technology of the Greek Ministry of Education.

References

1] Kopp JB; Rethinking hypertensive kidney disease: arterionephrosclerosis as a genetic, metabolic, and inflammatory disorder. Current opinion in nephrology and hypertension 2013;22:266-272.

2] Hultstrom M, Development of structural kidney damage in spontaneously hypertensive rats. Journal of hypertension 2012;30:1087-1091.

3] Bernatova I, Endothelial dysfunction in experimental models of arterial hypertension: cause or consequence? BioMed research international 2014;2014:598271.

4] Dornas WC, Silva ME, Animal models for the study of arterial hypertension. Journal of biosciences 2011;36:731-737.

5] Mullins LJ, Conway BR, Menzies RI, Denby L, Mullins JJ: Renal disease pathophysiology and treatment: contributions from the rat. Disease models & mechanisms 2016;9:1419-1433.

6] Hatziioanou D, Barkas G, Critselis E, Zoidakis J, Gakiopoulou H, Androutsou ME, Drossopoulou G, Charonis A, Vlahakos DV: Chloride Intracellular Channel 4 Overexpression in the Proximal Tubules of Kidneys from the Spontaneously Hypertensive Rat: Insight from Proteomic Analysis. Nephron 2017

7] Bernatova I, Conde MV, Kopincova J, Gonzalez MC, Puzserova A, Arribas SM: Endothelial dysfunction in spontaneously hypertensive rats: focus on methodological aspects. Journal of hypertension Supplement : official journal of the International Society of Hypertension 2009;27:S27-31.

8] Datta S, Malhotra L, Dickerson R, Chaffee S, Sen CK, Roy S: Laser capture microdissection: Big data from small samples. Histology and histopathology 2015;30:1255-1269.

9] Makridakis M, Vlahou A: GeLC-MS: A Sample Preparation Method for Proteomics Analysis of Minimal Amount of Tissue. Methods in molecular biology 2018;1788:165-175

10] Shannon P, Markiel A, Ozier O, Baliga NS, Wang JT, Ramage D, Amin N, Schwikowski B, Ideker T: Cytoscape: a software environment for integrated models of biomolecular interaction networks. Genome research 2003;13:2498-2504.

11] Bindea G, Mlecnik B, Hackl H, Charoentong P, Tosolini M, Kirilovsky A, Fridman WH, Pages F, Trajanoski Z, Galon J: ClueGO: a Cytoscape plug-in to decipher functionally grouped gene ontology and pathway annotation networks. Bioinformatics 2009;25:1091-1093.

12] Siragusa M, Fleming I: The eNOS signalosome and its link to endothelial dysfunction. Pflugers Archiv : European journal of physiology 2016;468:1125-1137.

13] Dilillo M, Pellegrini D, Ait-Belkacem R, de Graaf EL, Caleo M, McDonnell LA: Mass Spectrometry Imaging, Laser Capture Microdissection, and LC-MS/MS of the Same Tissue Section. Journal of proteome research 2017;16:2993-3001.

14] Ferrao FM, Lara LS, Lowe J: Renin-angiotensin system in the kidney: What is new? World journal of nephrology 2014;3:64 -76.

15] Ruiz-Ortega M, Lorenzo O, Egido J: Angiotensin III increases MCP-1 and activates NF-kappaB and AP-1 in cultured mesangial and mononuclear cells. Kidney international 2000;57:2285-2298.

16] Ruiz-Ortega M, Lorenzo O, Egido J: Angiotensin III up-regulates genes involved in kidney damage in mesangial cells and renal interstitial fibroblasts. Kidney international Supplement 1998;68:S41-45.

17] Padia SH, Kemp BA, Howell NL, Fournie-Zaluski MC, Roques BP, Carey RM: Conversion of renal angiotensin II to angiotensin III is critical for AT2 receptor-mediated natriuresis in rats. Hypertension 2008;51:460-465.

18] Kopf PG, Campbell WB: Endothelial metabolism of angiotensin II to angiotensin III, not angiotensin (1-7), augments the vasorelaxation response in adrenal cortical arteries. Endocrinology 2013;154:4768-4776.

19] Danziger RS: Aminopeptidase N in arterial hypertension. Heart failure reviews 2008;13:293-298.

20] Reaux A, Iturrioz X, Vazeux G, Fournie-Zaluski MC, David C, Roques BP, Corvol P, Llorens-Cortes C: Aminopeptidase A, which generates one of the main effector peptides of the brain renin-angiotensin system, angiotensin III, has a key role in central control of arterial blood pressure. Biochemical Society transactions 2000;28:435-440.

21] Chou TC, Yen MH, Li CY, Ding YA: Alterations of nitric oxide synthase expression with aging and hypertension in rats. Hypertension 1998;31:643-648.

22] Huang CF, Hsu CN, Chien SJ, Lin YJ, Huang LT, Tain YL: Aminoguanidine attenuates hypertension, whereas 7-nitroindazole exacerbates kidney damage in spontaneously hypertensive rats: the role of nitric oxide. European journal of pharmacology 2013;699:233-240.

23] Dendorfer A, Wolfrum S, Wagemann M, Qadri F, Dominiak P: Pathways of bradykinin degradation in blood and plasma of normotensive and hypertensive rats. American journal of physiology Heart and circulatory physiology 2001;280:H2182

-2188.

24] Ersahin C, Simmons WH: Inhibition of both aminopeptidase P and angiotensin-converting enzyme prevents bradykinin degradation in the rat coronary circulation. Journal of cardiovascular pharmacology 1997;30:96-101.

25] Mihout F, Shweke N, Bige N, Jouanneau C, Dussaule JC, Ronco P, Chatziantoniou C, Boffa JJ: Asymmetric dimethylarginine (ADMA) induces chronic kidney disease through a mechanism involving collagen and TGF-beta1 synthesis. The Journal of pathology 2011;223:37-45.

26] Tomlinson JA, Caplin B, Boruc O, Bruce-Cobbold C, Cutillas P, Dormann D, Faull P, Grossman RC, Khadayate S, Mas VR, Nitsch DD, Wang Z, Norman JT, Wilcox CS, Wheeler DC, Leiper J: Reduced Renal Methylarginine Metabolism Protects against Progressive Kidney Damage. Journal of the American Society of Nephrology : JASN 2015;26:3045-3059.

27] Rivera JC, Noueihed B, Madaan A, Lahaie I, Pan J, Belik J, Chemtob S: Tetrahydrobiopterin (BH4) deficiency is associated with augmented inflammation and microvascular degeneration in the retina. Journal of neuroinflammation 2017;14:181.

28] Grobe AC, Wells SM, Benavidez E, Oishi P, Azakie A, Fineman JR, Black SM: Increased oxidative stress in lambs with increased pulmonary blood flow and pulmonary hypertension: role of NADPH oxidase and endothelial NO synthase. American journal of physiology Lung cellular and molecular physiology 2006;290:L1069-1077.

29] Kim HL, Park YS: Maintenance of cellular tetrahydrobiopterin homeostasis. BMB reports 2010;43:584-592.

30] Liu X, Fan Q, Yang G, Liu N, Chen D, Jiang Y, Wang L: Isolating glomeruli from mice: A practical approach for beginners. Experimental and therapeutic medicine 2013;5:1322-1326.

31] Takemoto M, Asker N, Gerhardt H, Lundkvist A, Johansson BR, Saito Y, Betsholtz C: A new method for large scale isolation of kidney glomeruli from mice. The American journal of pathology 2002;161:799-805.

32] Ponzone A, Spada M, Ferraris S, Dianzani I, de Sanctis L: Dihydropteridine reductase deficiency in man: from biology to treatment. Medicinal research reviews 2004;24:127-150.

33] Lee CK, Han JS, Won KJ, Jung SH, Park HJ, Lee HM, Kim J, Park YS, Kim HJ, Park PJ, Park TK, Kim B: Diminished expression of dihydropteridine reductase is a potent biomarker for hypertensive vessels. Proteomics 2009;9:4851-4858.

34] Tojo A, Welch WJ, Bremer V, Kimoto M, Kimura K, Omata M, Ogawa T, Vallance P, Wilcox CS: Colocalization of demethylating enzymes and NOS and functional effects of methylarginines in rat kidney. Kidney international 1997;52:1593-1601.

35] Wang QZ, Gao HQ, Liang Y, Zhang J, Wang J, Qiu J: Cofilin1 is involved in hypertension-induced renal damage via the regulation of NF-kappaB in renal tubular epithelial cells. Journal of translational medicine 2015;13:323.

36] Flydal MI, Martinez A: Phenylalanine hydroxylase: function, structure, and regulation. IUBMB life 2013;65:341-349.

37] Lee CT, Ng HY, Lee YT, Lai LW, Lien YH: The role of calbindin -D28k on renal calcium and magnesium handling during treatment with loop and thiazide diuretics. American journal of physiology Renal physiology 2016;310:F230-236.

38] Chang IY, Yoon SP: The changes of calretinin immunoreactivity in paraquat-induced nephrotoxic rats. Acta histochemica 2012;114:836-841.

39] Zheng H, Lu GM: Reduction of prohibitin expression contributes to left ventricular hypertrophy via enhancement of mitochondrial reactive oxygen species formation in spontaneous hypertensive rats. Free radical research 2015;49:164-174.

40] Zhou TB, Qin YH, Lei FY, Huang WF, Drummen GP: Prohibitin attenuates oxidative stress and extracellular matrix accumulation in renal interstitial fibrosis disease. PloS one 2013;8:e77187.

41] Ising C, Bharill P, Brinkkoetter S, Brahler S, Schroeter C, Koehler S, Hagmann H, Merkwirth C, Hohne M, Muller RU, Fabretti F, Schermer B, Bloch W, Kerjaschki D, Kurschat CE, Benzing T, Brinkkoetter PT: Prohibitin-2 Depletion Unravels Extra-Mitochondrial Functions at the Kidney Filtration Barrier. The American journal of pathology 2016;186:1128-1139.